A geochemical and field study of the Ingeli and Horseshoe lobes, Mount Ayliff Complex, South Africa, and its potential for magmatic sulphide ores

By

Bart Hunter Albrechtsen

Submitted in partial fulfillment of the requirements for the degree

Magister Scientiae

in the Faculty of Natural & Agricultural Science

University of Pretoria

Pretoria

November, 2002

ABSTRACT

The Mount Ayliff Complex (MAC) is situated on the border between Kwa-Zulu Natal and the Eastern Cape provinces in the Republic of South Africa, approximately 90 km due west of Port Shepstone. The Complex forms part of the Karoo Igneous Province and includes five lobes (Ingeli, Insizwa, Tonti, Tabankulu, and Horseshoe) that are the remnants of a single continuous intrusive sheet that had an original extent of 18,000km^2. The current outcrop is estimated at 800km^2. The lobes all show extensive internal differentiation, from basal ultramafic cumulates to diorites and monzonites at the top, while most other intrusions in the Karoo Igneous Province cooled rapidly enough to produce relatively homogenous dolerites.

Most work conducted on the Complex thus far has centered on the Insizwa lobe due to the presence of a Ni-sulphide occurrence near the base of the lobe at Waterfall Gorge. The setting of the ores has analogies to the Noril'sk-Talnakh deposits, which has raised considerable exploration interest on the Mount Ayliff Complex over the last century.

The current study investigates the Ni-Cu sulphide potential of the Ingeli and Horseshoe lobes, which have been poorly studied in the past. To this effect, a stream sediment survey was conducted around the Ingeli lobe to try and detect potentially hidden magmatic sulphide ores. Further, the five lobes of the Complex have been compared in terms of lithology and lithogeochemistry. Analytical techniques used for the current study include: XRF, ICP-MS and electron microprobe. Stream sediment samples were analysed using XRF and ICP-OES.

Olivines from the ultramafic cumulates of the Ingeli and Insizwa lobes are undepleted in Ni, whereas olivines from the Horseshoe and Tabankulu lobes are strongly depleted in Ni. This suggests that the rocks of the latter two lobes crystallized from parental magmas that interacted with a sulphide liquid and that the magmatic flow direction was from the north to the south.

The data indicate that the ultramafic rocks of the Complex plot on or near control lines between olivine and Karoo dolerite indicating that the rocks are mixtures of cumulus olivine and trapped melt of Karoo dolerite composition. There appears to be a copper enrichment towards the top of the ultramafic package in the Ingeli lobe. This pattern corresponds to other studies conducted in the Insizwa lobe and suggests that the two lobes had originally been connected. The lowermost cumulates of the Ingeli lobe contain an enhanced crustal component suggesting some in situ contamination.

No significant sulphide enrichments were encountered in the Basal Zone rocks of the Ingeli lobe. However, the stream sediment data indicate localized PGE enrichment indicating the possible presence of a localized hidden sulphide occurrence of the type found at Waterfall Gorge. Small amounts of sulphides were found associated with the Basal Zone rocks in the Horseshoe lobe consistent with the trends of Ni-depletion of olivines. However, a lack of Co depletion in the ultramafic rocks of this lobe suggests that any sulphide segregation event that did take place was of a relatively small scale.

SAMEVATTING

Die Mount Ayliff Kompleks (MAK) is geleë op die grens van die Kwa-Zulu Natal en Oos-Kaap provinsies in die Republiek van Suid-Afrika, ongeveer 90 km wes van Port Shepstone. Die Kompleks vorm deel van die Karoo Stollings Provinsie en sluit vyf lobbe in (Ingeli, Insizwa, Tonti, Tabankulu en Horseshoe) wat die oorblyfsels is van 'n enkel aaneenlopende intrusiewe plaat met oorspronklike oppervlakgrootte van 18 000 km^2. Die lobbe toon almal 'n groot mate van interne differensiasie, van basale ultramafiese kumuliet tot dioriete en monsoniete aan die bokant, terwyl meeste ander intrusies in die Karoo Stollings Provinsie vinnig genoeg afgekoel het om redelik homogene doleriete te vorm.

Die meeste werk wat tot dusver gedoen is op die Kompleks, het gefokus op die Insizwa lob as gevolg van 'n Ni-sulfied voorkoms naby die basis van die lob by Waterfall Gorge. Die plasing van die erts toon ooreenkomste met die Noril'sk-Talnakh afsettings, wat groot belangstelling in eksplorasie op die Mount Ayliff Komples laat ontstaan het gedurende die laaste eeu.

Die huidige studie ondersoek die Ni-Cu sulfied potensiaal van die Ingeli en Horseshoe lobbe wat in die verlede slegs oppervlakkig bestudeer is. Met inagname hiervan, is 'n stroomsediment opname rondom die Ingeli lob gedoen om bedekte magmatiese sulfiederts te probeer opspoor. Die vyf lobbe van die Kompleks is ook vergelyk in terme van litologie en litogeochemie. Analitiese metodes wat vir die huidige studie gebruik is sluit die volgende in: XRF, ICP-MS en elektron mikrosondering. Stroomsediment-monsters is geanaliseer deur middel van XRF en ICP-OES.

Oliviene wat voorkom in die ultramafiese kumuliet van die Ingeli an Insizwa lobbe is Ni-ryk, terwyl oliviene van die Horseshoe en Tabankulu lobbe Ni-arm is. Dit impliseer dat die gesteentes van die laasgenoemde twee lobbe gekristalliseer het van ouer-magmas wat met 'n sulfied vloeistof in kontak was en dat die magmatiese vloeirigting noord na suid was.

Die data toon dat die ultramafiese gesteentes van die Kompleks op of naby die kontrolelyne tussen olivien en Karoo doleriet plot, wat beteken dat die gesteentes

mengsels is van kumulus olivien en ingeslote smeltsel van Karoo doleriet samestelling. Dit wil voorkom asof daar koperverryking is na die bokant van die ultramafiese pakket in die Ingeli lob. Hierdie patroon stem ooreen met ander studies wat gedoen is op die Insizwa lob en impliseer dat die twee lobbe oorspronklik verbind was. Die heel onderste kumuliet van die Ingeli lob bevat 'n verhoogde kors komponent wat in situ kontaminasie impliseer.

Geen belangrike sulfiedverrykings het in die Basale Sone van die gesteentes van die Ingeli lob voorgekom nie. Die stroomsediment data dui egter wel gelokaliseerde PGE-verryking aan wat die moontlike voorkoms van 'n gelokaliseerde versteekte sulfiedvoorkoms soos die tipe wat by Waterfall Gorge gevind word, aandui. Klein hoeveelhede sulfiedes is geassosieer met die Basale Sone van die Horseshoe lob wat ooreenstem met die Ni-verarming van die oliviene. Die afwesigheid van Co-verarming in die ultramafiese gesteentes van hierdie lob impliseer egter dat enige sulfied-skeidingsgebeurtenis op 'n relatiewe klein skaal plaasgevind het.

DECLARATION

I, the undersigned, hereby declare that the work contained in this thesis is my own original work and has not been previously in its entirety, or in part, been submitted at any university for a degree.

SIGNATURE:

Date:

ACKNOWLEDGEMENTS

The author would like to thank Prof. W.D Maier for his outstanding guidance in this project. Without his academic assistance, motivation and time spent on improvements, this thesis would not have been possible.

I am grateful to my fellow research students Lori Tuovilla, Taffy Gomwe, Adam Bumby and Dr. Ian Graham who contributed in various ways to this thesis. Additionally I would like to thank the technical staff at the University of Pretoria: Marco and Peter in the thin section lab, Maggie Loubscher, Sabine Verryn, and Peter Gräser for his help with understanding the microprobe, and proof reading. The academic staff at UP including: Prof. deWaal, Prof. P. Eriksson, Prof. R. Merkle, Prof. H. Theart and Prof. J. de Villers. I would also like to thank Melinda de Swart and Wiebke Grote for being the glue that binds the geology department at UP. Thanks to Magdel Combrink for translating the abstract into Afrikaans. I would also like to thank Raynard Macdonald for proof reading.

I would also like to thank Set Point Technologies for the analytical work done on the stream sediments.

Thanks are also due to the microprobe staff at Rhodes University. They include Siksha Bramdeo and Dr. Malcolm Roberts who did not give up on me.

I am grateful to Falconbridge Ventures of Africa; their financial support during my studies in Pretoria and in the field was invaluable. My knowledge of the industrial side of geology increased greatly during those months. I would also like to thank Andrew Pedley, of Falconbridge, for his guidance in the stream sediment geochemistry portion of the project.

I would like to thank CERMOD for the financial support given to me and to fellow students at the University of Pretoria and to the quest of bringing industry and academia closer together.

I would like to thank my parents who gave so much more than they could ever know they gave. To my friends who stuck by me through my long absences from their lives.

Lastly I would like to thank the late Glen Ruby, for instilling the love of geology and of the Earth into the soul of my father and to my father who would further instill it in me.

CONTENTS

ABSTRACT.....i

SAMEVATTING.....iii

DECLARATION.....v

List of Contents, Figures, Tables, and Plates.....vi

1. Introduction.....1

1.1 ***Aims and Objectives***.....1

1.2 ***Location of the Field Area***.....1

1.3 ***Climate and Drainage***.....6

1.4 ***General Geology of the Field Area***.....7

1.4.1 Karoo Supergroup.....7

1.4.2 Magmatic Rocks of the Study Area.....9

1.4.3 Mount Ayliff Complex.....10

1.5 Topography, Soils and Overburden, Vegetation, Settlements.....12

1.6 ***Mining History of the Mount Ayliff Complex***.....14

1.7 Methodology.....15

1.7.1 Air Photo Interpretation with Regards to the Ingeli Lobe.....15

1.7.2 Fieldwork.....16

2. Previous Work.....18

3. Petrography.....27

Ingeli Lobe

3.1 Introduction**.....27**

3.2 Basal Olivine Gabbronorite (BOG)**.....29**

3.3 Peridotite Unit (PU)**.....35**

3.4 Central Olivine Gabbronorite (COG)**.....40**

3.5 Central Gabbronorite (CG)**.....43**

3.6 Upper Olivine Gabbronorite (UOG)**.....46**

3.7 Upper Gabbronorite (UG)**.....49**

Horseshoe Lobe

3.8 Introduction**.....52**

3.9 Horseshoe Olivine Gabbronorite (HSOG)**.....53**

3.10 Horseshoe Gabbro (HSG)**.....58**

4. Mineral Chemistry.....61

4.1 Introduction.....61

4.2 Ingeli Lobe.....62

4.2.1 Olivine.....62

4.2.2 Mg# in Orthopyroxene and Clinopyroxene.....64

4.2.3 An in Plagioclase.....64

4.3 Horseshoe Lobe.....65

4.3.1 Olivine.....65

4.3.2 Mg# in Orthopyroxene and Clinopyroxene.....65

4.3.3 An in Plagioclase.....67

4.4 Ni versus Fo content in Olivine.....67

5. Whole Rock Geochemistry.....69

5.1 Introduction.....69

5.2 Binary Variation Diagrams.....69

5.2.1 Major Element Chemistry.....69

5.2.2 Trace Element Geochemistry 73

5.3 Spider diagrams.....80

5.4 Compositional variations against Elevation Above Base.....82

***5.4.1 Ingeli*.....82**

5.4.2 Horseshoe Lobe.....90

6. Stream Sediment Geochemistry.....96

6.1 Introduction.....96

6.2 Sampling Procedure.....99

6.3 Different Methods of Analysis.....101

6.4 Fe and Mn Oxides.....102

6.5 Binary Variation Diagrams.....102

6.6 Pt and Pd.....104

7. Discussion.....106

7.1 Introduction.....106

7.2 Lithological Comparison Between the Different Lobes of the MAC.....106

7.3 The Nature of the Parental Magma.....108

7.4 Interconnectivity of the Lobes of the MAC.....109

7.5 Flow Direction of Magmas in the MAC.....109

7.6 Open or Closed System Crystallization? 114

7.7 The Origin of the Crustal Component.....114

7.8 The Potential for Pulphide Ores; in the Ingeli and Horseshoe lobes, MAC.....115

8. Conclusions.....118

References.....119

ACKNOWLEDGEMENTS

APPENDIX I

APPENDIX II

APPENDIX III

APPENDIX IV

LIST of FIGURES

Fig. 1.1 Locality map of the Mount Ayliff Complex.....2

Fig. 1.2 Location of Tiger Hoek traverse.....3

Fig. 3.1 Classification of igneous rocks (Le Maitre et al., 1989).....30

Fig. 3.2 Stratigraphy of the Ingeli and Horseshoe lobes.....31

Figs. 3.3 (a)-(f) Modal mineral variation versus EAB in the Ingeli lobe...32

1. Introduction

1.1 *Aims and Objectives*

Based on analogies in the geological setting with Ni-sulphide bearing sub-volcanic intrusions at Noril'sk-Talnakh, the Mount Ayliff Complex (MAC) of South Africa has been the focus of extensive exploration efforts by mining companies over the last 80 years. The present study was initiated during the latest such programme, by Falconbridge Ventures of Africa and Impala Platinum, to investigate the petrogenesis and magmatic Ni-sulphide potential of the Ingeli and Horseshoe lobes of the Mount Ayliff Complex. The methods by which these goals have been pursued include:

(i) Lithological, petrographical, and compositional comparison of the Ingeli and Horseshoe lobes to the other lobes of the Mount Ayliff Complex.

(ii) A stream sediment sampling programme around the Ingeli lobe.

1.2 *Location of the Field Area*

The Mount Ayliff Complex is situated on the border between Kwa-Zulu Natal and the Eastern Cape provinces of the Republic of South Africa. The areas of principle interest within the Complex have the following locations: Ingeli lobe (Fig 1.2) centres on 29° 15'E longitude, 30° 36'S latitude, and is located approximately 90 km due west of the town of Port Shepstone, which is on the Kwa-Zulu Natal coast. Figure 1.2 was derived from published data from government geological maps, Maske (1966), field mapping completed by the

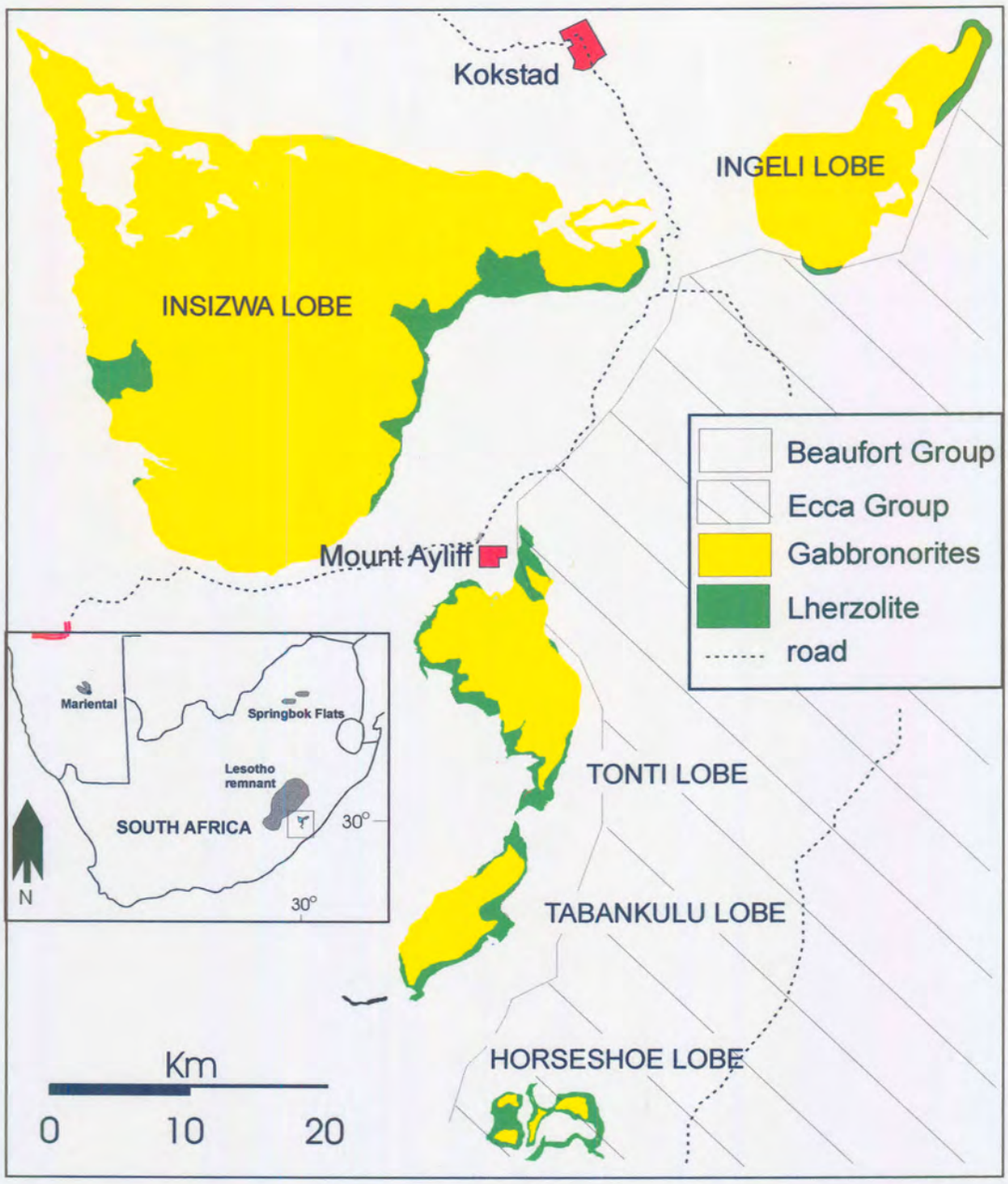

Fig. 1.1 Locality map showing the Mount Ayliff Complex (adapted from Maier et al., 2002).

Figure 1.2: Location of Tiger Hoek Peak Traverse

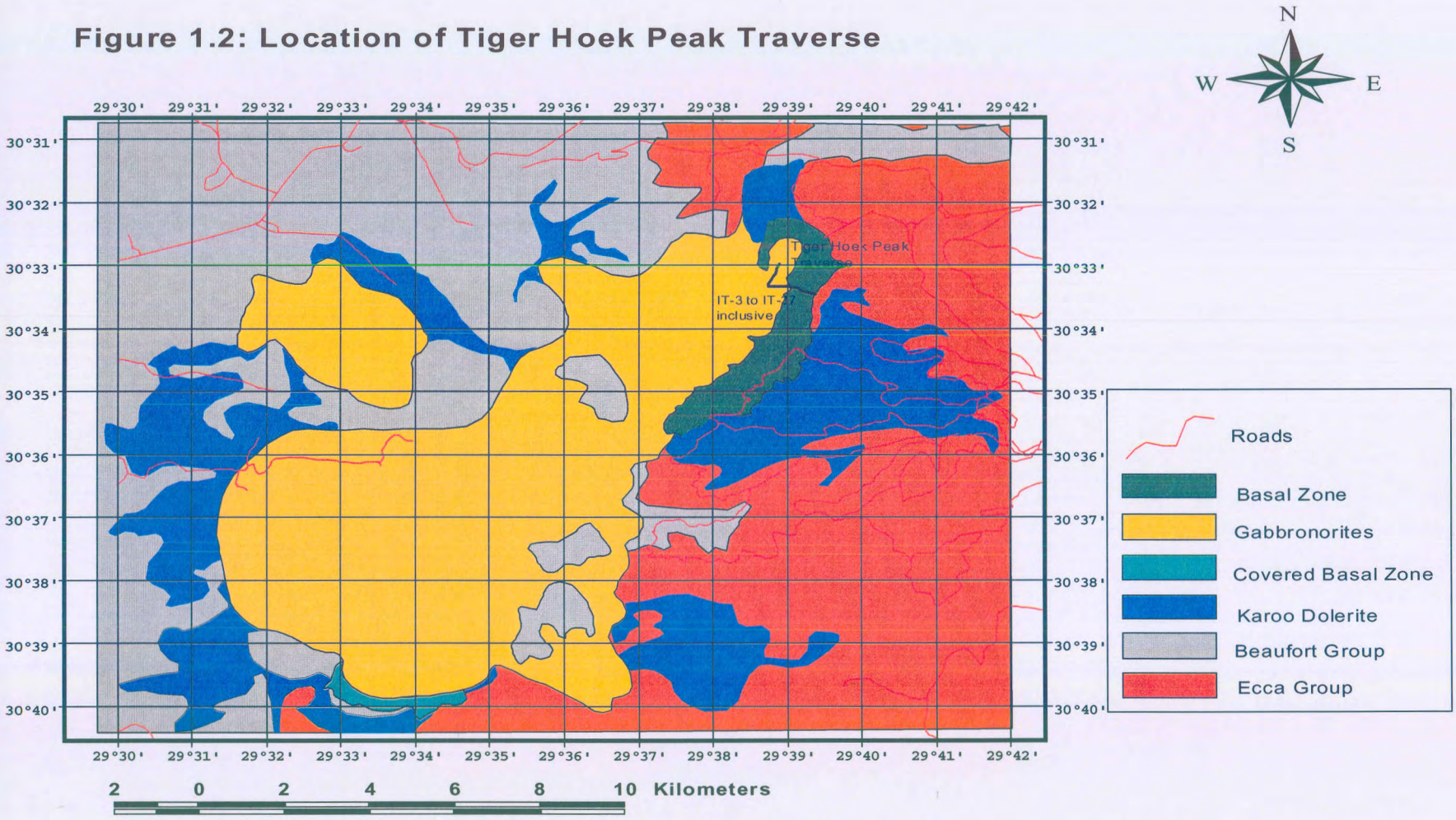

Plate 1: Tiger Hoek peak, Ingeli lobe, viewed from the NE. Distinctive layering is apparent. The analysed traverse is located towards the left of the massif.

Plate 2: The Mzintlava river in the Horseshoe lobe. The Horseshoe sill forms the central light-coloured portion of the mountain face in the centre of the photograph.

Plate 3: Steeply dipping Basal Olivine Gabbronorite in the northwestern part of the Ingeli lobe.

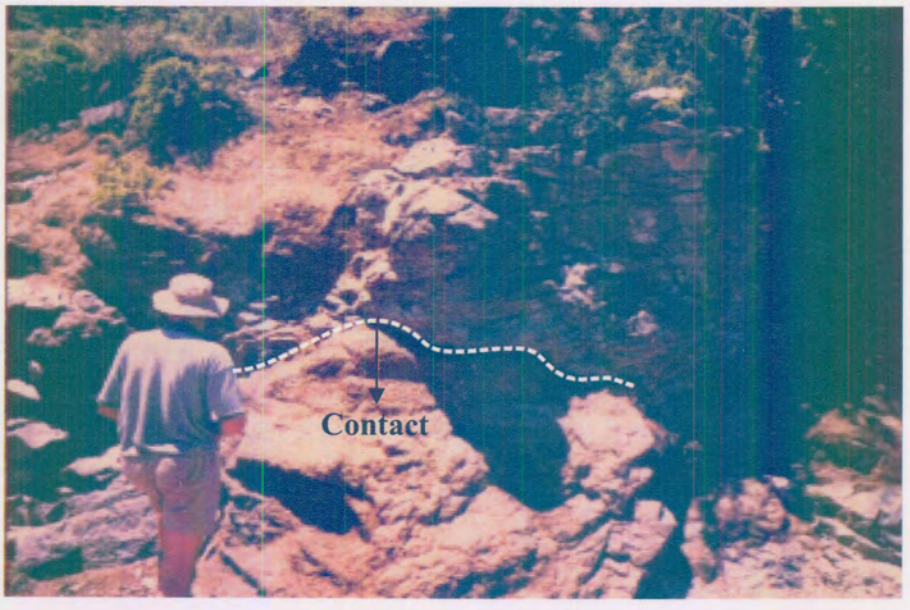

Plate 4: The basal contact of the Horseshoe lobe with the country rock.

author and photogeological mapping. The Insizwa lobe centres on 29° 15'E longitude, 30°45'S latitude and can be found on the following 1:50.000 topographical maps: 3029 CA, 3029 CB, 3029 CC, and 3029 CD. The Insizwa lobe is located some 10 km due west, across Brook's Neck, from the Ingeli lobe. The Horseshoe lobe centres on: 29° 26'E longitude, 31° 35'S latitude.

The Mount Ayliff Complex itself can be found on the following government geological maps at a scale of 1-250,000:

- Umtata (Karpetra and Johnston, 1979) 3128
- Kokstad (Decker, 1981) 3028

1.3 *Climate and Drainage*

The climate in the field area is temperate, with annual precipitation from between 750 mm and 1000 mm per annum. Average temperatures range from 15°C in winter to 32°C in summer. Most of the rains fall from October to April. According to Maske (1966), rock weathering tends to be deep because of high rainfall, and soil cover is thick except on the steepest slopes. This soil cover and high precipitation support lush grassland-type vegetation.

The Mount Ayliff Complex is drained by many perennial and non-perennial streams. These streams are generally first and second order streams, with an occasional third order stream on the shallower slopes. The streams tend to widen out as the angle of the slope decreases and eventually merge "off-lobe" (Pedley, 2000). The larger streams become tributaries that feed the Mtamvana, Mzintlava, Mzimvubu, Umtamvuna, and the Ibisi rivers.

The rivers that are fed by streams of the Ingeli lobe are noteworthy in this study and include; Ibisi, which finds its tributaries from the northwestern portion of the lobe. The streams that drain the western portion of the lobe tend to flow into the Mzintlava River. The streams that drain to the east tend to flow into the Umtamvuna River (Maske, 1966).

1.4 *General Geology of the Field Area*

1.4.1 Karoo Supergroup

According to Tankard et al. (1982), the Karoo Supergroup is a gently dipping structural basin which is filled by sedimentary rocks. Remnants of the sedimentary sequence are preserved in these various countries; Botswana, Malawi, Mozambique, Namibia, South Africa, Swaziland, Tanzania, Zambia and Zimbabwe.

The Karoo Basin became active in the Permo-Carboniferous (280 ma), and accumulated sediments for some 100 million years. The maximum outcrop area of the Permian basins was 4.5 million km². The present outcrop of Karoo rocks is about 300,000 km², with an estimated thickness of 8000 m (Smith et al., 1993).

At the base of the Karoo Supergroup is the Dwyka Formation which consists of tillites that formed when Gondwanaland moved over the South Pole, resulting in major ice sheets (Smith et al., 1993).

A Carbonaceous ocean, fed by melt water, intruded over the sediments left by the retreating glaciation. The subsequent erosion of sediments from the south and the east provided the marine clays and mud stones that would become the Lower Ecca Group. The "Gondwanide" mountains were formed after the subduction of the paleo-Pacific plate. As these mountains eroded, they provided the material that would accumulate in large deltas to become the upper Ecca Group (Smith et al., 1993). The Ecca Group is dominantly argillaceous and reaches a maximum thickness of 3050 m (Maske, 1966). The Ecca shales are low energy indicators, yellow to brown in colour and contain high amounts of clay. When in contact with intrusives they become microcrystalline hornfels, which break in concoidal fracture. Original bedding can often be made out, except in areas of extreme metamorphism.

By the late Permian the climate had warmed and the fluvio-lacustrine sediments of the Beaufort Group were laid down over subsiding alluvial plains (Smith et al., 1993). The arenaceous sediments of the Beaufort Group were deposited during times of desiccation interspersed with times of flooding. The Basin at the time was experiencing a gentle down warping, accelerating the accumulation of approximately 3,400 m of the Beaufort Group sediments (Maske, 1966). The Beaufort sediments are of the same colour as the Ecca sediments, but tend to have higher loam content. When in contact with intrusives, the Beaufort rocks experience a similar metamorphism producing microcrystalline hornfels.

However, being more arenaceous, these sediments tend to produce porphryblasts of alkali feldspar (Maske, 1966).

After the deposition of the Beaufort Group the Molteno Beds, Red Beds, and the Cave Sandstone were deposited (Tankard et al., 1982). The depositional cycle of the Karoo Supergroup ended when the basic magma flows and extensive sub-volcanic intrusions (including the MAC) began, which marked the beginning break up of Gondwanaland. The elevation of the area since the end of the Mesozoic caused the erosion of strata exposing the Mount Ayliff Complex.

1.4.2 Magmatic Rocks of the Study Area

The Karoo Igneous Province is considered one of the largest flood basalt provinces on Earth. The age of the province is estimated to be approximately 182 million years (Marsh et al., 1997). In southern Africa the lavas currently cover some 140,000 km^2. It is thought, however, that the original extent of the lavas was between 1,500,000 and 2,000,000 km^2. These estimates are based on the extent of sub-volcanic dykes, sills and ring intrusions (Marsh et al., 1997). Concordant sills, transgressive sheets, cone sheets, dykes, bell-jar intrusions and laccoliths have all been described in the Karoo Province.

Only the largest intrusive bodies show any form of magma differentiation. The smaller intrusions cooled rapidly enough to create typical Karoo dolerites, consisting of; fine to medium grained, dark gray rock characterized by plagioclase

and ophitic augite. Occasionally samples contain olivine, alkali feldspar and quartz (Walker and Poldervaart, 1948).

Maske (1966) postulated that the magma conduits, leading to the intrusions, were caused by tensional strain that resulted from the subsiding strata of the central basin.

1.4.3 Mount Ayliff Complex

The Mount Ayliff Complex formed from hyper shallow intrusions of magma into the Karoo sedimentary rocks. Maske and Cawthorn (1986) thought that the Complex could represent the eruptive centre that produced the extensive Drakensberg lava flows. It outcrops over some 800 km² in extent and reaches a thickness of some 1200 m. The Mount Ayliff mafic sill contains the most ultramafic cumulates and also the most differentiated rocks in all known occurrences of Karoo dolerites (Bruynzeel, 1957). The Mount Ayliff Complex consists of five distinct lobes including: Insizwa, Ingeli, Tonti, Tabankulu and Horseshoe. The Horseshoe lobe is a fraction of the thickness of the other lobes and is made up of lherzolite overlaid by gabbro. Past authors have hypothesized that the lobes are thought to represent the remnants of a single continuous intrusive sheet that had an original extent of approximately 18,000 km² (Maske and Cawthorn, 1986). Subsequent erosion cut the body and exposed the sedimentary floor rocks between the lobes (Maske and Cawthorn, 1986).

Sander (1996) suggested that the different lobes were fed by the Tabankulu picrite dyke, the Taylor's Koppie olivine gabbronorite dyke and the Insizwa picrite dyke.

Lightfoot and Naldrett (1984) showed that the Complex formed from multiple injections of a low-MgO parental magma of Lesotho-type characteristics. This resulted in the formation of several distinct lithological units e.g. (Lightfoot and Naldrett (1984) after the work of: Scholtz (1936), Bruynzeel (1957), Maske (1966), Lightfoot (1982) and Lightfoot and Naldrett (1984a)):

- *Basal Zone*- consists predominantly of lherzolites, with olivine gabbronorites particularly near the base.
- *Central Zone*- is composed of an olivine gabbronorite
- *Roof Zone*-consists of quartz diorites and monzonites.

All of the exposed mountain masses of the Complex show trough shaped or lower contacts, which dip towards the center of the intrusion by as little as 15° and as much as 40° (Plate 3) (Bruynzeel, 1957). These inward dipping relationships of the lower contact show that the remaining mountain masses could be the preserved remnants of trough portions, while the thinner intervening dome sections have been removed by erosion, making the sheet non-continuous. The upper roof contact with the lower Beaufort sediments has only been preserved in portions of the Insizwa and Ingeli lobes (Maske and Cawthorn, 1986).

The Ingeli lobe is the second largest of the lobes (Plate 1) of the Mount Ayliff Complex. The width of the Ingeli range is 5-6.5 km, and it is approximately 16

km long. The highest elevations range from 1830 m in the north to 2100 m in the southern portion (Maske,1966). Maske also proposed that the Ingeli lobe was fed by magma that flowed laterally from the Insizwa lobe. In contrast, the Horseshoe lobe is the smallest of the lobes of the MAC and is 6-7 km in length and 4-5 km in width (Plates 2, and 4).

1.5 Topography, Soils and Overburden, Vegetation, Settlements

The Mount Ayliff Complex is depicted by areas of high relief that prevail over the surrounding mean average elevation. Slopes in the field area range from gentle rolling slopes to sub-vertical/vertical precipitous cliff lines that dominate the surrounding views. The rugged nature of the topography results from the deeply incised characteristics of the meandering Mtamvuna, Mzimvubu and Mzintlava rivers. The surrounding topography consists of prominent mountains, precipitous cliffs and steep talus strewn slopes (Maske and Cawthorn, 1986). According to Maske (1966), there are five peaks in the Ingeli range over 1830 m. From north to south they are: Tiger Hoek (1855 m), Beestekraal (1948 m), Abergeldie (2146 m), Ingeli (2268 m) and Poholo (2127 m).

In general, the soil cover is less than 1-2 m thick, and usually ranges between a true laterite and a red-podzol. The ultramafic rocks of the intrusion tend to weather in typical sphereoidal weathering forms. This weathering can be as deep as 10 m (Pedley, 2000). Colluvium is best developed on the steeper margins of the lobes and is characterized by angular fragments of gabbro, troctolite (where

applicable) and gabbronorite of the steeper slopes. Fragments such as these tend to be hosted in a sand/clay matrix, which is the weathering product of the intrusion. Creep movements are abundant. While these movements expose fresh rock on the higher slopes, they tend to cover up outcrop in the lower portions (Maske, 1966). In the Ingeli section, the southern extremity is most affected by creep and talus accumulations that cover all the ultramafic rock outcrops.

Over the whole of the basal sections and the intervening valleys the vegetation is dominated by long grass and low scrub. On the wind and rain facing sides of the lobes, indigenous forest sections follow up the stream gorges and into the manmade forest plantations. Two lobes in particular, Ingeli and Insizwa, have their lower slopes on the rain sides covered in plantations. The Weza Plantation of the Ingeli Lobe covers several 100 km^2. These plantations, while giving road access, have grown over large sections of the basal units in both lobes and bring with them pine trees and thorned brush.

The area surrounding the MAC is settled by predominantly Xhosa speaking peoples. Their main livelihood is farming and their settlements and towns are scattered about the base of the lobes. Mount Ayliff is the largest town in the area. Most small settlements are set up around numerous small perennial streams that drain each lobe and often provide road access to the lobes. While the upper slopes lack habitation because of the steepness, they are still used for grazing of sheep, cattle and goats. This grazing helps to expose rock outcrop that would

otherwise have been covered by grasses. Wood gathering occurs in the indigenous forests that follow up the stream gorges.

1.6 *Mining History of the Mount Ayliff Complex*

In 1865, Rudlin, a prospector, discovered the Waterfall Gorge deposit. Later he would claim that he had to abandon the prospect because of "hostilities with the natives" (Maske and Cawthorn, 1986). In 1908, A.L. Du Toit was sent to investigate reports of copper, nickel and platinum. He was sent to the area by the Cape Government, who commissioned him to complete a geological survey for the whole area. This work was completed in 1910 (Maske and Cawthorn, 1986). Du Toit's presence in the area sparked mining and prospecting camps to spring up around the base of the Insizwa lobe. Most of these efforts concentrated on the Waterfall Gorge area and Brook's Adit was driven into the southwestern bank of the stream. The adit was approximately 200 m long and disclosed numerous veins and lenses of massive sulphide as well as disseminated sulphides (Maske and Cawthorn, 1986). Further exploration in the area concentrated efforts on the massive bodies of ore that tended to occur around the contact with the footwall. Because of the patchy nature of the ore, mining operations came to a close by 1915. At this stage, mining had opened some 825 m of adit length, exposing a strike length of some 400 m (Maske and Cawthorn, 1986).

In 1937, thanks to D.L Scholtz's monograph of the deposit (completed in 1936), interest in the area began to unfold again. Prospecting rights were acquired by the

New Witswatersrand Gold Exploration Company and diamond drilling commenced. Some 1273 m of drill core showed negative results and further exploration was abandoned for more than a decade (Maske and Cawthorn 1986). By 1986, five companies had prospected the intrusion and all of them showed negative results. Techniques included: geological mapping, magnetic and electromagnetic geophysical surveys, soil sampling (40,000 samples) and more than 20 boreholes. All effort failed to reveal a deposit of economic importance (Maske and Cawthorn 1986).

In 1996, Falconbridge Ventures of Africa and Impala Platinum took up exploration efforts to see if there may be another mineralized deposit outside of Waterfall Gorge in the Mount Ayliff Intrusion. After nearly five years the joint venture stopped exploration efforts in November of 2000. The reason for the abandonment was that only insignificant and patchy mineralization was encountered associated with the basal contact of the intrusion.

1.7 Methodology

1.7.1 Air Photo Interpretation with Regards to the Ingeli Lobe

The different lithologies of the Complex tend to weather at different rates. This lends itself well to photogeological mapping. Using photogeology, one could effectively determine the boundary between these two lower zones. However, the boundaries between individual intervals of the basal section could not be determined with this technique because the weathering patterns of the Basal

Olivine Gabbronorite and the overlying Peridotite unit are very similar. Both of these units tend to form slopes, while the central and upper units tend to form precipitous cliffs. Another problem encountered when using photogeology on the Ingeli lobe is related to the forestry plantations which may cover up large areas of the Basal Zone. The main advantages in using photogeology in the field where:

(i) Locating possible areas of exposed basal units.

(ii) Locating possible streams that could be used for the stream orientation survey.

1.7.2 Fieldwork

Fieldwork was conducted between August 15th and November 27th 2000. Maps used for the fieldwork were governmental maps that had been digitized by Falconbridge Ventures of Africa. Most fieldwork was conducted on the Ingeli lobe. However, an additional traverse was conducted in the Horseshoe lobe. All samples were taken in situ, and their location was determined using a Global Positioning System. Samples were taken from the base to the top of the intrusion. Samples were taken at regular intervals since most lithological contacts could not be identified in the field because of overburden and gradational contacts.

Stream sediment samples were collected in perennial and non-perennial streams around the Ingeli lobe. These samples where collected "off-lobe", up to within a kilometer of the intrusive. Because it was an orientation survey, samples were collected at the merging of two first-order streams, where possible. Third-order

streams (two second-order streams merging) were left out of the orientation survey. Sediment samples were collected from "traps", behind boulders or on bedrock. Clay and organic-rich areas were avoided. Stream sediment samples were wet sieved down to two size fractions, 250-75 μ, and –75 μ.

2 Previous Work

2.1 Introduction

Most of the work done thus far on the Mount Ayliff Complex centres around the Insizwa lobe. This is mainly because of the occurrence of Ni-sulphides at Waterfall Gorge.

2.2 Insizwa and Tabankulu lobes

The initial work done on the Mount Ayliff Complex was carried out by A.L. Du Toit (1910). He was commissioned by the Cape Government to conduct a geological survey over the area. He hypothesized that four of the five intrusions (Insizwa, Ingeli, Tonti, and Tabankulu) had originally been linked to form a continuous massive sheet.

Scholtz (1936) worked on the Waterfall Gorge occurrence and re-awakened the mining interest in the Mount Ayliff Complex. He also proposed a lithological subdivision of the intrusion, comprising of a Basal Zone, a Central Zone, and a Roof Zone. He suggested that basaltic magma was injected into the Karoo sediments in an area of active subsidence. Vast amounts of lavas were additionally ejected to the surface as the weight of the overlying sedimentary rocks exerted pressure on the growing magma chamber. Thus he suggested that the MAC was formed from at least two (but probably more) synchronous magma pulses. The first influx of magma partially chilled against the contact with the Karoo sediments. From multiple injections of magma, large olivine crystals

accumulated at the base of the chamber to form the Basal Zone. The smaller crystals would be partially or completely reabsorbed and converted to pyroxene. Scholtz went on to suggest that the Complex crystallized as an example of a closed system with a chamber pressure of about 750 atm. With regards to the sulphides found at Waterfall Gorge, Scholtz suggested that sulphide supersaturation was achieved within the magma by the concentration of minute ore components (formerly homogenously distributed throughout the magma) in the upward migrating magmatic differentiate and that the sulphide liquid was able to concentrate in the form of globules. The globules would coalesce and form droplets of sulphide large enough so as to be able to settle through the cumulate pile and interstitial melt, to troughs at the base of the intrusion. The vein-type ores most likely exploited fractures which developed near the floor contact. He further suggested that large amounts of ore could be expected in the lower levels of the intrusion. The disseminated sulphides in the Basal Zone rocks were thought to represent ore droplets that segregated relatively late and were unable to settle through the solidifying cumulates. These droplets would then be held in a state of suspension between the voids of crystalline material.

Bruynzeel (1957) gave a detailed petrographic description of the basal 650 m portion of the Insizwa intrusion at Waterfall Gorge. Seventeen chemical analyses were conducted. Based on the chemical analysis of the chilled rocks, she was the first to suggest that some of the parental magmas to the MAC were of tholeiitic composition close to that of average Karoo dolerite. She suggests that the first

influx of magma was of primary olivine basaltic composition that had been contaminated at depth with sialic material and originally had a tholeiitic character.

Dowsett and Reid (1967) reported on an extensive exploration programme for massive Ni-Cu deposits in the MAC, but conducted no petrographic studies of the rocks.

Cawthorn (1980), Tischler (1981), Cawthorn et al. (1985), and Cawthorn et al. (1992) observed that the chilled margins of the Insizwa lobe are anomalously enriched in MgO compared to other intrusions in the Karoo Igneous Province and concluded that the parental magmas of the MAC were of high-MgO composition. Eales and Marsh (1979) argued that Karoo dolerites that contained greater than 10 % MgO were not representative of true liquids, but contained cumulus olivine. Cawthorn (1980) responded by saying that the low proportion of olivine found by Scholtz (1936) in the chilled rocks with 13.4 % MgO demonstrated that the magmas were not enriched in olivine. Cawthorn et al. (1996) also found magnesium ilmenites in the Basal Zone that are not observed in other Karoo dolerites and used this to back up their arguments. Cawthorn et al. (1992) went on to suggest that the cumulates of the MAC had undergone a "trapped liquid shift". The primary composition of the cumulus olivine was originally (Fo_{84-86}), but reaction with the residual trapped melt shifted this to lower values (Fo_{77-83}). This could account for the reversed differentiation trend in olivine compositions. Cawthorn (1980) and Tischler (1981) argued that the sulphide melt segregated

from the magma because of crustal contamination. They suggested that the association of biotite with sulphide could support the idea that there had been an addition of siliceous material. They cite as evidence the high amounts of SiO_2, Na_2O, and K_2O content in the chilled margins relative to Karoo dolerite. The occurrence of sulphide in the chilled margin was interpreted as evidence for sulphide entrainment from depth. They suggest that the sulphur is most likely magmatic in origin and was not derived from the country rocks.

Lightfoot and Naldrett (1983, 1984b) and Lightfoot and Naldrett et al. (1984a, 1987) favored a low-MgO parental magma of Karoo doleritic composition with 6-7 % MgO, based on the following arguments:

1. The forsterite content of the most Mg-rich olivine is in equilibrium with a low-Mg Lesotho-type parental magma.
2. The lower Basal Zone rocks plot on or near control lines between Karoo dolerite and olivine in terms of most major and trace elements.

The authors postulated that the presence of cumulus olivine caused the compositional variation in the Basal Zone. The increase in modal olivine and Fo contents with elevation in the complex was explained by intrusions of successively less-fractionated batches of magma carrying more suspended olivine. They also suggested that fewer olivine crystals found at the base could be explained by increased supercooling of the magma near the floor. Based on the Ni depletion of the olivines in the Basal Zone rocks of the Tabankulu and Insizwa lobes they suggested there may be large amounts of Ni-sulphides in the floor of

the Mount Ayliff Complex. They dispute the idea of Cawthorn (1980) and Tischler (1981) that there had been significant amounts of crustal contamination. However, they noted that granophyre and hornfels xenoliths are associated with sulphide in the Waterfall Gorge area, although no observed equivalent had been observed at Tabankulu or at Ingeli (Maske, 1966).

Maske and Cawthorn (1986) gave a summary of the mining history in the Mount Ayliff Complex, and reaffirmed the suggestion that there is a high potential for a large Ni-Cu-PGE deposit in the floor of the Complex.

Cawthorn et al. (1986) suggested that at least some of the sulphide could be found at the basal contact of the MAC. They further proposed that the immiscible sulphide liquid did not separate by crustal contamination, as proposed by Cawthorn (1980), and Tischler (1981), but in response to the mixing of compositionally distinct magmas. Isotopic and trace element data was used to determine that multiple intrusions of at least 3 different magma pulses did take place.

Sander and Cawthorn (1996) postulated that there were several hidden feeder dykes below the MAC using geophysical gravity methods. They also suggested that the Insizwa lobe contained significant amounts of hidden Basal Zone rocks that could be a new target for sulphide mineralization. A borehole (INS1) sunk in the central portion of the lobe by Rand Mines confirmed this model by

intersecting 410 metres of Basal Zone rocks. However, no sulphides were encountered in the hole.

Dodd (2000) provides a summary of the results of the exploration efforts of Falconbridge Ventures of Africa from 1995-2000.

Pedley (2000) conducted a stream sediment survey over the eastern margin of the Insizwa lobe and "off-lobe" areas. The purpose of the survey was to assess the suitability of stream sediment geochemistry for the exploration of Cu-Ni-Co and PGE deposits.

Marsh and Allen (2002) suggested that the rocks found within 3 m of the basal contact of the Insizwa lobe (chilled samples) show a wide variation in MgO and olivine contents. This would be consistent with olivine enrichment of a parental magma of Karoo dolerite composition. They found no evidence of a high-MgO parental magma. Geochemical evidence suggests that the Basal Zone olivine gabbronorites and lherzolites found at Insizwa and the gabbronorites of the Central Zone are compositionally different from each other. This was discovered using P/Zr, Sr/Zr, and other incompatible element ratios. They suggested that multiple pulses of magma built the Insizwa lobe. Based on textural and mineralogical evidence, they argued that the rocks of the Central Zone were thermally metamorphosed whereas the rocks of the Basal Zone showed primary igneous textures. This would suggest that the Central Zone rocks were emplaced

before the Basal Zone rocks. Using Sr-isotopes, Marsh and Allen suggest that at least some of the Insizwa magmas were contaminated at depth, but not in situ. However, the initial Sr-Isotope work on the MAC was first conducted by Lightfoot et al. (1984) also suggest this. Incompatible element data from the Central Zone and from Taylor's Koppie Dyke show that the dyke could have been a feeder to the Central Zone rocks. Ni contents of the Taylor's Koppie dyke suggest that the magma may have lost sulphides before emplacement and was not part of the system that fed the Basal Zone rocks. Variable Sr-isotope ratios suggest that the Insizwa lobe was a large open magmatic system that saw repeated injections of fresh magma that deposited cumulate crystals while the melt continued to ascend.

Maier et al. (2002) suggested that if the footwall chill of the Insizwa lobe is representative of the parental magma, then the magma forming the Insizwa lobe was PGE depleted before emplacement and contained no entrained sulphides. However, the magma was not depleted in Ni or Cu, suggesting that major sulphide segregation at depth did not occur. This observation is in contrast to Scholtz (1936) who noted sulphides in the chill, suggesting either variable sulphide contents of the magma, or that sulphides percolated down from above exploiting fractures prior to solidification. The Taylor's Koppie dyke was examined to determine if it was a possible magma conduit to the Insizwa lobe. The exits of conduits into magma chambers are important targets for magmatic sulphide ores (Li and Naldrett, 1998). However, the Taylor's Koppie dyke shows

a much stronger PGE depletion than the Basal Zone cumulates, suggesting that it could not have formed a magma conduit to this zone. Maier et al. (2002) suggest that the distribution patterns of the PGE, including those of the Waterfall Gorge ores, can be explained by segregation of sulphides from magma of the chilled margin composition and that more than one compositionally distinct magma need not be incorporated into the model.

2.3 Ingeli Lobe

Maske (1966) believed that the primary factors responsible for the formation of the Ingeli lobe are as follows:

1. Injection of olivine basaltic magma of Karoo dolerite composition.
2. Freezing of the magma near the contact to the country rocks.
3. Fractional crystallization of early olivine followed by accumulation of the cumulus olivine at the bottom of the chamber, and upward displacement of intercumulus melt. This would have produced a progressively more evolved residual magma.
4. Crystallization of trapped intercumulus liquid within the crystalline mush of the cumulus phases.

Based on the cyclic layering of the lobe, he suggested that the magma chamber was replenished by two distinct magma influxes, similar to the Insizwa lobe. He noted an upward increase in modal proportion of olivine in the Basal Zone rocks of the Ingeli lobe. This, he thought, was caused by decreasing amounts of trapped melt. Using field observations, Maske also suggested that the Ingeli magma was

emplaced laterally from the Insizwa lobe because he found no feeder dyke near the contact of the Ingeli lobe.

Nordin (1987) conducted geochemical soil sampling and whole rock geochemistry for Helmuth Redinger Exploration and Development and for Gencor. He found an increase in Cu contents towards the top of the Basal Zone, similar to that determined by Maier et al. (2002). He proposed that further exploration using I.P. survey should be carried through even though exploration results up to that point had not been positive.

3. PETROGRAPHY

Ingeli Lobe

3.1 Introduction

The rocks in the study areas are classified based on the recommendations of the IUGS Subcommission on Igneous Rocks (Le Maitre et al., 1989) (Fig. 3.1). Figure 3.2 shows the statigraphy of the Ingeli and Horseshoe lobes. The abbreviations used in figure 3.2 include: BOG (Basal Olivine Gabbronorite), PU (Peridotite Unit), COG (Central Olivine Gabbronorite), CG (Central Gabbronorite), UOG (Upper Olivine Gabbronorite), and UG (Upper Gabbronorite). The divisions into rock units are based on petrographic subdivisions based largely on the work of Maske and IUGS. Maske uses the term 'picrite' to describe the PU unit. However, Le Maitre et al. (1989) propose that a picrite is a volcanic rock, and therefore the term Peridotite Unit (lherzolites and dunites in this case) has been adopted here.

The Basal Zone consists of two units, the BOG, and the PU. The BOG is an olivine cumulate rock with intercumulus and minor amounts of cumulus plagioclase (between 10-21 %). The PU rocks are also olivine cumulates, however, they have less plagioclase (<10 %) and they do not contain cumulus plagioclase. However, It-13 does show more than 10 % plagioclase but this could be because the sample is quite altered, making accurate point counting difficult. The COG unit is a gabbronorite, with minor amounts of olivine (6 %). The CG unit is also a gabbronorite but with negligible olivine (<5 %). The UOG unit

consists of gabbronorite with >6 % olivine and the UG unit is an olivine free gabbronorite.

Figures 3.3 (a)-(f) show mineral modes plotted versus EAB. Within the BOG unit, olivine progressively increases in abundance to reach a plateau of about 80 % in the PU. At the same time, plagioclase, orthopyroxene and combined mica, orthoclase and quartz decrease in abundance. Clinopyroxene remains fairly constant in abundance, while combined opaques show a slight increase with height. The four gabbroic units are olivine poor, but some olivine is found in the COG and the UOG. Amongst the other minerals, plagioclase and orthopyroxene tend to decrease with height, while clinopyroxene and combined mica, orthoclase and quartz increase. The abundance of opaques is markedly lower than the Basal Zone. Minor sulphides are observed towards the top of the UG unit.

Table 3.1 lists the abbreviations used in the following plates.

Table 3.1 Abbreviations

Ol = Olivine
Py = Pyroxene
Opx = Orthopyroxene
Cpx = Clinopyroxene
PL = Plagioclase
IPL = Intercumulus Plagioclase
CPL = Cumulus Plagioclase
Sul = Sulphides

3.2 Basal Olivine Gabbronorite (BOG)

This is the basal unit of the intrusion and is in contact with the floor rocks of the Ecca and Beaufort Groups. In some places a fine-grained contact chill is developed at its base. However, at the Tiger Hoek traverse, such a chill was not found. The unit has a thickness of approximately 165 m and makes up roughly 1/3 of the Basal Zone at the Tiger Hoek Traverse. Olivine is the major cumulus mineral, at up to 69.7 volume % of the rock. The other major cumulus phase is chromite, at less than 2.5 % by volume. In some cases, minor cumulus plagioclase may appear (generally less than 2 vol. %.) Plagioclase is the most abundant of the postcumulus phases. Additional postcumulus phases include, in order of decreasing abundance, orthopyroxene, clinopyroxene and mica. In rare cases, interstitial sulphides are also found, the bulk of which is pyrrhotite. Interstitial plagioclase, orthopyroxene and clinopyroxene can all show a poikilitic texture, enclosing both olivine and chromite.

Olivine

The cumulus olivine crystals tend to be equigranular. Rare exceptions of large grains of olivine can exceed 3 mm. However, most of the olivine grains average between 0.7 mm to 1.3 mm in size. Most of the grains are subhedral, but euhedral grains are not uncommon. Well-formed crystal faces of olivine tend to occur when olivine is in direct contact with plagioclase (Plate 5). All of the olivine grains are fractured and in some cases alteration products have formed along the

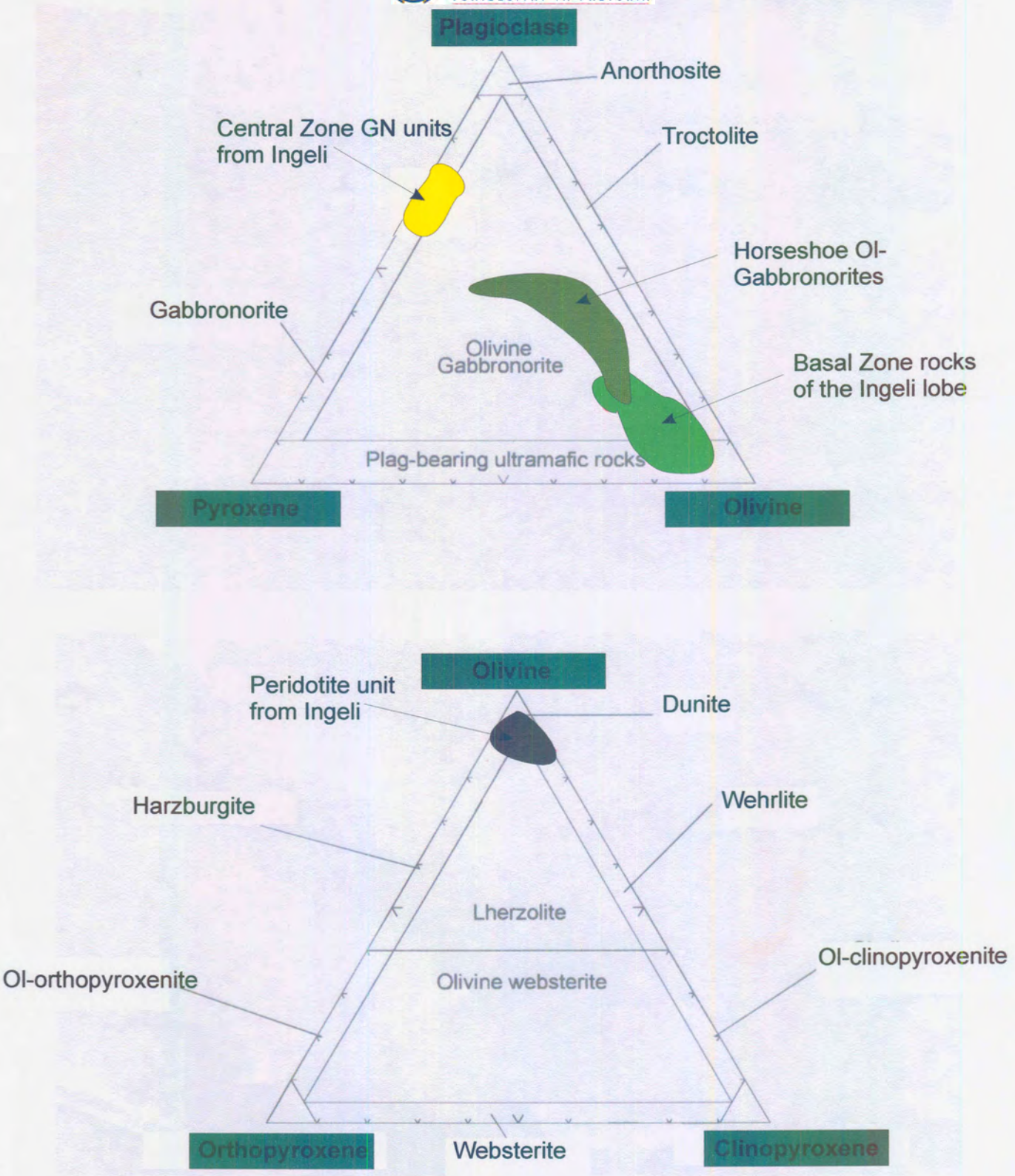

Fig.3.1 Classification of igneous rocks of the Ingeli and Horseshoe lobes, MAC. Classification based on IUGS Subcommission on Igneous Rocks (Le Maitre et al., 1989)

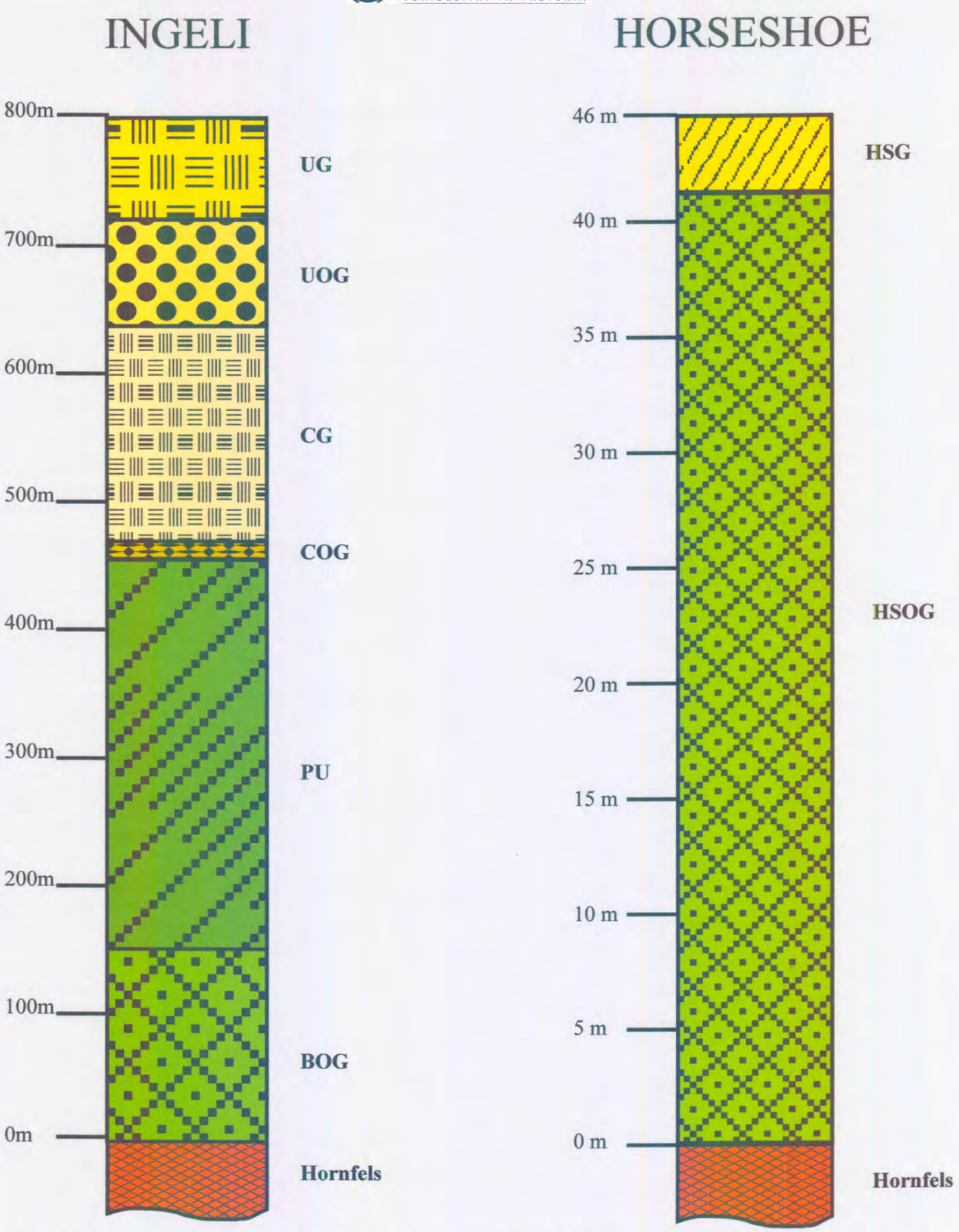

Fig. 3.2 The statigraphy of the Ingeli and Horseshoe lobes, MAC. The two profiles have different scales because the Horseshoe lobe is only a fraction of the thickness of the Ingeli lobe.

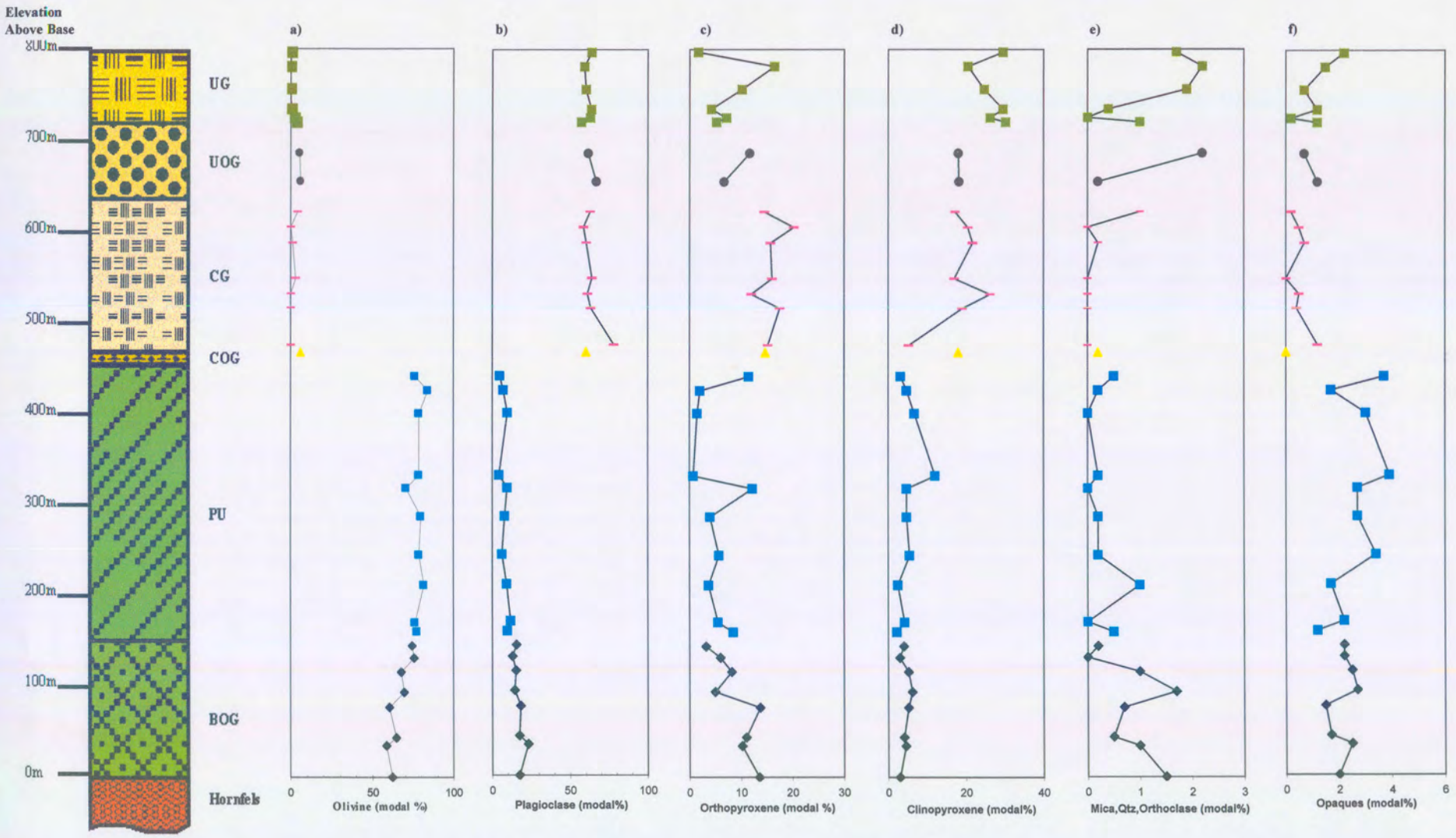

Figs. 3.3 (a)-(f): Modal mineral variation versus EAB in the Ingeli lobe

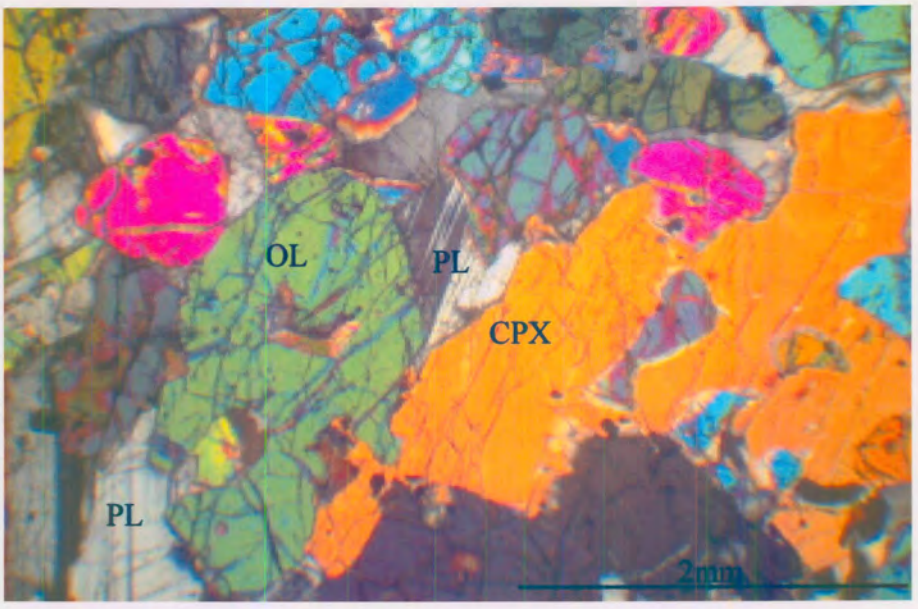

Plate 5: Photomicrograph of typical BOG (sample It-3). Plagioclase shows both a cumulus and intercumulus habit in this unit. Note inclusion of plagioclase in olivine.

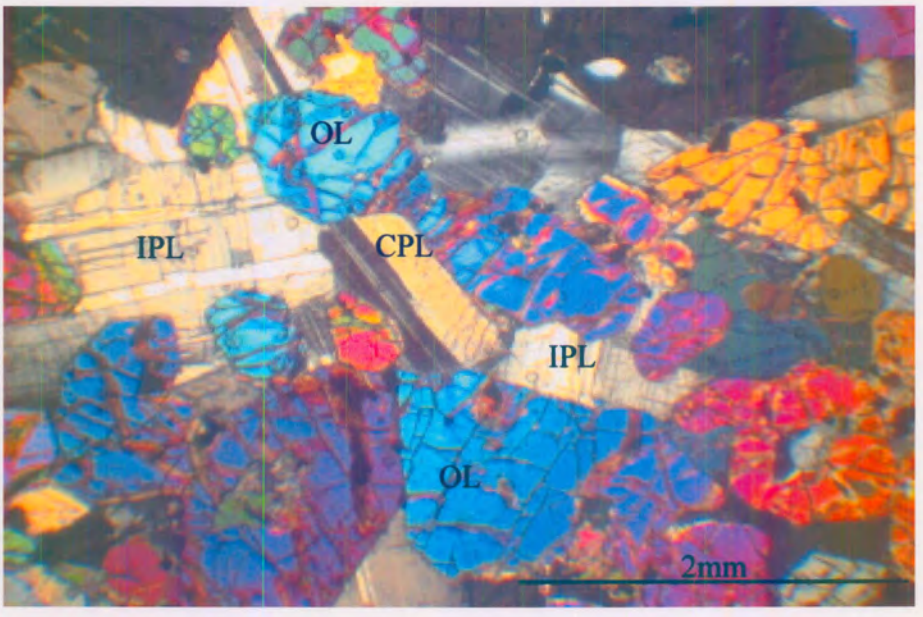

Plate 6: Photomicrograph of typical BOG (sample It-4). Plagioclase shows cumulus and intercumulus habit. Note that olivine in conctact with plagioclase is euhedral.

fracture planes. In some cases, mica, chromite, plagioclase and clinopyroxene were found to be completely included in olivine (Plate 6).

Chromite

Chromite is commonly euhedral or subhedral, with octahedral crystal shapes. Most grains are smaller than 0.1 mm. Chromite grains are commonly associated with or included in olivine in this rock and the overlying peridotite unit, indicating that it was an early crystallization phase. Additional chromite occurs enclosed by interstitial plagioclase and pyroxene.

Plagioclase

Cumulus plagioclase tends to occur as subhedral elongated laths. Most commonly, they are 2/3 mm to 1 mm in length and are roughly ½ mm wide. Intercumulus plagioclase is the most abundant postcumulus phase, at an average modal percentage of between 16-17 %. Grains average from 0.7 mm to 1.5 mm in size. In some cases, plagioclase can form oikocrysts between 2-3 mm in size, which can enclose olivine and chromite grains.

Orthopyroxene

Orthopyroxene tends to make up approximately 12 % of the volume of the rock. This phase is more likely to form oikocrysts than the plagioclase. Most grains have an average size of 1 mm, but large oikocrysts can reach 2-3 mm in size. Clinopyroxene exsolution lamellae and blebs are common throughout the mineral.

Clinopyroxene

Intercumulus clinopyroxene makes up approximately 4-5 % of the volume of the rock. It can be found either as oikocrysts up to 3-4 mm in size, or as interstitial fillings between olivine grains. Clinopyroxene tends to be unaltered and less fractured than olivine and orthopyroxene.

Accessory Minerals

Mica can be found as rims around sulphide blebs, and can also exist as isolated flakes throughout the unit. Sulphides, mainly pyrrhotite and rare chalcopyrite, make up nearly 2 % of the volume of the unit. The sulphides occur as disseminated blebs that are associated with postcumulus phases. They are often in contact with mica flakes.

3.3 Peridotite Unit (PU)

The Peridotite Unit makes up the thickest rock package in the Ingeli Lobe, at approximately 300 m. Olivine is the major cumulus phase and comprises 78-80 % of the rock. Apart from olivine, the most abundant cumulus phase is chromite, which in some cases can reach over 3 % of the rock. There is relatively little cumulus plagioclase, usually less than 0.5 % of the rock. Plagioclase is the most abundant intercumulus phase at approximately 10 % on average. The next most abundant intercumulus phase is orthopyroxene, at about 7 % on average and

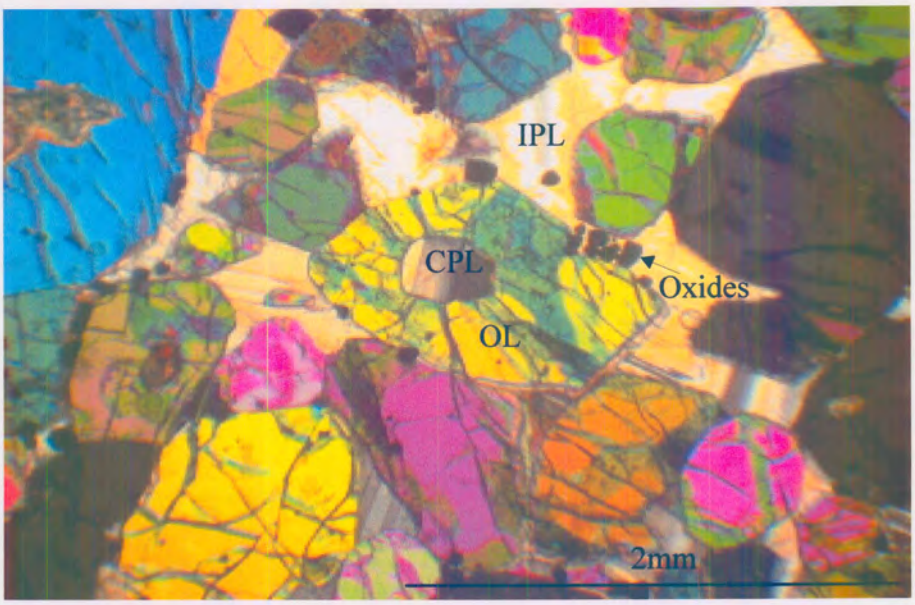

Plate 7: Photomicrograph of typical PU (sample It-15). Photo shows subhedral olivine grain in centre surrounded by intercumulus plagioclase and subhedral oxides. Note the inclusion of plagioclase in olivine.

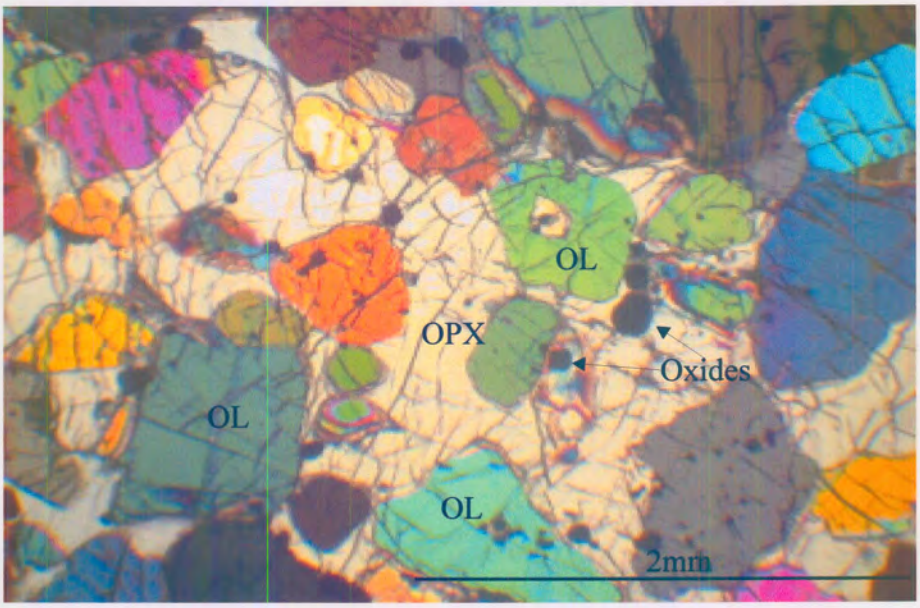

Plate 8: Photomicrograph of typical PU (sample It-16). Photo shows interstitial orthopyroxene oikocryst enveloping cumulus olivine and oxide grains.

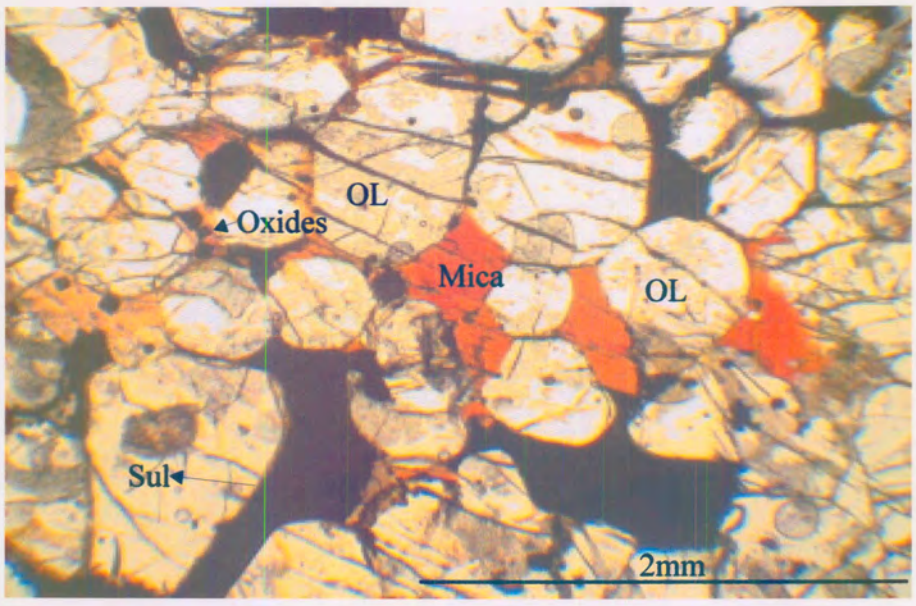

Plate 9: Photomicrograph of the PU in ppl (sample It-15). Note association between biotite, sulphides, and oxides.

ranging between 0.7 % and 12 %. Intercumulus clinopyroxene normally averages 4-5 % by volume, but in one sample reached 12 % by volume. Mica makes up less than 0.5 % of this rock unit. Irregular grains of sulphides are often associated with mica, and can make up to 2 % of the rock. Intercumulus plagioclase, orthopyroxene and clinopyroxene can all occur as oikocrysts, enclosing olivine and oxides.

Olivine

Olivine grains are equigranular, euhedral and subhedral, and normally range in size from 0.7 mm to 1.3 mm, but in some case may reach 3-4 mm in size. Olivine grains show no apparent preferred orientation even though the largest grains may show elongation. The grains are all highly fractured, and some show serpentine alteration along fracture planes. Inclusions in olivine include: chromite, mica, pyroxenes and rare plagioclase (Plate 7). When olivine is included in oikocrysts of orthopyroxene the olivine grains tend to be anhedral. Whereas olivine included in plagioclase, tends to be euhedral (Plate 7). In rare cases, fluid inclusion trails can be seen across olivine grains.

Chromite

Chromite can be found throughout the unit. It is found included in all major rock forming phases. However, grains tend to be smaller when included in olivine (0.1-0.15 mm) as opposed to being included in plagioclase and pyroxene (> 0.3 mm) (Plate 8).

plagioclase

Plagioclase found in the peridotite unit normally exists as large oikocrysts that can be over 3 mm in diameter. These oikocrysts mainly include olivine and chromite. Plagioclase can also be found to fill the interstices between other phases. Cumulus plagioclase is rare.

Orthopyroxene

Large orthopyroxene oikocrysts are common in this rock unit (Plate 8). These anhedral grains can reach sizes of 5-7 mm in diameter and can encompass many olivine and chromite chadacrysts. Orthopyroxene may also occur as reaction rims around olivine. Orthopyroxene almost always shows clinopyroxene exsolution lamellae and blebs. In some cases, orthopyroxene does not form oikocrysts, but instead fills interstices between olivine grains. In these cases, the grains may be much smaller, approximately 1 mm in size.

Clinopyroxene

This phase may comprise 4-5 % of the rock and occurs as oikocrysts that enclose olivine and chromite chadacrysts. In rare cases, it can also envelop plagioclase. The oikocrysts are generally smaller than those of orthopyroxene and average from 0.7 mm to 1.5 mm. However, some large grains do exist and can be over 5 mm in size. In some cases, olivine has a reaction corona with the clinopyroxene and zoning has occurred in the clinopyroxene grain.

Accessory Minerals

Sulphides are concentrated midway through the unit where they can reach 2 modal % in abundance. In the remainder of the unit, sulphides make up between 0 and 0.7 modal % of the rock. Sulphides and mica are commonly found associated (Plate 9), but mica is less abundant than in the underlying unit and now represents less than 0.5 % of the rock.

3.4 Central Olivine Gabbronorite (COG)

This is a relatively thin package of rocks with a thickness of approximately 10 m. Maske (1966) described a troctolite unit directly overlying the peridotite unit. No such unit was encountered at the Tiger Hoek traverse, but whether this was due to lack of outcrop remains unclear. The unit is composed mostly of cumulate plagioclase making up some 60 % of the total volume of the rock. Unlike the underlying units, the COG contains no cumulus chromite, the only other cumulus phase being olivine at about 6 modal % of the rock. The most abundant postcumulus phase in this unit is clinopyroxene, which can account to 18 % of the rock. Intercumulus orthopyroxene accounts for another 14-15 %, on average. Mica and sulphides are rare and can account for 0.2 % of the unit.

Plagioclase

Cumulus plagioclase grains are roughly equigranular. Laths average 0.7 mm to 1 mm in length, and rarely up to 2 mm. Most laths are euhedral or subhedral. Small fracture planes exist and normally cut across the C-crystallographic axis,

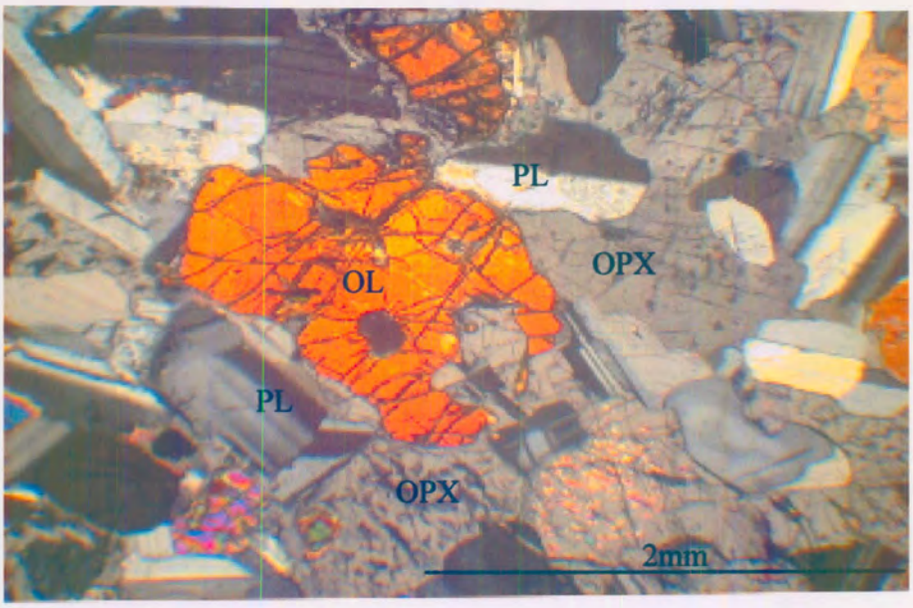

Plate 10: Photomicrograph of the COG (sample It-22). Photo shows cumulus olivine surrounded by cumulus plagioclase, and intercumulus orthopyroxene.

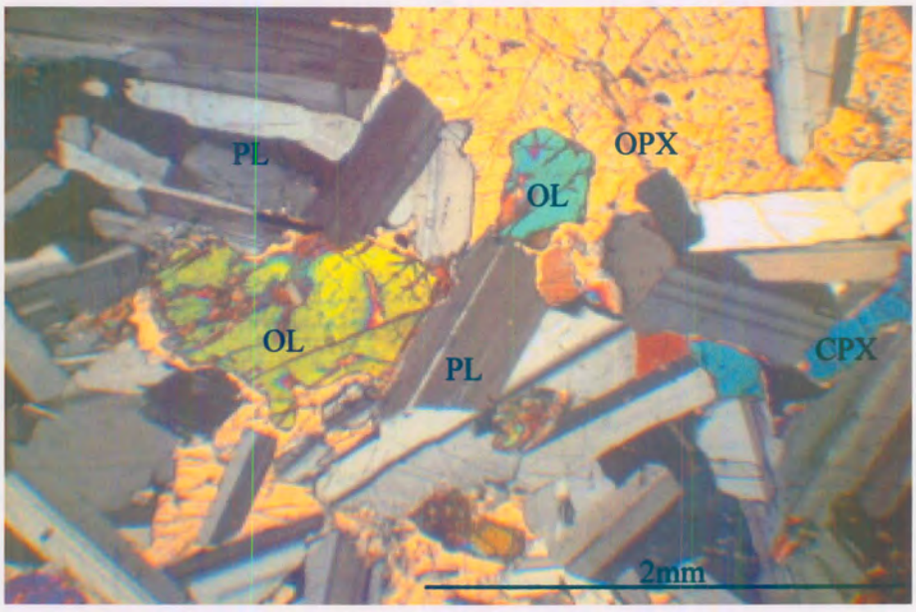

Plate 11: Photomicrograph of the COG (sample It-22). Photo shows olivine grains surrounded by cumulus plagioclase, and intercumulus orthopyroxene.

often at angles as high as 45°. Of all phases observed, plagioclase shows the least amount of internal alteration. No preferred orientation of plagioclase has occurred, so no flow direction is apparent.

Olivine

Olivine grains are equigranular and range from 0.5 mm to 1.3 mm in size. Olivine tends to be anhedral and well rounded. Grains tend to be heavily fractured. Olivine is almost always associated with pyroxenes (Plates 10 and 11), and is often in direct contact or even surrounded by them. Olivine is generally free of other mineral inclusions except in one rare case where plagioclase and mica inclusions were found in separate grains. In some cases alteration products such as serpentine are found along the fracture planes of olivine.

Clinopyroxene

This mineral tends to fill interstices between plagioclase laths. Clinopyroxene can often form an interconnecting network of grains associated with orthopyroxene. The grains vary in size, but most are in the range of 0.5-0.7 mm. Cumulus clinopyroxene was not found. Often grains of clinopyroxene are rimed by orthopyroxene.

Orthopyroxene

Orthopyroxene also fills interstices between plagioclase grains. However, unlike clinopyroxene, orthopyroxene can make up oikocrysts of up to 4 mm in size.

Most grains, however, do not form oikocrysts, and range from 0.5 mm to 0.7 mm. Orthopyroxene is often in contact with both olivine and clinopyroxene. Orthopyroxene usually contains clinopyroxene exsolution lamellae and blebs.

Accessory Minerals

The main accessory phase in this unit is mica. Mica makes up a very small percentage of the rock, and is generally associated with pyroxenes. Most grains are smaller than 0.3 mm. In one sample, mica was found as an inclusion in an olivine grain.

3.5 Central Gabbronorite (CG)

This unit is approximately 73 m thick. Plagioclase is again the major cumulus phase with modal percentages up to 78.2 modal %. However, in most samples plagioclase averages 61 modal %. Olivine can reach up to 4 % by volume and the occasional rare magnetite can also be found in modal percentages from 0.2-0.5 %. The most abundant postcumulus phase is clinopyroxene, which can make up as much as 26 % of the rock however, clinopyroxene can also be found in a cumulus state (Plate 12). Orthopyroxene makes up most of the remainder of the intercumulus phases, and is present in quantities of 12-18 %. Other phases are rare, with mica making up less than 0.2 % and sulphides less than 1 %.

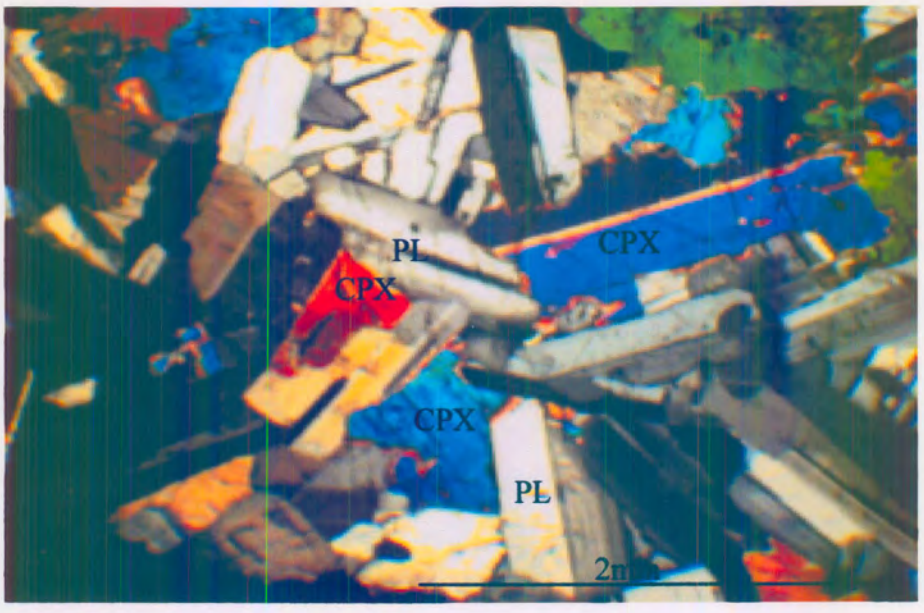

Plate 12: Photomicrograph of the CG (sample It-25). Photo shows cumulus plagioclase, cumulus clinopyroxene, and intercumulus clinopyroxene..

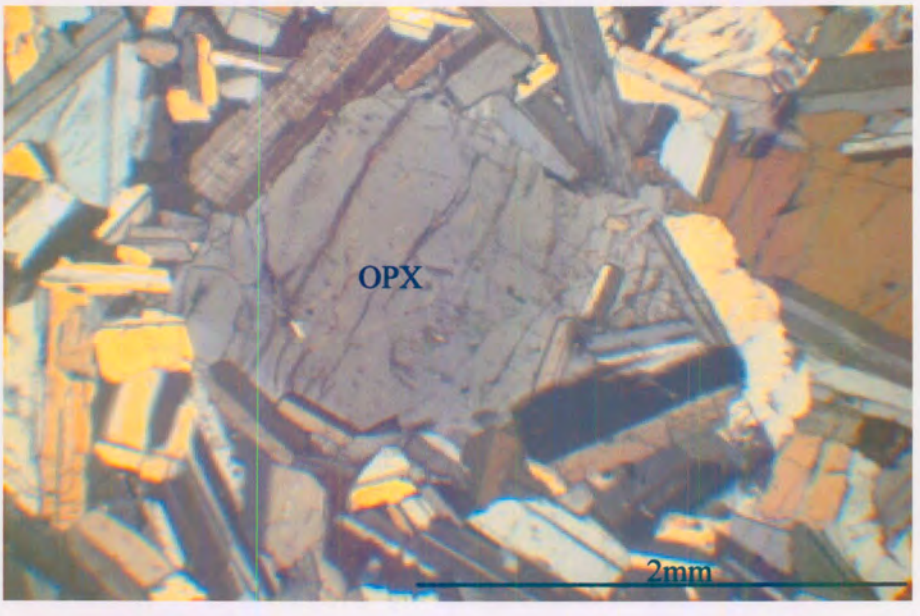

Plate 13: Photomicrograph of the CG (sample It-28). Photo shows large orthopyroxene grain, surrounded by cumulus plagioclase.

Plagioclase

Cumulus plagioclase grains are equigranular and euhedral or subhedral. Their well-formed crystal laths range in size from less than 0.7 mm to greater than 2 mm. Grains are arranged in a random manner with no predominant orientation being observed (Plate 13). Small fracture planes are often found to cut across the laths. Anhedral grains are rare and the size of those grains tends to be small by comparison with the rest of the plagioclase in the unit.

Olivine

Olivine only occurs in two samples. The grains are equigranular and range from 0.7 mm to 1.5 mm. They are subhedral and anhedral, and commonly enclose small plagioclase laths. Olivine grains are always in contact with either clinopyroxene or orthopyroxene. Grains tend to be heavily fractured, and fracture planes are commonly filled by alteration products. Small amounts of mica are also found to exist around the margins of heavily altered olivine grains.

Clinopyroxene

The mineral tends to fill the triangular voids between plagioclase grains. Most of the grains are anhedral and relatively small averaging between 0.7 mm to 1 mm. The grains are often associated with large orthopyroxene oikocrysts even though the clinopyroxene itself does not tend to form oikocrysts in this unit. Some clinopyroxene occurs as cumulus grains. These grains tend to be smaller, at less

than 0.7 mm, subhedral and form stumpy prisms and laths. The grains tend to show simple twins. Most clinopyroxene grains have rims of orthopyroxene.

Orthopyroxene

This phase characteristically forms large anhedral grains that can exceed 3 mm in diameter. Small plagioclase laths that do not exceed 0.3 mm in size often penetrate these grains producing a sub-ophitic texture. In the stratigraphically elevated portion of the unit, the orthopyroxene tends to fill in interstices between plagioclase and clinopyroxene laths. Exsolution lamellae and blebs of clinopyroxene in the orthopyroxene are common throughout the unit.

Accessory Minerals

Mica flakes are extremely rare (<0.5 %) and are sometimes found to associate with equally rare, small interstitial blebs of sulphide.

3.6 Upper Olivine Gabbronorite (UOG)

This unit is approximately 32 m thick. Cumulus plagioclase is the major phase in this rock unit and constitutes up to 66.9 modal % of the minerals. Olivine is the next most abundant cumulus phase, and can make up 5.5-6 % of the rock. Clinopyroxene is the most abundant postcumulus phase and averages 17 % of the unit. Orthopyroxene is the other major postcumulus phase and ranges from 7-12 modal % of the unit. Minor amphibole, mica and sulphides are also found within

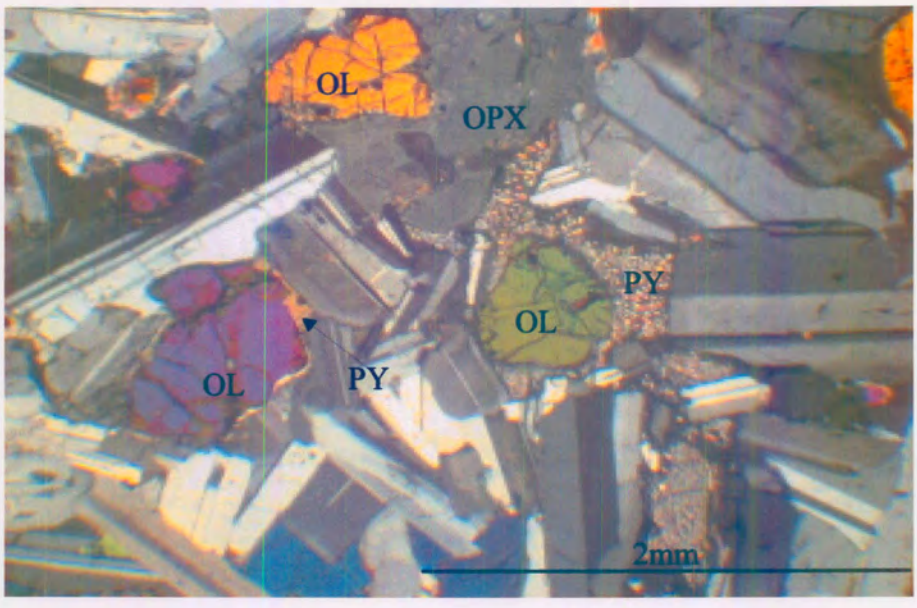

Plate 14: Photomicrograph of the UOG (sample It-30). Photo shows olivine grains surrounded by cumulus plagioclase, and intercumulus pyroxene.

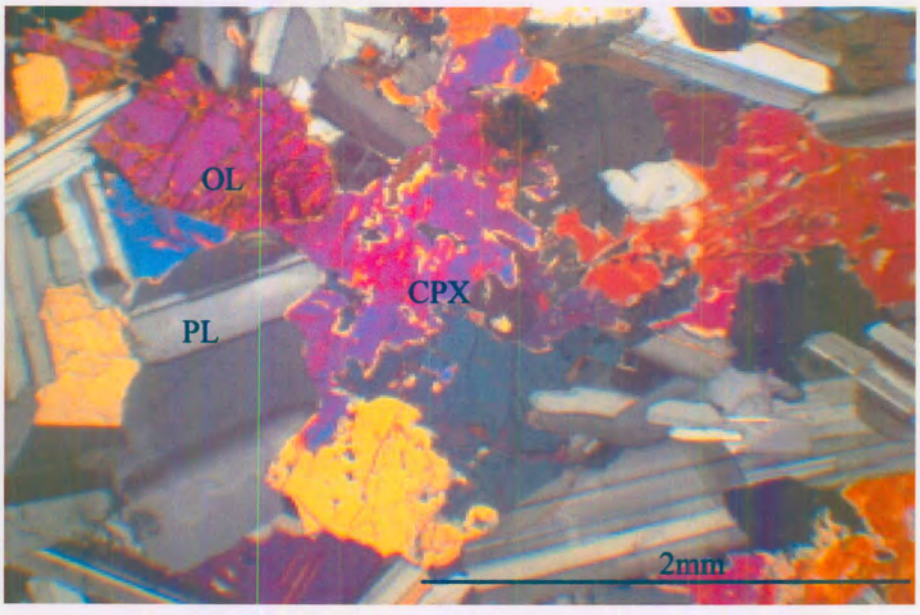

Plate 15: Photomicrograph of the UOG (sample It-31). Photo shows olivine surrounded by cumulus plagioclase, and interlocking interstitial clinopyroxene grains.

the unit, but in abundances of less than 1 %. Alkali feldspar occurs in abundances that average less than 1.5 %.

Plagioclase

The mineral occurs as euhedral and subhedral laths, up to 2 mm in diameter and averaging 0.7 mm in length. In general, the plagioclase grains seem smaller and more euhedral than in the underlying rock unit.

Olivine

Olivine tends to be equigranular, and grains average approximately 1.3 mm in diameter. In rare cases they are smaller than 0.5 mm. Olivine crystals tend to be anhedral, and are always connected in some fashion to a pyroxene grain (Plate 14). Some olivine grains are wholly enveloped by pyroxenes. Olivine tends to be highly fractured, and alters to serpentine along fracture planes and around grain margins. Plagioclase, amphibole, clinopyroxene and mica form inclusions in olivine.

Clinopyroxene

Clinopyroxene tends to form small interlocking anhedral grains. These interconnected grains pierce though the interstices of plagioclase grains, and form an interlocking network of crystals. Most of these smaller grains average 0.7 mm in diameter, but some grains reach 2 mm in diameter.

Orthopyroxene

Orthopyroxene tends to form large oikocrysts that can be over 3 mm in diameter. The mineral tends to associate with olivine, and can be found to form coronas around olivine grains. Most orthopyroxene contains exsolution lamellae and blebs of clinopyroxene. In some cases, orthopyroxene shows a graphic intergrowth with clinopyroxene.

Accessory Phases

Mica flakes and sulphides tend to be associated although neither is very abundant in this rock unit. Alkali feldspar becomes more predominant towards the top of this unit, but never exceeds 2.2 % by volume. No quartz was found in this unit.

3.7 Upper Gabbronorite (UG)

The upper most 127 m of the traverse consists of the upper gabbronorite unit. Plagioclase remains the dominant cumulus mineral phase averaging between 57.2 –63.9 modal %. Olivine is the next most abundant cumulus phase and can form up to 3.7 modal % of the rock. Clinopyroxene is the most abundant postcumulus phase, contributing between 20-30 modal %. Orthopyroxene is the other important postcumulus phase, which can be found in quantities from 2-16 modal %. Magnetite, as well as sulphides, alkali feldspar, amphibole and quartz are accessory phases.

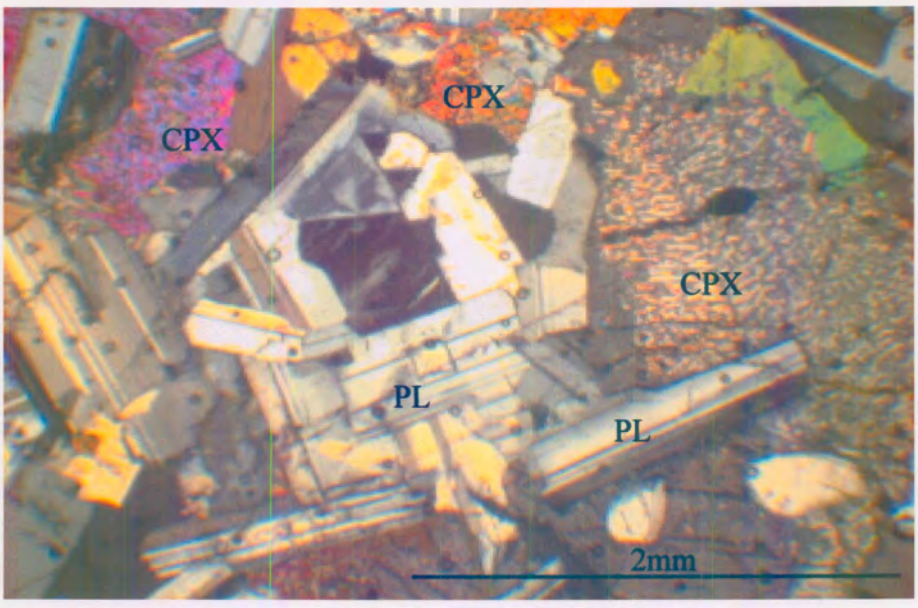

Plate 16: Photomicrograph of the UG (sample It-35). Photo shows plagioclase cumulate with clinopyroxene. The clinopyroxene on the right shows a "herring bone" texture.

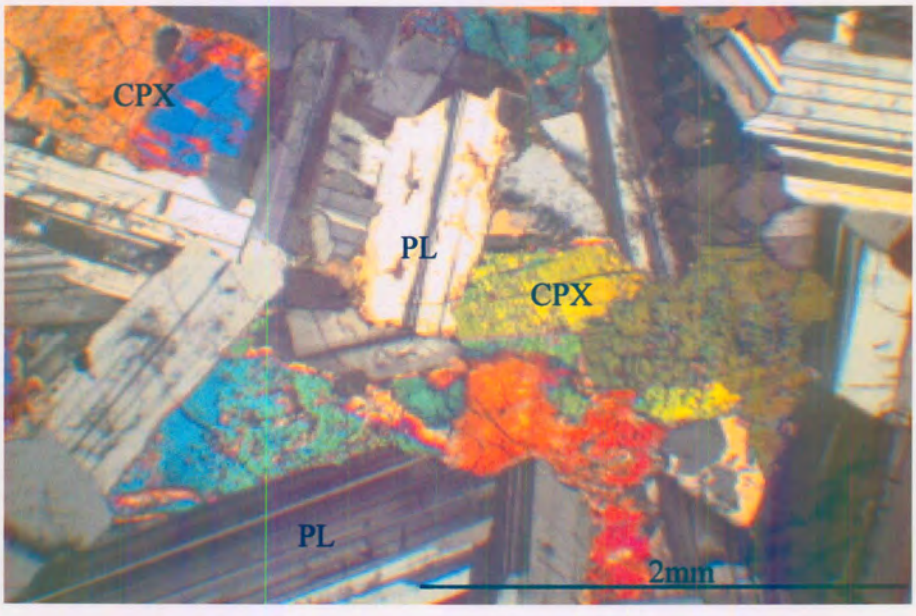

Plate 17: Photomicrograph of the UG (sample It-37). Photo shows apparent size increase of the cumulus plagioclase grains at the top of the Ingeli lobe.

Plagioclase

A characteristic feature of this unit is that the cumulus plagioclase laths have become larger (Plate 17). This lends to a coarser grained rock unit than the underlying units. Plagioclase laths normally average 1.5 mm in length, reaching 2.5 mm in some cases. The grains are mostly subhedral, but some of the smaller grains maybe anhedral. Microfracturing tends to cut across the C-axis of some laths. No preferred orientation was found in plagioclase. No interstitial plagioclase was found.

Olivine

Olivine is rare in this unit, making up less than 1 %. The few grains found range from 0.7 mm- 2 mm in length. The larger ones often enclose small laths of plagioclase. Olivine grains tend to be heavily altered to serpentine and fractured. Often these grains are surrounded by orthopyroxene coronas, which maybe altered to mica or amphibole.

Clinopyroxene

Clinopyroxene grains tend to occur as large anhedral interlocking crystals, 2-3 mm in size. Grains can also occur as small isolated grains, as in the underlying unit. Many of the grains are pervasively altered, and rims of orthopyroxene are found around most specimens. Alteration of both types of pyroxenes, to form secondary amphibole and mica, becomes progressively more intense in the higher stratigraphic levels.

Orthopyroxene

Orthopyroxene generally forms grains from 0.7 mm to 1.3 mm in diameter. They generally fill interstices between plagioclase grains. They are subhedral and anhedral, and commonly form coronas around olivine grains. They generally are intergrown with clinopyroxene and have clinopyroxene exsolution blebs and lamellae forming a "herring-bone" texture (Plate 16).

Accessory Phases

Sulphides, mica, and amphibole are found throughout the layer. Sulphides can reach up to 2.2 modal %. Mica is commonly associated with sulphides and amphibole, and is often an alteration product of clinopyroxene. Oxides are more prevalent in the lower portion of the layer, where they are normally associated with olivine. Minor quartz grains up to 1 mm in length are also found. Rare alkali feldspar forms graphic intergrowths with quartz.

Horseshoe Lobe

3.8 Introduction

The Horseshoe lobe is made up of two lithological units, the Horseshoe olivine gabbronorite (HSOG), and the Horseshoe gabbro (HSG) with less than 5 % opx (Fig. 3.2). The HSOG makes up the bulk of the intrusion, and is very similar in terms of mineral modes to the BOG unit in the Ingeli lobe.

Figures 3.4 (a)-(e) show modal mineral percentages through the Horseshoe intersection. As seen at the Ingeli lobe, olivine shows a slight increase in abundance with height. As in the Ingeli lobe, modal plagioclase shows an inverse behaviour to olivine. Orthopyroxene and clinopyroxene show little variation through the HSOG. The HSG has almost no orthopyroxene but close to 40 % clinopyroxene. This is broadly similar to the UG unit of the Ingeli lobe. This could possibly suggest that the PU, COG, CG and the UOG units of the Ingeli lobe are not developed at Horseshoe.

3.9 Horseshoe Olivine Gabbronorite (HSOG)

The Horseshoe olivine gabbronorite unit makes up approximately 90 % of the Horseshoe lobe. Olivine is the major cumulus phase with the exception of the uppermost sample of this unit where plagioclase becomes the major cumulus phase. Olivine makes up between 40 and 60 % of the phases in the unit, but the uppermost sample only contains 20 modal % olivine. Throughout the unit there are varying amounts of cumulus and intercumulus plagioclase ranging between 17 and 40 %. Except for the top sample, intercumulus plagioclase is more common than the cumulus variety. Orthopyroxene is the next most abundant intercumulus phase from 10 to 18 modal %. Clinopyroxene varies dramatically in modal percentage from 0 to 21 %. Chromite is not as abundant as in the Ingeli lobe. Most grains are associated with olivine. Mica is present in small amounts, and commonly encloses sulphide blebs.

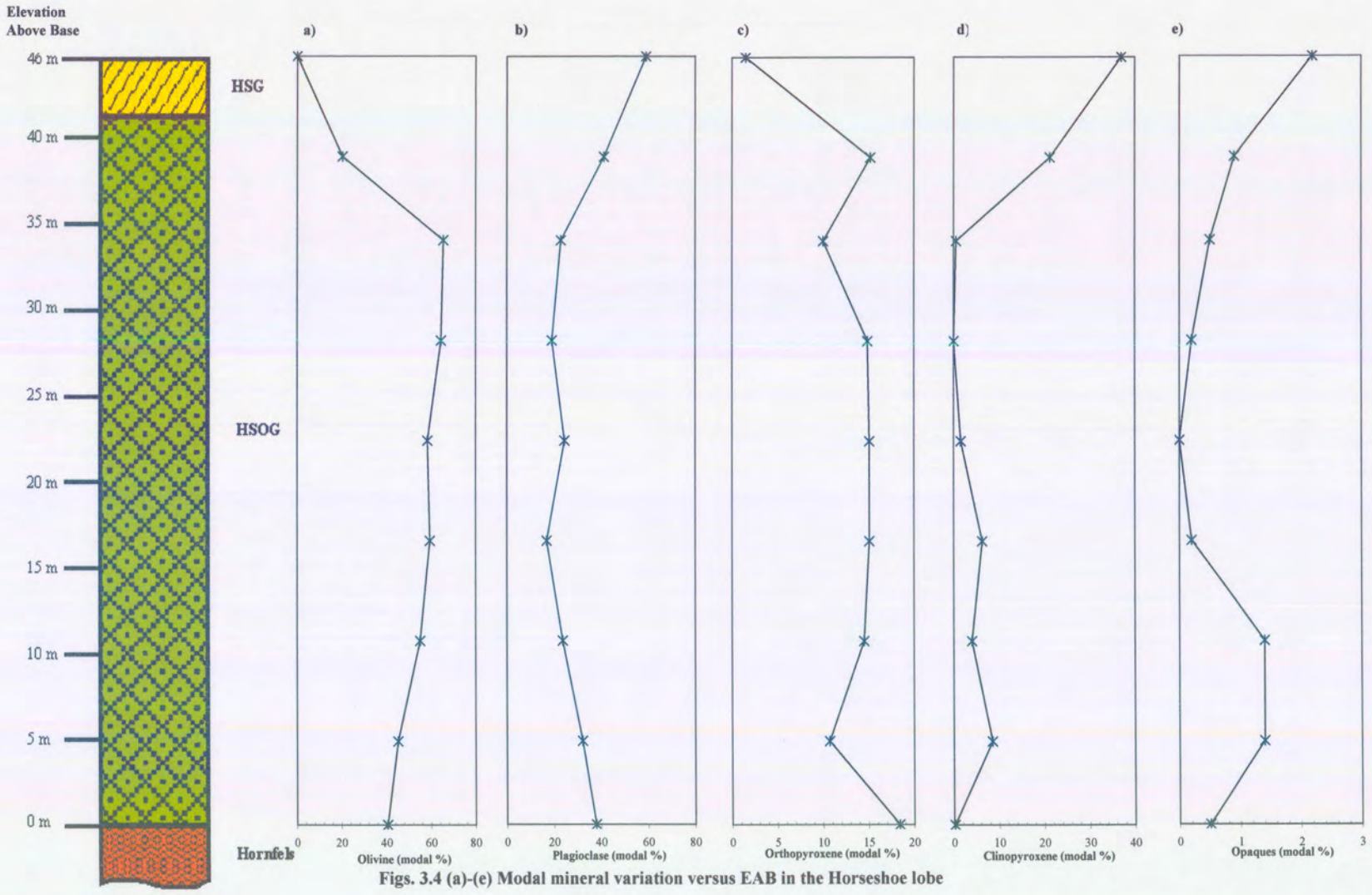

Figs. 3.4 (a)-(e) Modal mineral variation versus EAB in the Horseshoe lobe

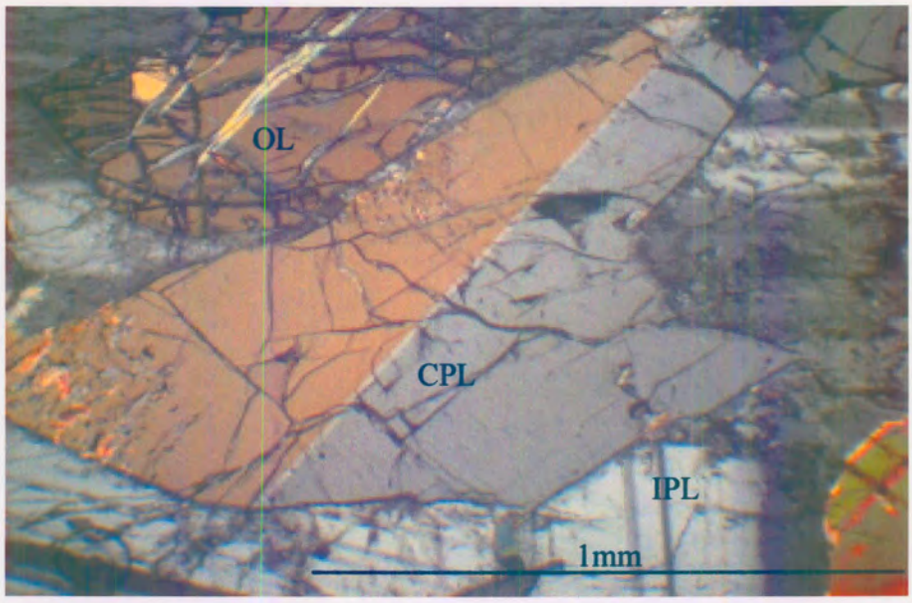

Plate 18: Photomicrograph of the HSOG (sample Hs-12). Photo shows cumulus plagioclase surrounded by intercumulus plagioclase.

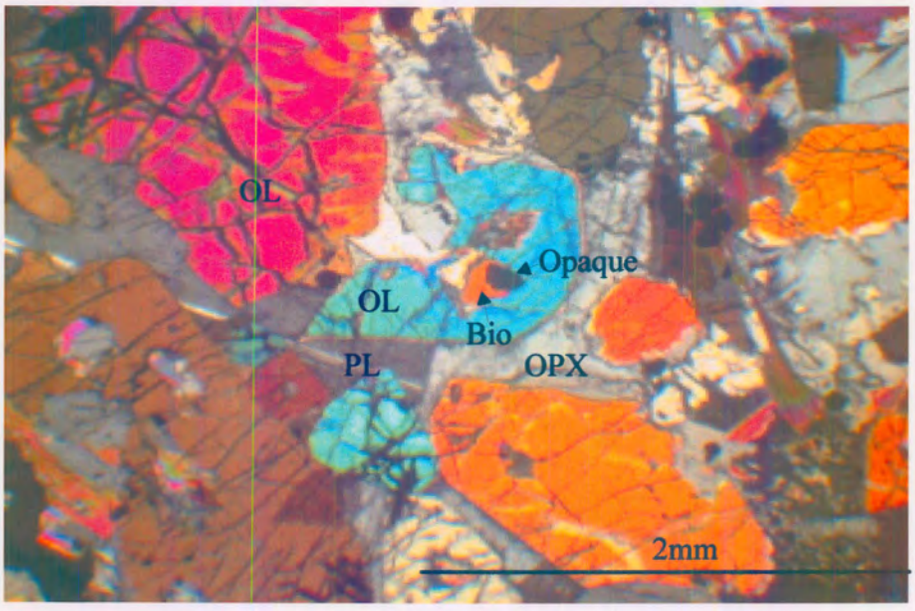

Plate 19: Photomicrograph of the HSOG (sample Hs-13). Photo shows cumulus olivine surrounded by orthopyroxene, and plagioclase. Olivine grain in the centre encloses biotite and opaque.

Olivine

Olivine grains range in size from 2/3 mm to over 3 mm. However, most grains range between 1 and 1 ½ mm. Most grains are anhedral and highly fractured. Rare subhedral grains can exist. Serpentinization commonly occurs along the fracture faces of the grains. Olivine sometimes contains small plagioclase, mica and oxide inclusions. The uppermost sample in the unit shows a subhedral to anhedral olivine often associated with both types of pyroxenes.

Chromite

Small amounts of chromite appear throughout the HSOG unit, but seem less abundant than in the BOG unit of the Ingeli lobe. Chromite is commonly found enclosed by olivine grains (Plate 19), and becomes progressively less abundant with height in the stratigraphy.

Plagioclase

Plagioclase forms either interstitial filling between olivine that can be more than 3 mm in size, or as lath like cumulus phases which can be from 1/3 mm to over 2 mm in length (Plate 18). The proportion of cumulus plagioclase increases with height similar to the pattern observed in the BOG unit of the Ingeli lobe. Cumulus grains in the highest sample of the unit tend to be subhedral, small (less than 2/3 mm) and free of alteration. Commonly these plagioclase laths dictate the shape of the olivine grain faces.

Orthopyroxene

Orthopyroxene is generally found as large oikocrysts that often enclose small plagioclase laths as well as, chromite and olivine. Some orthopyroxene have clinopyroxene exsolution blebs. Grains can range from 1 mm to over 3 mm in length. Most orthopyroxene in the lower samples are relatively unaltered. In the uppermost sample orthopyroxenes becomes larger and more altered and it has more clinopyroxene exsolution blebs. Orthopyroxene often encloses olivine grains in this sample.

Clinopyroxene

Clinopyroxene can be fairly abundant in some samples, but is absent in others. Clinopyroxene typically makes up small grains, up to 0.3 mm. The uppermost sample of the unit shows a high abundance of small interlocking clinopyroxene that are commonly associated with olivine grains and interstitial orthopyroxene grains. These grains are often found to be severely altered and show orthopyroxene reaction rims when in contact with other phases.

Accessory Phases

Minor amounts of mica are found in the lowest samples of the unit, but become progressively less abundant with height. Sulphides are also more common in the lowest samples and are often found associated with mica, or completely enclosed by this phase.

3.10 Horseshoe Gabbro (HSG)

The Horseshoe gabbro is approximately 4 m thick and caps the intrusion. Plagioclase is the only cumulus mineral phase, at approximately 60 modal %. Clinopyroxene is the most abundant postcumulus phase, and makes up approximately 37 modal %. Orthopyroxene occurs as a minor postcumulus phase, at 1.5 modal %. Olivine is not present in this rock unit. Small amounts of interstitial sulphides are found within the interstices of cumulus plagioclase.

Cumulus Plagioclase

In general, cumulus plagioclase laths in the HSG are much smaller than those of the feldspathic units of the Ingeli lobe (Plate 20). Large laths may be in the 0.7 mm range, but most grains tend to be smaller than 0.3 mm. Most grains are subhedral and unaltered.

Clinopyroxene

Clinopyroxene predominantly occurs as and interstitial phase. Most grains range in size from 0.3 to 0.7 mm. The crystal grains form anhedral, interlocking amalgamations in the interstices of the cumulus plagioclase. Rare cumulus clinopyroxene grains can also be found. Most clinopyroxene is pervasively altered.

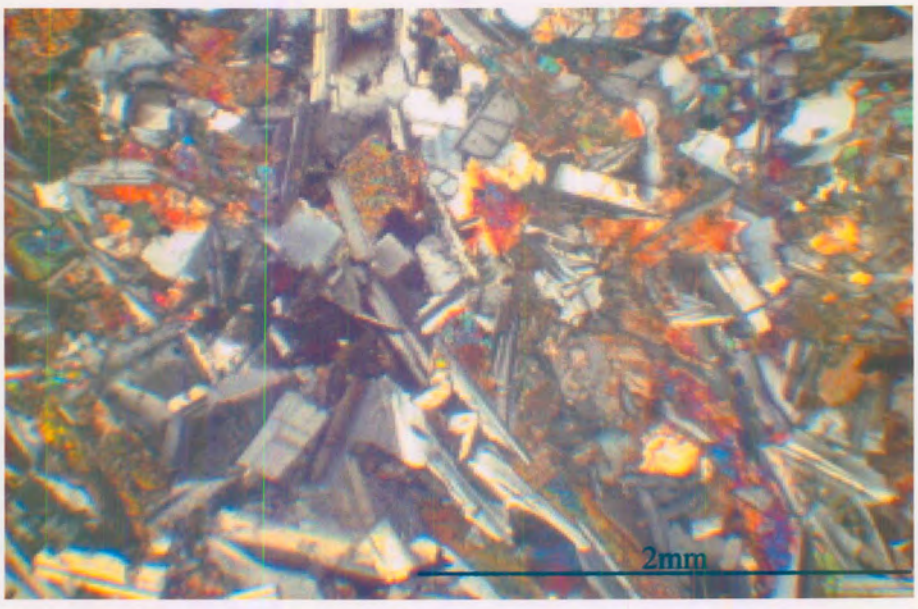

Plate 20: Photomicrograph of the HSG (sample Hs-8).

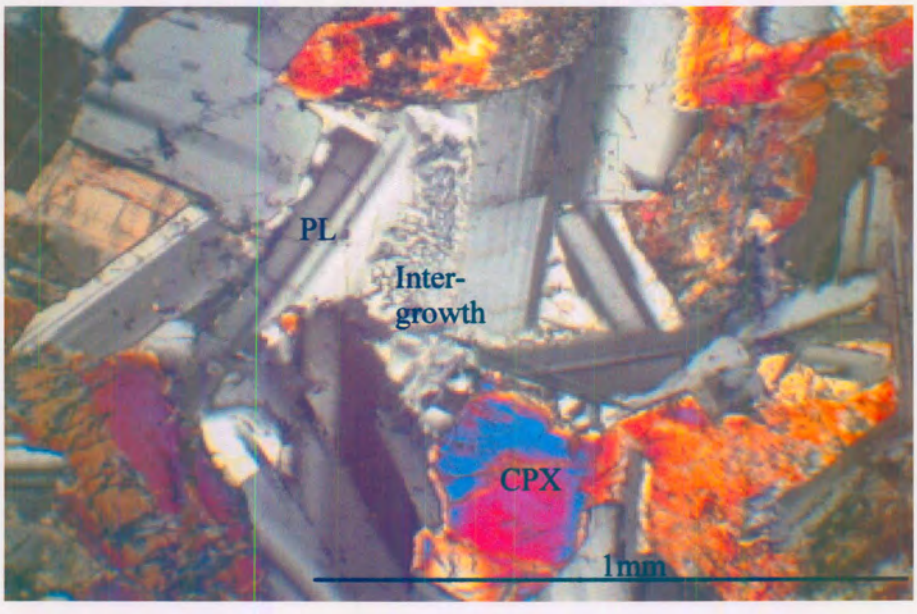

Plate 21: Photomicrograph of the HSG (sample Hs-8). Alkali feldspar and quartz are intergrown in the centre of the photo.

Orthopyroxene

Orthopyroxene is rare in the unit. However, the few grains that were found were over 1 mm in length, making them the largest phase in the unit. Grains were found to be less altered than clinopyroxene. Orthopyroxene tends to envelop smaller plagioclase laths producing a sub-ophitic texture.

Micrographic Intergrowths

As in the Ingeli lobe, micrographic intergrowths between quartz and alkali feldspar do occur in the uppermost unit of the Horseshoe lobe, but they are more frequent here (Plate 21).

Accessory Phases

Rare mica flakes are found to be included between interlocking clinopyroxene grains. Sulphide blebs are often found between the junctions of multiple cumulus plagioclase grains.

4. Mineral Chemistry

4.1 Introduction

The major rock forming minerals of the Ingeli and Horseshoe lobes of the MAC are; olivine, plagioclase, orthopyroxene, clinopyroxene and chromite. The present study is confined to the first four phases. The data are tabulated in Appendix II a total of 533 grains were analysed in the study. Table 4.1 shows how many grains of each phase were analysed in the Ingeli and Horseshoe lobes.

Table 4-1: Numbers of grains analysed

	olivine	plag	opx	cpx
Ingeli	92	126	98	110
Horseshoe	29	31	26	21
total	121	157	124	131

Grains were analysed in the core domain of the minerals. Analytical reproducibility was tested by repeat analysis on one spot on 4 grains of each phase. Table 4.2 below lists the coefficients of variation (calculated at 100* standard deviation/ mean concentration in wt %) based on repeat analysis.

Table 4-2: Coefficients of variation

Mineral	SiO2	Al2O3	TiO2	Cr2O3	FeO	MnO	MgO	NiO	CaO	Na2O	K2O
Ol	0.32	-	-	-	1.27	4.19	0.34	16.20	4.70	-	-
opx	0.59	10.96	14.08	8.77	1.47	19.95	0.44	74.80	2.33	59.35	-
cpx	0.47	5.88	7.02	6.47	2.59	10.21	0.88	103.60	1.71	18.77	-
Plag	1.83	2.37	47.00	-	18.18	-	-	-	6.44	9.43	11.72

Coefficients of variation are 0.3-3 % for concentrations within the ranges 5-50 + wt %, and rise above 3 % as concentration levels approach 1 %.

4.2 Ingeli Lobe

4.2.1 Olivine

A plot of Ni in olivine versus elevation above base is shown in figure 4.1. The graph shows that the concentration of Ni in olivine is highest in the three lowermost samples of the BOG unit reaching 2500 ppm. In the remainder of the BOG and throughout much of the overlying PU, Ni contents in olivine are between 1100 and 2000 ppm.

The Ni concentration in the olivine of the COG unit is the lowest in the profile, at just under 700 ppm. There is only one sample in the CG unit that contains olivine, (at 621 m EAB) and the olivine contains 900 ppm. In the UOG unit the Ni concentration in olivine increases to 1000-1300 ppm. In the UG unit (the last unit in the traverse) Ni contents are broadly similar as in the UOG.

Fo contents of olivine show much less variation than Ni contents. Within the BOG and the PU, Fo contents plot between 81 and 85, with the lowest values observed at the base of the intrusion. In the overlying gabbroic units, Fo varies between 59 and 62. The data shows that Ni and Fo contents of olivine in the Ingeli lobe are decoupled, i.e., there is considerable scatter in Ni within the ultramafic rocks, at relatively constant Fo contents.

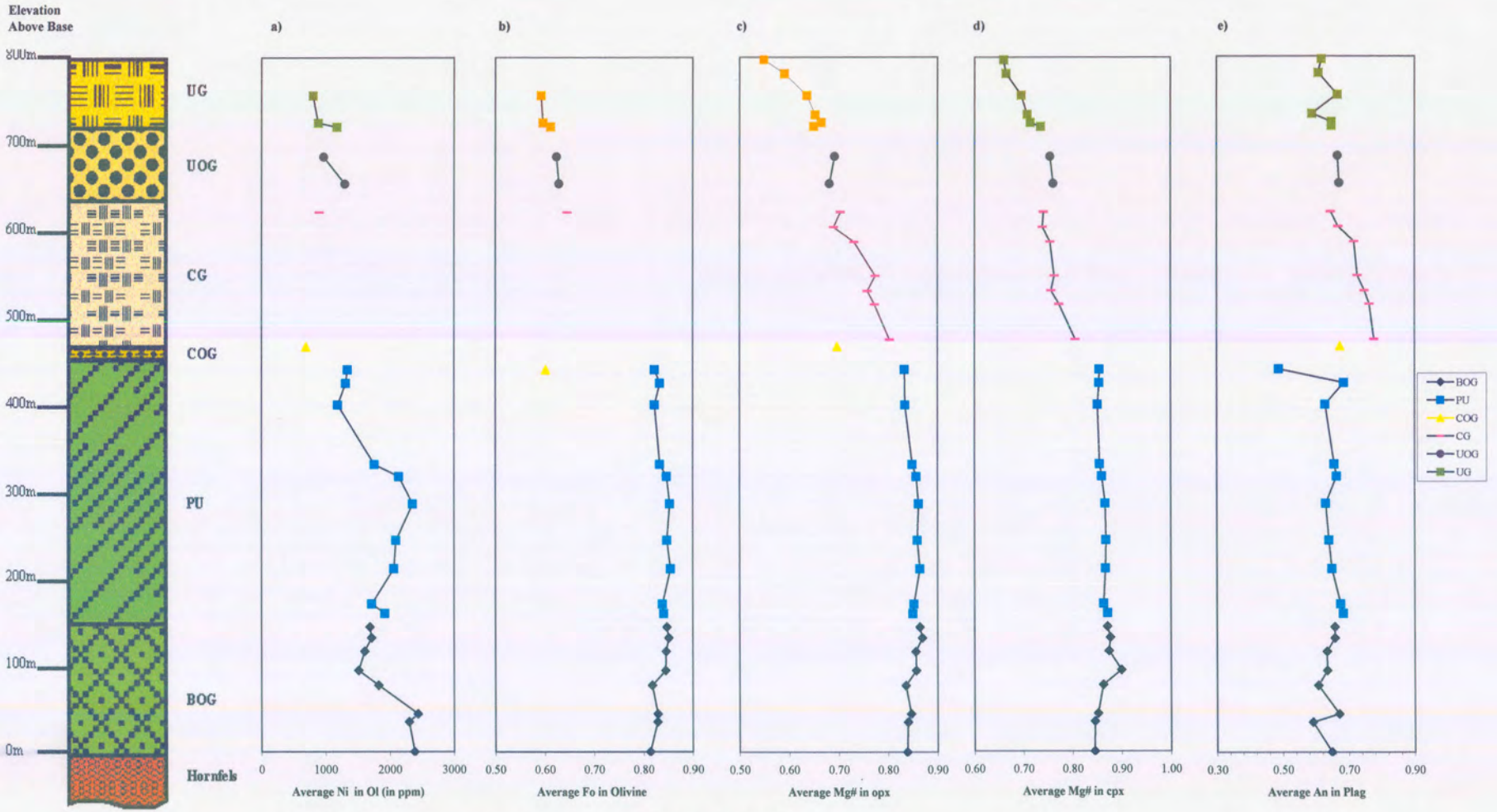

Fig. 4.1 (a)-(e): Mineral compositional variation versus EAB in the Ingeli lobe

4.2.2 Mg# in Orthopyroxene and Clinopyroxene

Mg# of orthopyroxene is plotted versus EAB in figure 4.1. Variation in Mg# ranges from 0.66 to 0.87. The values are relatively constant (0.83-0.87) in the basal ultramafic rocks (BOG and PU units), in accord with the compositional variation of olivine. The COG unit appears to have a relatively low Mg#, but the overlying CG unit shows a progressive decrease in Mg# of orthopyroxene from 0.80 to 0.70 with height. This trend continues through the UOG and UG units, with the latter showing the lowest Mg# of orthopyroxene of the intrusion at approximately 0.65.

The trends of Mg# in clinopyroxene essentially mirror that of orthopyroxene.

4.2.3 An in Plagioclase

An contents of the BOG unit vary from An_{59} to An_{67}. Within the PU unit, plagioclase is largely intercumulus by nature, but compared to intercumulus plagioclase in Bushveld ultramafic cumulates (Maier, 1992) An contents are surprisingly constant, from An_{65} to An_{62}. This suggests relatively little compositional zoning of the grains. The uppermost sample of the unit has markedly less calcic plagioclase, at An_{48}. The COG has broadly similar An contents as the PU. There is a marked increase in An content of plagioclase at the base of the CG unit (0.8), from thereon the An content decreases progressively to fall back to the levels observed in the PU towards the top of the CG and in the overlying UOG and UG units.

4.3 Horseshoe Lobe

4.3.1 Olivine

The Ni concentration of olivine in the Horseshoe lobe is significantly lower than that in the Ingeli lobe (Fig. 4.2 a). On average, the Ni concentration plots between 400 and 900 ppm, whereas in the Ingeli lobe Ni contents of olivine reach 2500 ppm. In general, the Ni content of olivine decreases with height in the Horseshoe lobe. Figure 4.3 b shows average Fo contents in Horseshoe olivines plotted versus EAB. The plot shows a small increase in concentration with height through the basal 5 m of the intrusion, but from then on the Fo contents remain steady before decreasing sharply in the uppermost olivine gabbronorite sample. In general, the Fo content of olivines in the Horseshoe lobe is lower than that of olivines in the Ingeli lobe (fig. 4.1 b).

4.3.2 Mg# in orthopyroxene and clinopyroxene

(Fig. 4.2 c) shows a plot of average Mg# in orthopyroxene versus EAB. The Mg# ranges from approximately 0.7 to nearly 0.85 with a progressive increase in the basal 35 m of the intrusion and a sharp drop in the topmost ten m. This is compared to the Ingeli lobe, with values at 0.66 to 0.87 throughout the lobe, and 0.83-0.87 in the Basal Zone units.

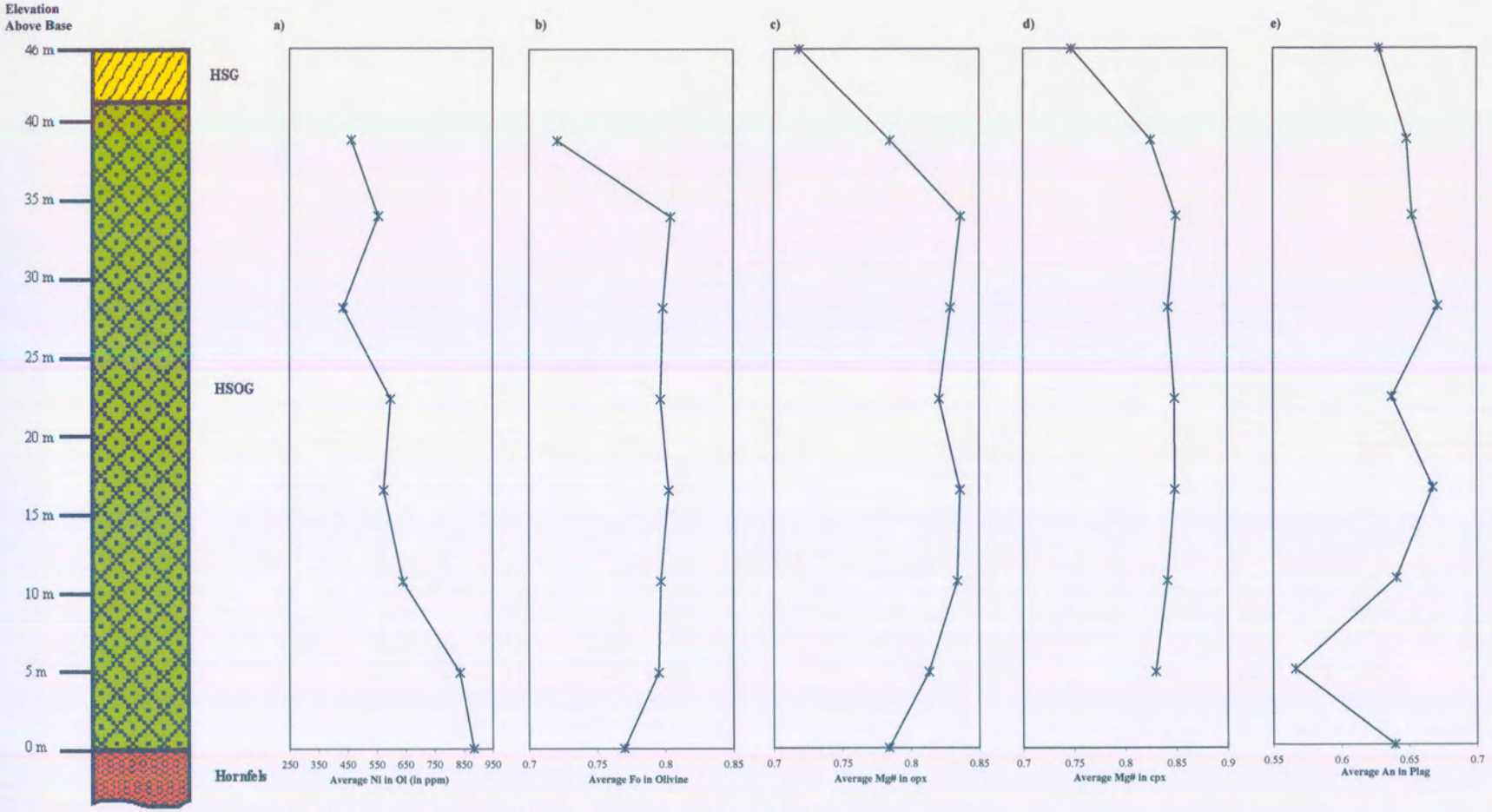

Fig. 4.2 (a)-(e): Mineral compostional variation versus EAB in the Horseshoe lobe

Variation in Mg# of clinopyroxene (Fig 4.2 d) effectively mirrors that of orthopyroxene, as it did in the BOG of the Ingeli lobe.

4.3.3 An in Plagioclase

(Fig. 4.2 e) shows average An content of plagioclase versus EAB. The plot shows large variability in the lowermost samples. This is due to the presence of intercumulus and cumulus plagioclase in these samples. The upper samples show less compositional variation, at between 0.6 and 0.65. Compared to the Ingeli lobe An contents are similar to those from the BOG unit, with values at 0.59 to 0.67.

4.4 Ni versus Fo content in Olivine

(Figure 4.2) shows a plot of Fo versus Ni in olivine. Relative to the field of layered intrusions (Simpkin and Smith, 1970), Ingeli olivines do not appear to be depleted in Ni. This implies that the Ingeli olivines did not crystallize from a magma that had undergone significant amounts of sulphide segregation prior to emplacement. In contrast, olivines in the Horseshoe lobe are depleted in Ni and plot below the field of layered intrusions. Thus the Horseshoe magma may have experienced sulphide segregation prior to emplacement.

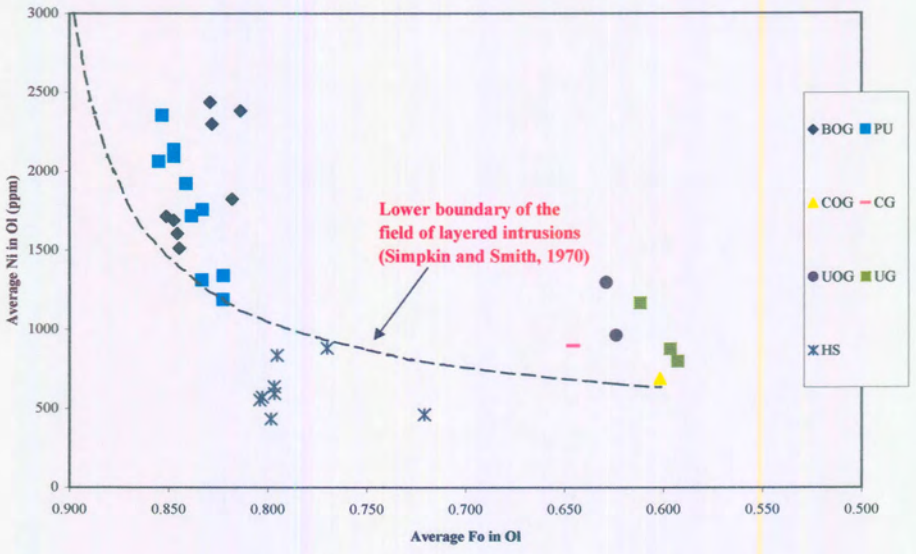

Fig. 4.3 Ni concentration plotted versus forsterite (Fo) content in olivine.

5. Whole Rock Geochemistry

5.1 Introduction

Thirty-five samples from the Ingeli lobe and nine samples from the Horseshoe lobe, representing all major lithological units encountered, were prepared for whole rock geochemical analysis using X-Ray Fluorescence. Analytical methods for the XRF analyses, as well as the data, are given in Appendix III. Additional trace elements, including REE, Ba, Rb, Th, K, Nb, Sr, Zr and Ti, were analysed in selected samples in the Ingeli traverse by inductively coupled plasma mass spectrometry. Analytical methods for ICP-MS are also given in Appendix III. CIPW norms were also compiled in this study and the data can be found in appendix (I).

5.2 Binary Variation Diagrams

5.2.1 Major Element Chemistry

Figs. 5.1 (a)-(h) show binary variation diagrams of major elements versus MgO (in wt %) in both the Ingeli and the Horseshoe lobes. The highest SiO_2 values are found in the gabbroic rocks of the Ingeli and Horseshoe lobes reaching a maximum of 54 wt% SiO_2. These levels are similar to the average Karoo dolerites (fig. 5.1 a) (Marsh, 1984). In the analysed samples, highly differentiated rocks were either eroded (i.e. at the Ingeli lobe), or not developed (i.e. at the Horseshoe lobe). The lowest SiO_2 contents are found in the ultramafic rocks of the Basal Zone (BOG and PU units of the Ingeli lobe). The olivine-rich

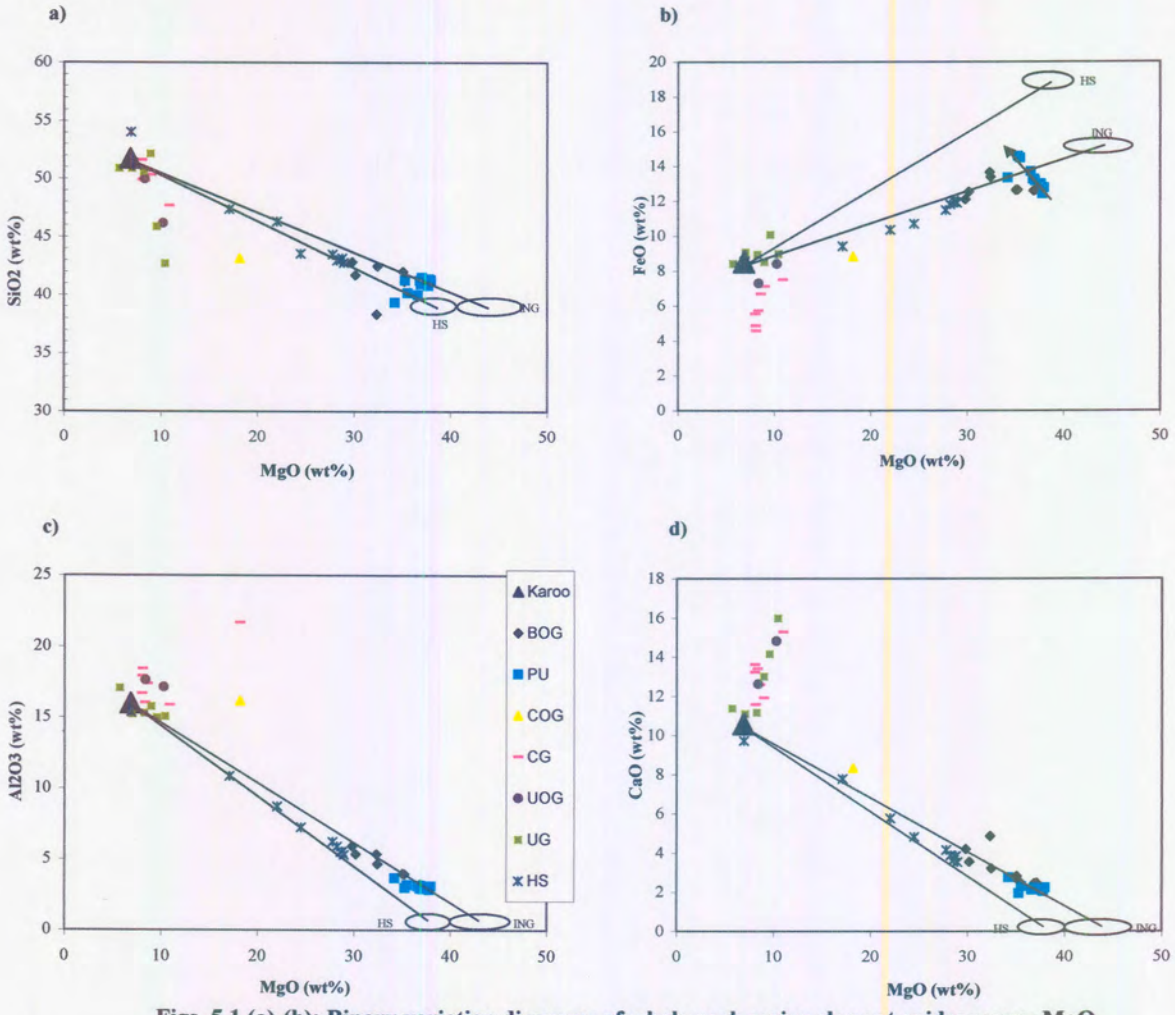

Figs. 5.1 (a)-(h): Binary variation diagrams of whole-rock major element oxides versus MgO. Open circles indicate approximate compositional range of olivine from the Ingeli (ING) and Horseshoe (HS) lobes. Composition of Karoo dolerite from Marsh and Eales (1984).

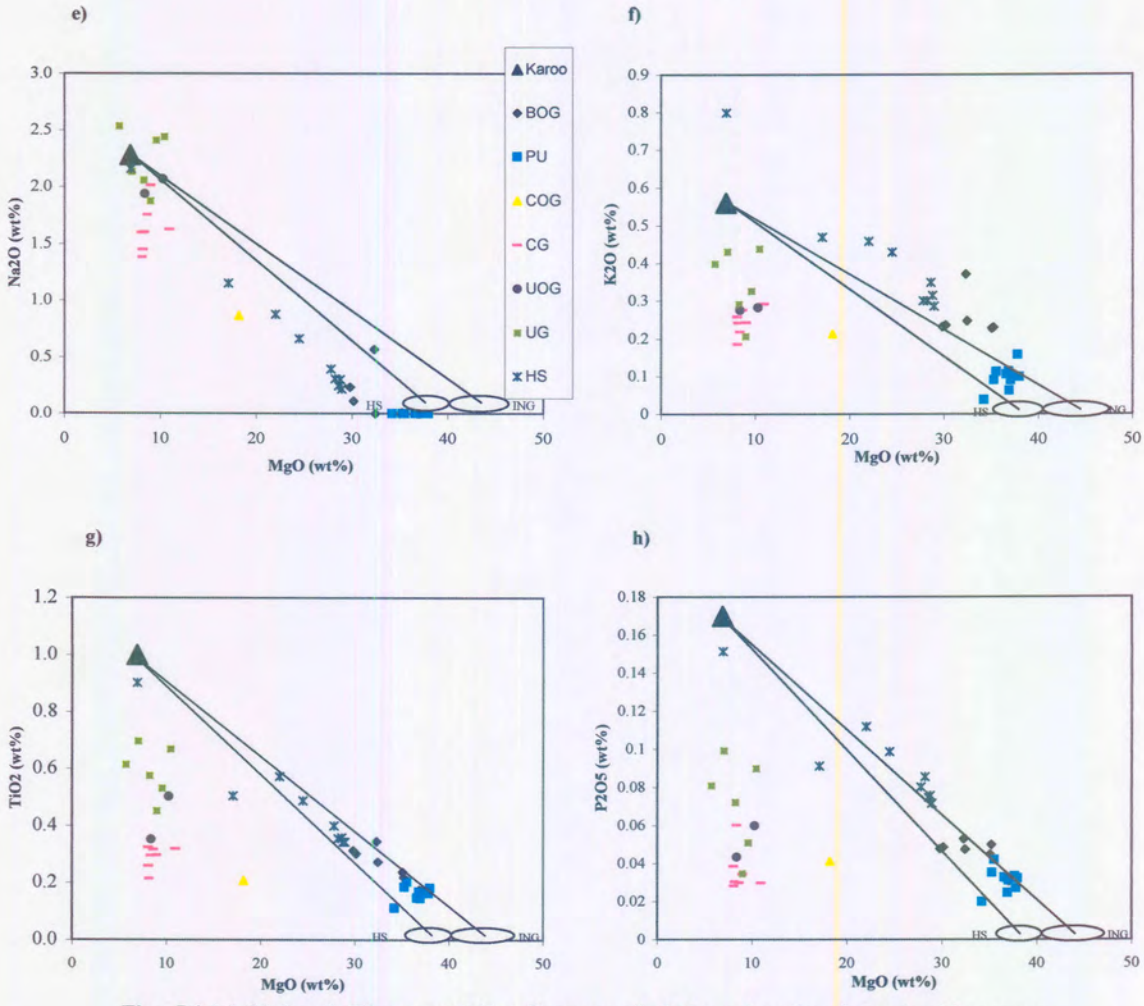

Figs. 5.1 (a)-(h) (cont): Binary variation diagrams of whole-rock major element oxides versus MgO. Open circles indicate approximate compositional range of olivine from the Ingeli (ING) and Horseshoe (HS) lobes. Composition of Karoo dolerite from Marsh and Eales (1984).

Horseshoe rocks generally have lower MgO contents than the ultramafic rocks of the Ingeli lobe.

FeO (Fig. 5.1 b) show the FeO contents of the MgO rich Ingeli and Horseshoe rocks fall between olivine control lines. Within the lherzolitic rocks a negative correlation between FeO and MgO is evident (as indicated by the arrow). This could be due to reaction of cumulus olivine with percolating, relatively evolved (i.e. FeO rich), intercumulus melt (Cawthorn, 1992).

Al_2O_3, CaO, and Na_2O (Figs. 5.1 c, d and e) concentrations are largely governed by modal amounts of plagioclase and clinopyroxene and values decrease with increasing MgO contents in the rocks of the Basal Zone, i.e. they show a negative correlation with MgO. The highest amounts of Al_2O_3, CaO and Na_2O are found in the plagioclase cumulates of the gabbronorite units (COG, CG, UOG and UG) in the Ingeli lobe and the HSG of the Horseshoe lobe. With regard to CaO and Al_2O_3 most of the Basal Zone rocks plot close to tie lines between Karoo dolerite and olivine. This suggests that plagioclase and clinopyroxene in these rocks largely crystallized from trapped melt and are not of cumulus origin. All of the gabbronoritic rocks have higher CaO contents than average Karoo dolerite (the highest being 16 wt %), suggesting control by cumulus plagioclase and clinopyroxene. The K_2O (Fig. 5.1 f) and Na_2O (Fig. 5.1 e) trends are notable because the ultramafic rocks plot off the olivine control lines. In the case of Na_2O an analytical problem is indicated.

TiO_2 values (Fig 5.1 g) in the Mg-rich rocks plot on olivine control lines and thus appear to be controlled by the amount of trapped melt in the rocks. The gabbroic rocks have TiO_2 contents below Karoo dolerite; this indicates that cumulus magnetite is rare in these rocks.

P_2O_5 is an incompatible element with respect to all of the major phases of the Mount Ayliff Complex. The oxide shows a negative correlation with MgO (wt %) and plots along olivine control lines (Figs. 5.1 h) in the olivine-rich rocks, suggesting that P_2O_5 contents are controlled by the trapped melt. The gabbroic rocks seem to be depleted in P_2O_5 relative to Karoo dolerite, indicating that these rocks are plagioclase-clinopyroxene cumulates, containing mostly <50% trapped melt.

5.2.2 Trace Element Geochemistry

Trace element partitioning within a melt is affected by a number of factors including; composition of the melt, size sites, ionic radii, temperature, pressure, accumulation rates, kinetic effects, and crystallization according to Rollinson (1993) and references therein. Figs. 5.2 (a)-(h) show binary variation plots of selected trace elements (Cr, Zr, Sr, V, Cu, Ni, Co and S) versus MgO.

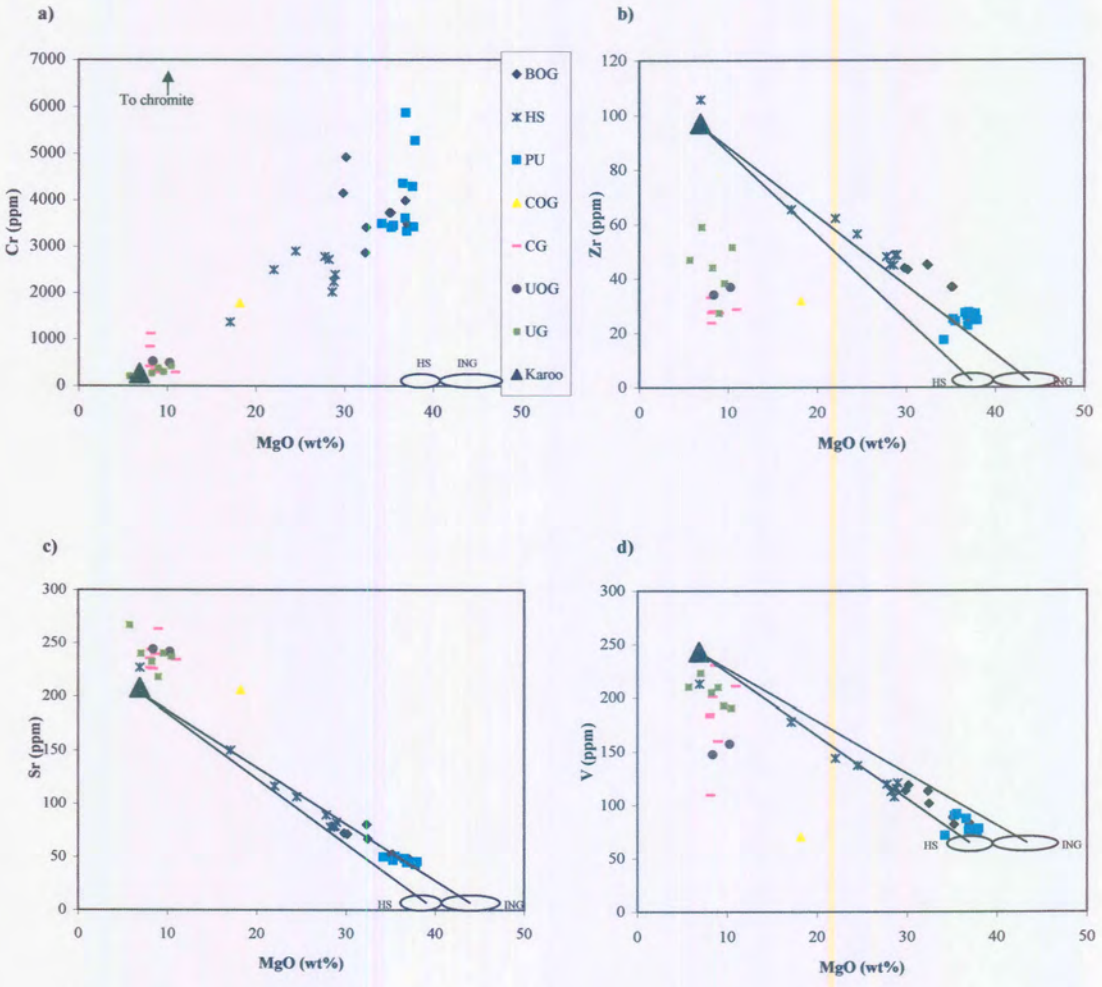

Figs. 5.2 (a)-(h): Binary variation diagrams of whole-rock minor and trace elements plotted versus MgO. Open circles indicate approximate compositional range of olivine from the Ingeli (ING) and Horseshoe (HS) lobes. Composition of Karoo dolerite is from Marsh and Eales (1984).

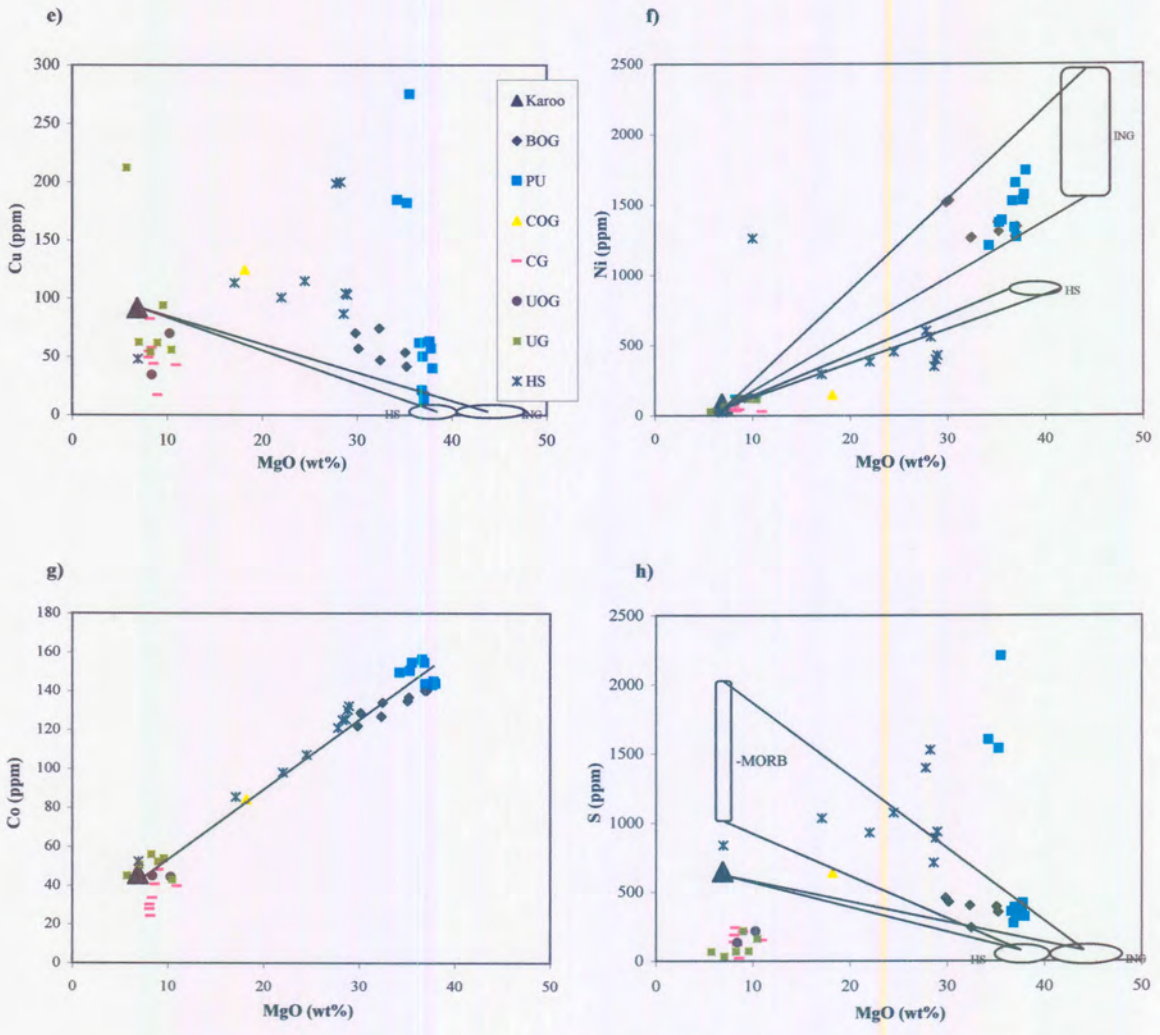

Figs. 5.2 (a)-(h): Binary variation diagrams of whole-rock minor and trace elements plotted versus MgO. Open circles indicate approximate compositional range of olivines from the Ingeli (ING) and Horseshoe (HS) lobes. Composition of Karoo dolerite is from Marsh and Eales (1984).

Chromium (fig. 5.2 a) has a high partition coefficient (D) with respect to chromite. With regard to orthopyroxene D_{Cr} is around 2, while $D(Cr)_{olivine/\ silicate\ melt}$ is most likely to be below unity according to Rollinson (1993) and references therein. The diagram shows a positive correlation between chromium and MgO, with the highest values in the PU unit at around 6,000 ppm Cr. The lowest Cr values are found in the gabbronorite units of the Ingeli lobe. The samples of the Horseshoe lobe plot in between the Basal Zone and the gabbronorites of the Ingeli Lobe.

The olivine-rich samples plot within a triangular field defined by the composition olivine, chromite and trapped melt as defined by Karoo dolerite. Interestingly, the relative proportion of olivine and chromite appears to be broadly constant in the ultramafic rocks. The major element data has shown that orthopyroxene and clinopyroxene are not important cumulus phases in these rocks and therefore cannot control chromium contents.

Zirconium (Fig. 5.2 b) has a high charge and a small radius. Zr does not enter significantly into cation sites of common cumulus minerals. Therefore, it is almost invariably concentrated in the trapped intercumulus liquid. The diagram shows considerable variation between the Basal Zone rocks and the gabbronorites. The olivine-rich rocks tend to plot above the tie line between Karoo dolerite and olivines. The ICP data indicate lower Zr contents and fall on

the tie line between dolerite and olivine, suggesting that Zr contents determined by XRF are inaccurate. The gabbronorite rocks plot to the far left of the tie lines. The gabbronoritic rocks have between 20-60 % Zr of the Zr content of the Karoo dolerites, indicating 20-60 % trapped melt in these rocks. This is broadly in agreement with the P_2O_5 data.

Strontium (Fig 5.2 c) has and ionic radius of 1.18 Å, and substitutes for Ca, and K (1.01 Å and 1.33 Å) in the feldspars (mainly in plagioclase). Therefore, the Sr content of a rock is mainly a reflection of the modal proportion of plagioclase. The figure shows a good negative correlation between MgO and Sr. The Basal Zone rocks have very little Sr, and the element is controlled by the trapped melt confirming that the rocks contain very little cumulus plagioclase. The rocks of the overlying gabbronorites that are dominated by cumulus plagioclase have the highest Sr values at 200-250 ppm. The Horseshoe Sr values plot between the Ol-rich rocks and the gabbronorites of the Ingeli lobe.

Vanadium (Fig. 5.2 d) has an extremely high D value into spinel, whereas for orthopyroxene D is around unity, and for olivine, clinopyroxene and plagioclase D is low according to Rollinson (1993) and references therein. Therefore, the V content of magmas and cumulate rocks increases with increasing differentiation until magnetite becomes a cumulus phase during the advanced stages of differentiation. The present data shows a good negative correlation between V and MgO in the rocks of the Basal Zone which is a result of trapped melt control.

In the gabbronoritic rocks, V contents show considerable variation at relatively constant MgO contents and can be assigned to the presence of cumulus magnetite, particularly in the uppermost UG sample. The Horseshoe rocks plot between the Ol-rich rocks and the gabbronorites of the Ingeli lobe.

Copper (Fig. 5.2 e) partitions preferentially into sulphides, and will show low values in any rock that is barren of sulphides. The D(Cu) sulphide melt/silicate melt is approximately 1000 (Rollinson and references therein, 1993). The only silicate phase that shows partition coefficients slightly above unity is clinopyroxene. However, this effect tends to be overprinted by the presence of sulphides. The figure shows tie lines between Karoo dolerite and olivine from Horseshoe and Ingeli. Any value that plots above the tie lines, indicates the presence of cumulus sulphides. Alternatively, there could have been some mobility of Cu during hydrothermal alteration of the rocks. Most of the Basal Zone rocks, and the Horseshoe rocks plot above the tie lines between Karoo dolerite and olivine and thus appears to contain small amounts of cumulus sulphide. Alternatively, there could have been some mobility of Cu during hydrothermal alteration of the rocks. The highest value is from a PU rock, at around 275 ppm. Of note is that most of the gabbronorite rocks plot below the Karoo average (from 15 to 60 ppm) indicating that these rocks contain little or no cumulus sulphides.

Nickel (Fig. 5.2 f) is strongly compatible with respect to chromite, olivine, orthopyroxene and sulphides. D values with respect to olivine may fall between 5 and 30 depending on the magma composition. D(Ni) sulphide melt/silicate melt = 350 for basaltic magma (Rollinson and references therein, 1993). Therefore, Ni contents are mainly governed by the concentration of sulphides. In (Fig. 5.2 f), tie lines are drawn between Karoo dolerite and the range of olivine composition at Ingeli and Horseshoe. Most of the samples fall within the olivine control fields. There is little evidence for the presence of cumulus sulphides, possibly suggesting that the variation in Cu content is due to mobility of Cu.

Cobalt (Fig 5.2 g) partitions preferentially into sulphides (D(Co) sulphide melt/ silicate melt =70, Rajamani and Naldrett, 1978), as well as into spinel and olivine. D values for orthopyroxene are about unity. Mg is often substituted by Co in olivine and opx, and this accounts for elevated Co levels in ultramafic rocks. (Fig. 5.2 g) shows Co versus MgO, with a "best fit" line drawn from Karoo average through samples. The graph shows that no sample is significantly enriched or depleted in Co. The lack of variation in Co is in sharp contrast to the variation in Cu and Ni between the Ingeli and the Horseshoe rocks.

Fig. 5.2 h shows S contents within the analysed rocks plotted versus MgO. S contents of Karoo magmas are poorly known, but if the S content of a sill below the Insizwa lobe analysed by Maier et al. 2002 (650 ppm) are representative, then most of the Horseshoe rocks, and several of the olivine-rich rocks at Ingeli, have

cumulus sulphides as they plot above the tie line between Karoo dolerite and olivine. If S contents of MORB are used (Wallace and Carmichael, 1992), then only a few samples from Horseshoe and Ingeli would contain cumulus sulphides. The gabbroic rocks are S-poor, at below 300 ppm, and appear to contain little or no cumulus sulphide.

5.3 Spider diagrams

Figures 5.3 (a)-(e) shows spider diagrams of incompatible trace elements (analysed using ICP-MS) normalized to primitive mantle. Sixteen samples were analysed through five of the units of the Ingeli lobe (BOG, PU, COG, CU, and UG). The rocks of the Horseshoe lobe and the UOG unit were not analysed in this study. The most important features of the diagrams are summarized in the following:

(i) The BOG unit has a generally higher concentration of incompatible trace elements than the overlying PU. This indicates larger amounts of trapped melt, bearing in mind that the concentration of incompatible trace elements in both units plot on control lines between olivine and Karoo dolerite (Fig. 5.2).

(ii) The shape of the patterns in the BOG and the PU is broadly similar. The patterns are fractionated with relative enrichment in the highly incompatible trace elements, and negative Nb and Ti anomalies. Both units show no positive Sr or Eu anomaly, indicating that the plagioclase observed in the rocks crystallized from trapped melt.

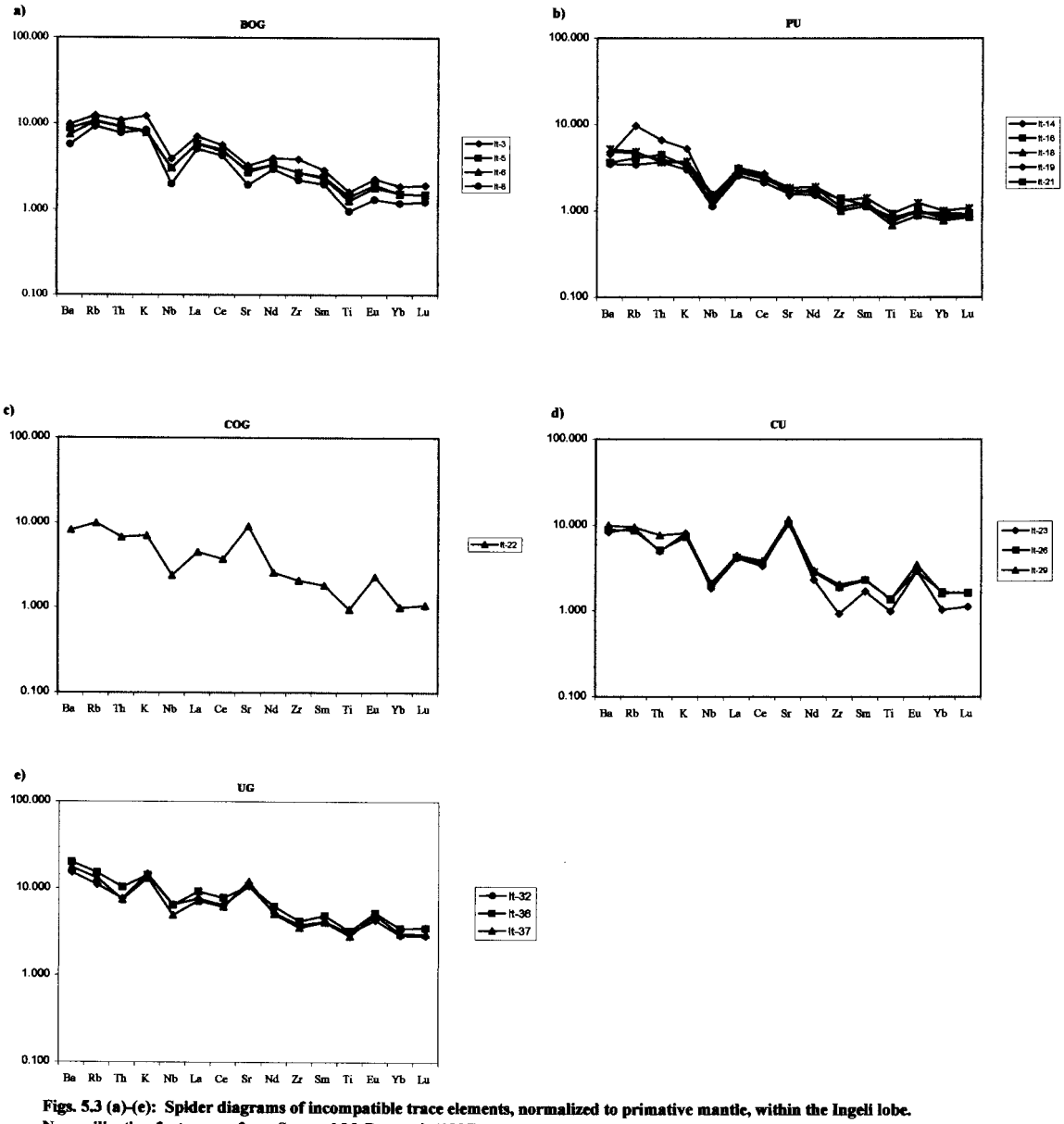

Figs. 5.3 (a)-(e): Spider diagrams of incompatible trace elements, normalized to primative mantle, within the Ingeli lobe. Normailization factors are from Sun and McDonough (1995).

(iii) The BOG has a slight negative Sr anomaly. The largest negative Sr anomaly is observed in the sample with the largest negative Nb and Ti anomaly. This may indicate crustal contamination of this sample with elements other than Nb, Ti, and Sr, which are retained by possibly refractory oxides and plagioclase. Alternatively, the sample could contain less trapped melt.

(iv) The normalized Nb/La ratio decreases with height through the Ingeli lobe, possibly indicating a progressively smaller crustal component in the rocks. The following list shows the average Nb/La ratios in each unit: BOG (0.520), PU (0.475), COG (0.551), CG (0.482) and UG (0.770).

(v) The gabbroic units have positive Sr and Eu anomalies indicative of the presence of cumulus plagioclase.

(vi) The positive Sr and Eu anomalies are less pronounced in the uppermost unit, whereas Ba is elevated. This is interpreted to be the result of lesser amounts of plagioclase relative to trapped melt and K-feldspar.

5.4 Compositional variations against Elevation Above Base

5.4.1 Ingeli

Figures 5.4 (a)-(p) show geochemical plotted against EAB (Elevation Above Base) for the Ingeli lobe. The figures are compiled from data collected by XRF (for major-minor-and some traces elements), and ICP-MS (for some trace elements).

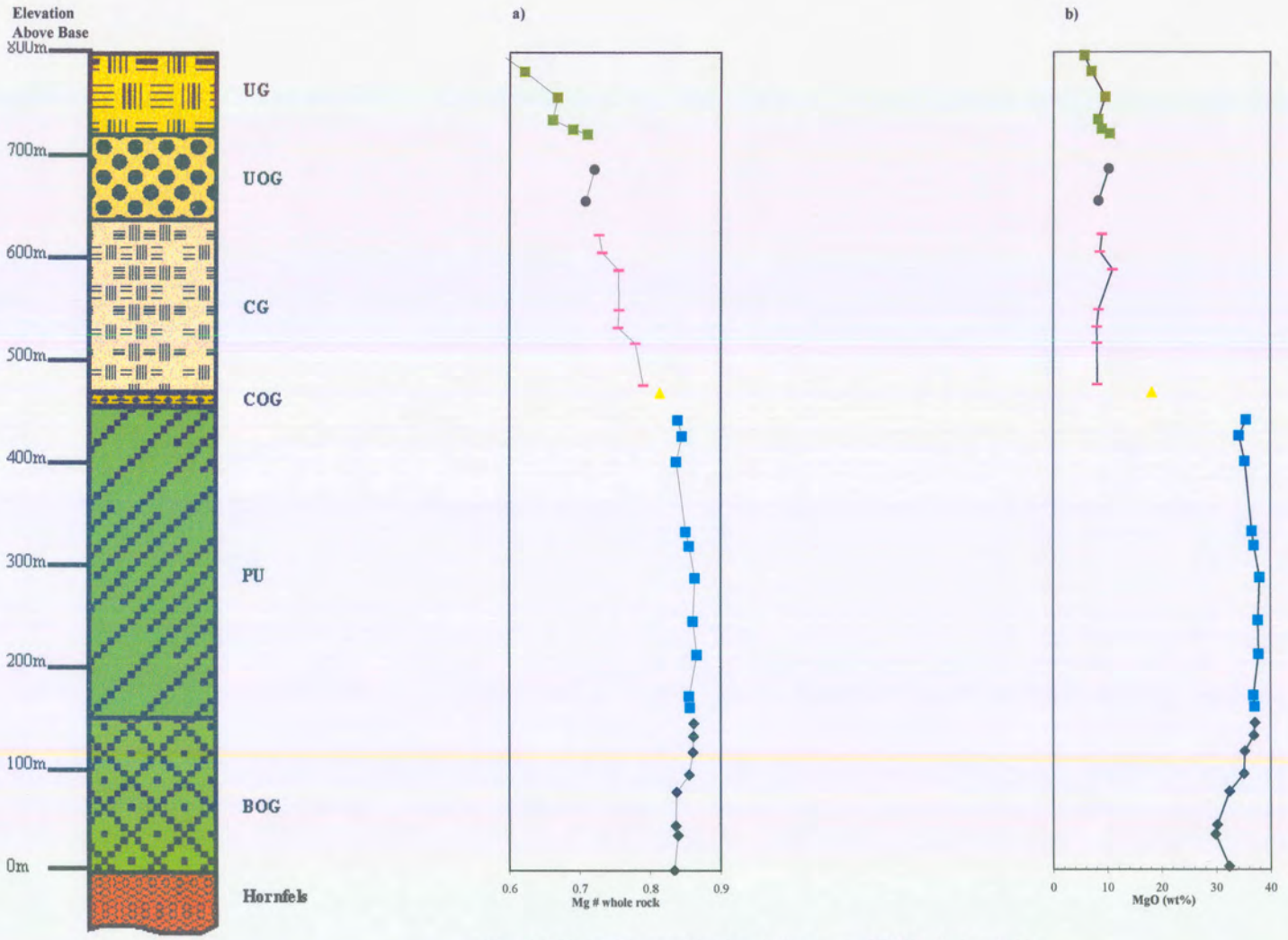

Figs. 5.4 (a)-(p): Compositional variation versus EAB in the Ingeli lobe

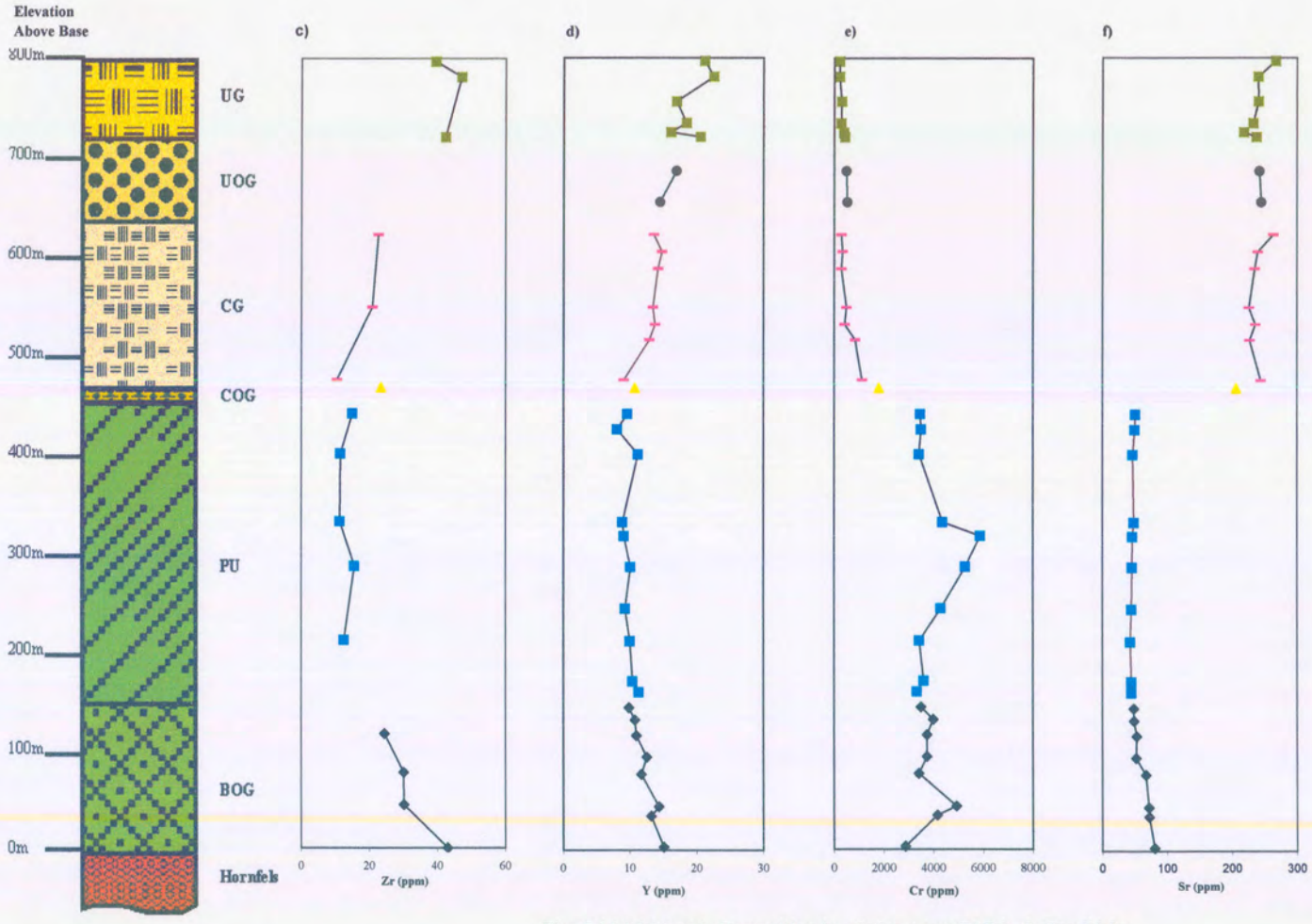

Figs. 5.4 (a)-(p) (cont): Compositional variation versus EAB in the Ingeli lobe

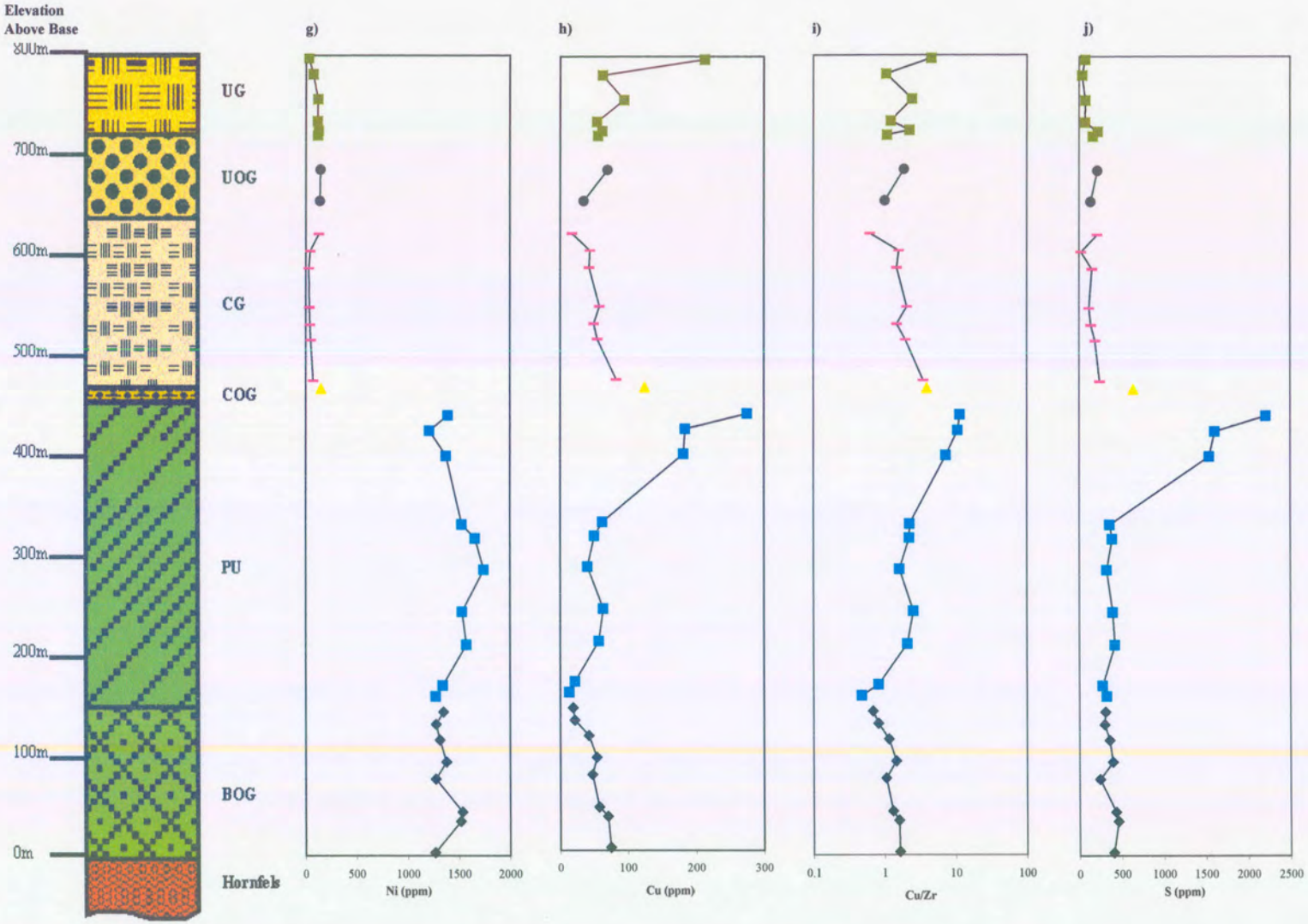

Figs. 5.4 (a)-(p) (cont): Compositional variation versus EAB in the Ingeli lobe

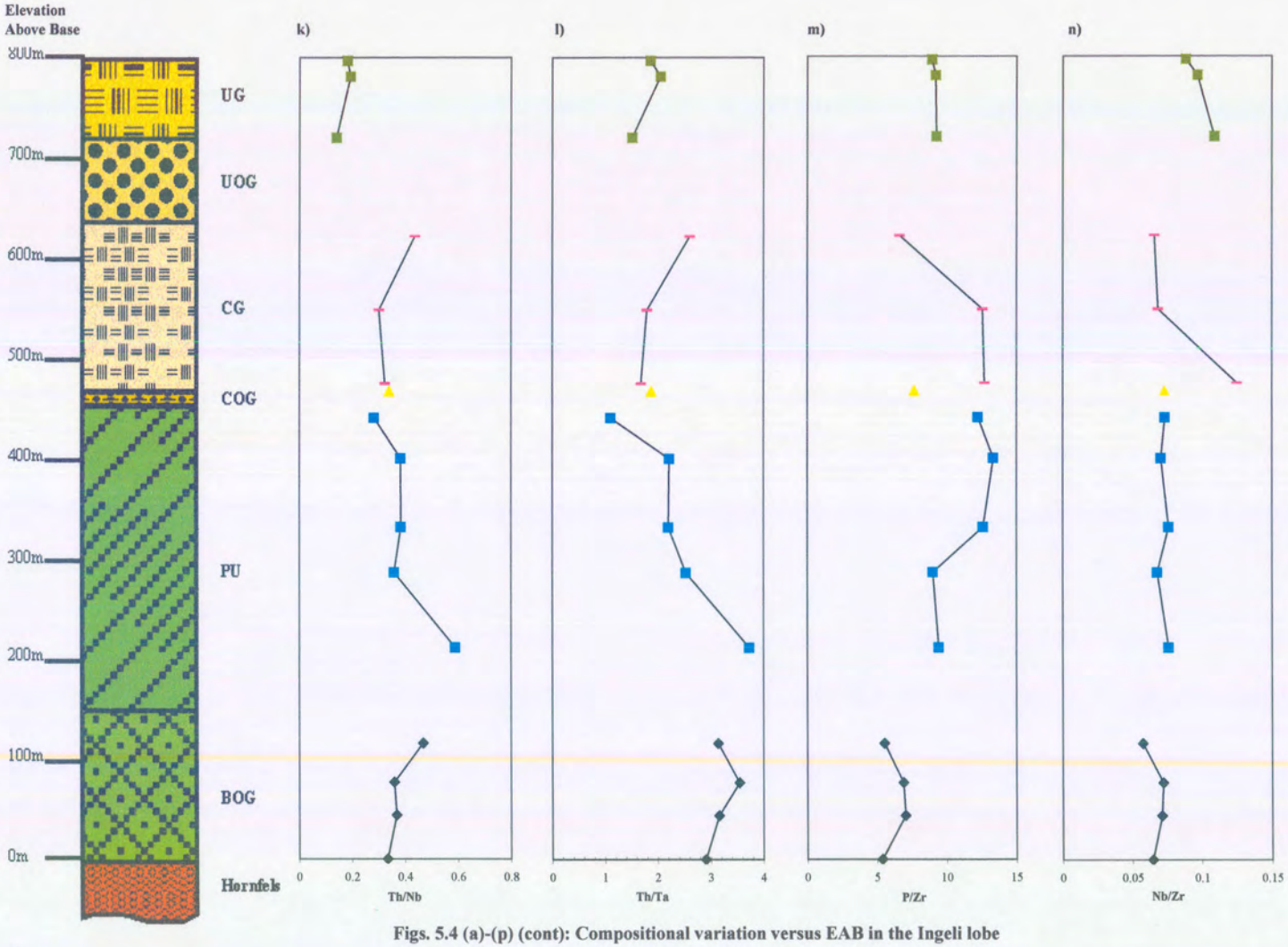

Figs. 5.4 (a)-(p) (cont): Compositional variation versus EAB in the Ingeli lobe

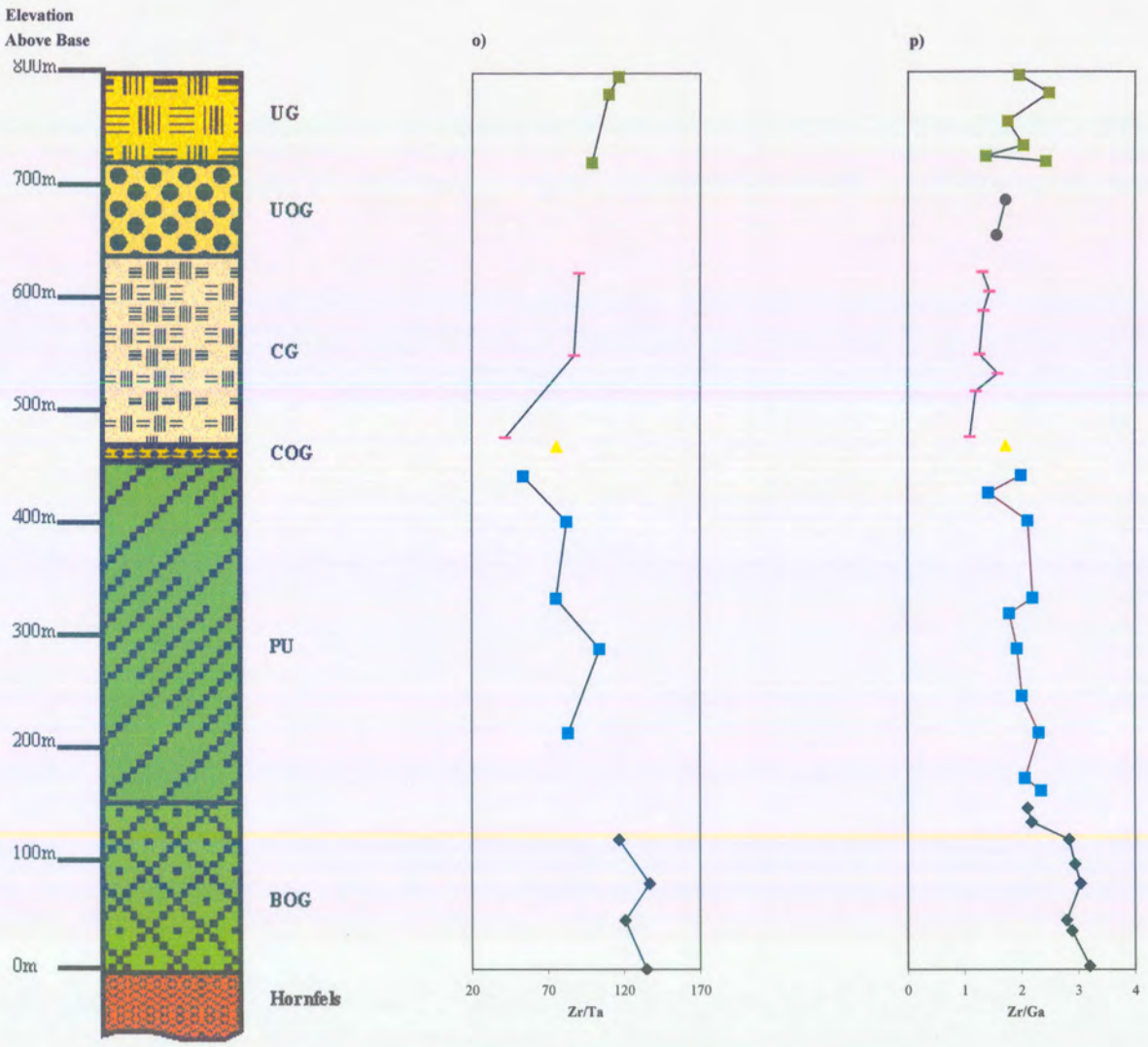

Figs. 5.4 (a)-(p) (cont): Compositional variation versus EAB in the Ingeli lobe

Figure 5.4 a. shows a plot of whole rock Mg# versus EAB. Throughout the BOG unit the Mg# progressively increases matching the compositional variation in olivine and pyroxene (Figs. 4.1 b-d). This could reflect the intruding magma becoming more primitive, or a decreasing amount of trapped melt. Throughout the PU unit, the Mg# remains fairly constant, but decreases slightly towards the top. From the COG unit to the top of the UG unit the Mg# decreases progressively. Unlike in the Insizwa lobe there are no sharp compositional breaks observed (Maier et al. 2002).

The MgO content (Fig. 5.4 b) of the rocks is controlled largely by the modal amounts of ferromagnesian phases (olivine and pyroxenes). In the Basal Zone, MgO contents closely reflect the modal abundance of olivine (fig. 3.3 a). In the topmost 3 gabbroic units, MgO plots between 4-6 wt %. The COG has an intermediate MgO content between the Basal Zone and the overlying gabbronorite units.

The incompatible trace elements Zr and Y show broadly similar variation through the intersection, with relatively elevated levels in the BOG, low values in the PU, and a progressive increase from the base of the COG unit to the top of the intersection. Based on a comparison to Karoo dolerite (Marsh and Eales, 1984), the BOG has approximately 20-40 % trapped melt, and the PU 10-20 % trapped melt.

The Cr concentration broadly mirrors the trend of modal olivine contents, indicating that chromite and olivine coprecipitated throughout the Basal Zone, but are rare throughout the overlying gabbroic rocks.

As expected, Sr contents closely mirror the abundance of plagioclase in the rocks with low values in the BOG and PU units and high values in the gabbroic units.

Ni contents broadly reflect the abundance of olivine, with high values (1100-1700 ppm) in the Basal Zone, and low values (200 ppm) in the Central Zone.

Cu contents are between 0-100 ppm throughout the intersection, but reach higher values in the uppermost portion of the PU (up to 300 ppm Cu), the COG unit (120 ppm), and towards the top of the UG unit (200 ppm). The copper peak towards the top of the PU unit has also been noted by Nordin (1987), in an earlier study of the Ingeli lobe, and by Maier et al. (2002) in the Insizwa lobe.

Cu/Zr ratios are sensitive to the presence of cumulus sulphides as both elements are incompatible in the absence of sulphides, but Cu partitions into sulphides. Karoo dolerites have Cu/Zr around unity, and most of the samples studied in the Ingeli lobe have values above this value suggesting either the presence of small amounts of cumulus sulphides, or mobility of Cu relative to Zr. The highest values are found in the PU unit, in the COG unit, and towards the top of the UG unit. Sulphur (Fig. 5.4 j) shows the same overall trend as copper except that there

is no enrichment in S at the top of the UG unit. The maximum S contents are observed at the top of the PU, at 2300 ppm. If it is assumed that the BOG unit has 20-40 % trapped melt (Fig 5.4 c), and little or no cumulus sulphide, then the Ingeli magma had some 1500 ppm S, broadly similar to MORB (Wallace and Carmichael, 1992).

Th, Nb, Ta, P, Zr and Ga are all elements that do not partition into any of the major minerals of the Ingeli lobe. Variation in the inter-element ratios should therefore reflect variation in the mantle source of the magmas or crustal contamination during ascent and/or emplacement. It is evident (Figs. 5.4 k-p) that Th/Nb, Th/Ta, Zr/Ta and Zr/Ga, in the BOG is higher than in the overlying units, possibly indicating an enhanced crustal component. This is in accord with low, P/Zr and Nb/Zr ratios in the BOG.

5.4.2 Horseshoe Lobe

In terms of Mg# and MgO (Figs. 5.5 a-b), the HSOG is slightly less primitive and ultramafic than the BOG of the Ingeli lobe. However, as in the Ingeli lobe, there is a progressive increase in Mg# and MgO. A reversal towards more evolved compositions is only observed in the uppermost 10 m of the intrusion.

Orthopyroxene and clinopyroxene show little variation through the HSOG. The HSG has almost no orthopyroxene but close to 40 % clinopyroxene. This is broadly similar to the UG unit of the Ingeli lobe. This could possibly suggest that

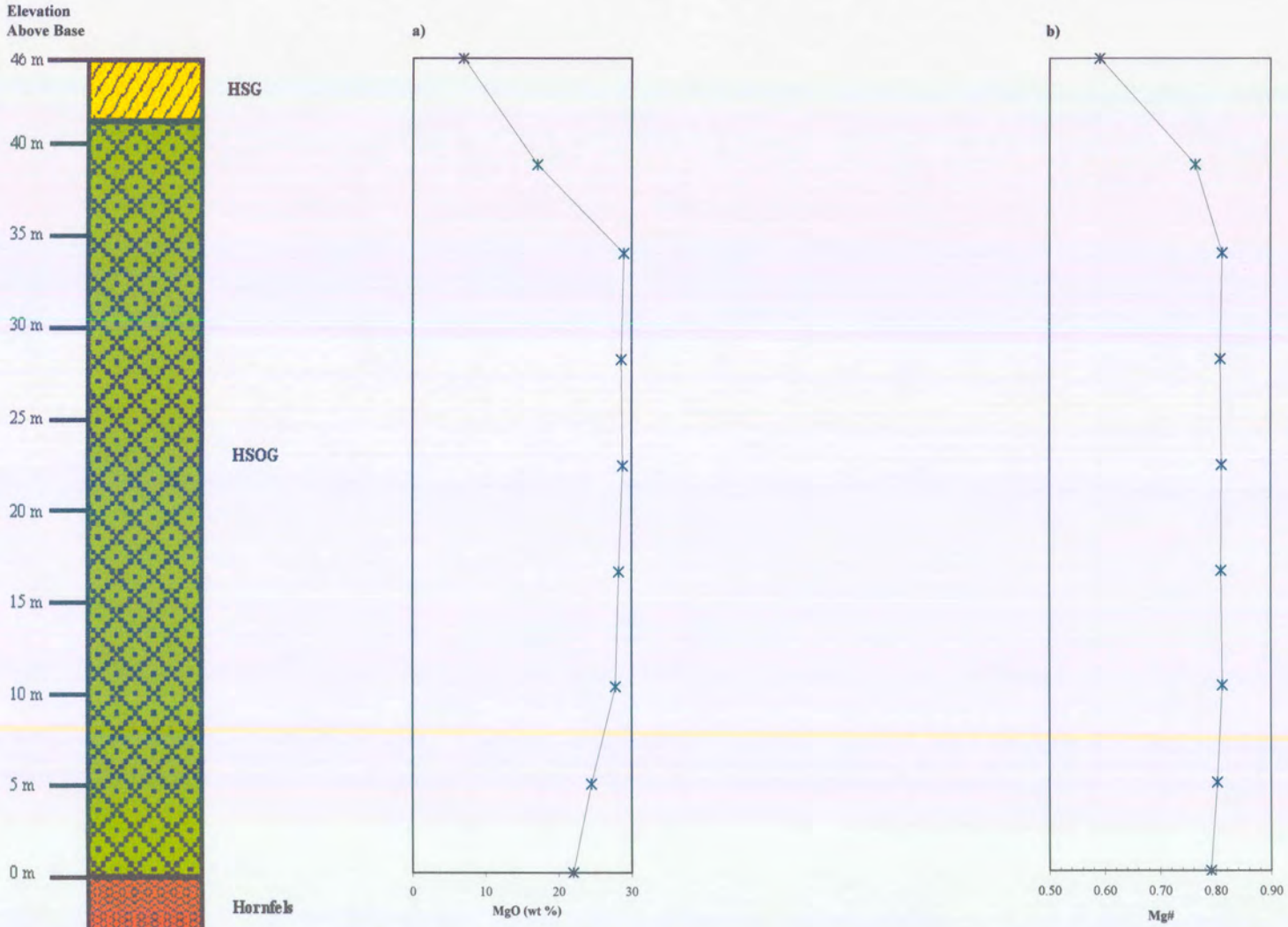

Figs. 5.5 (a)-(k): Compositional variation versus EAB in the Horseshoe lobe

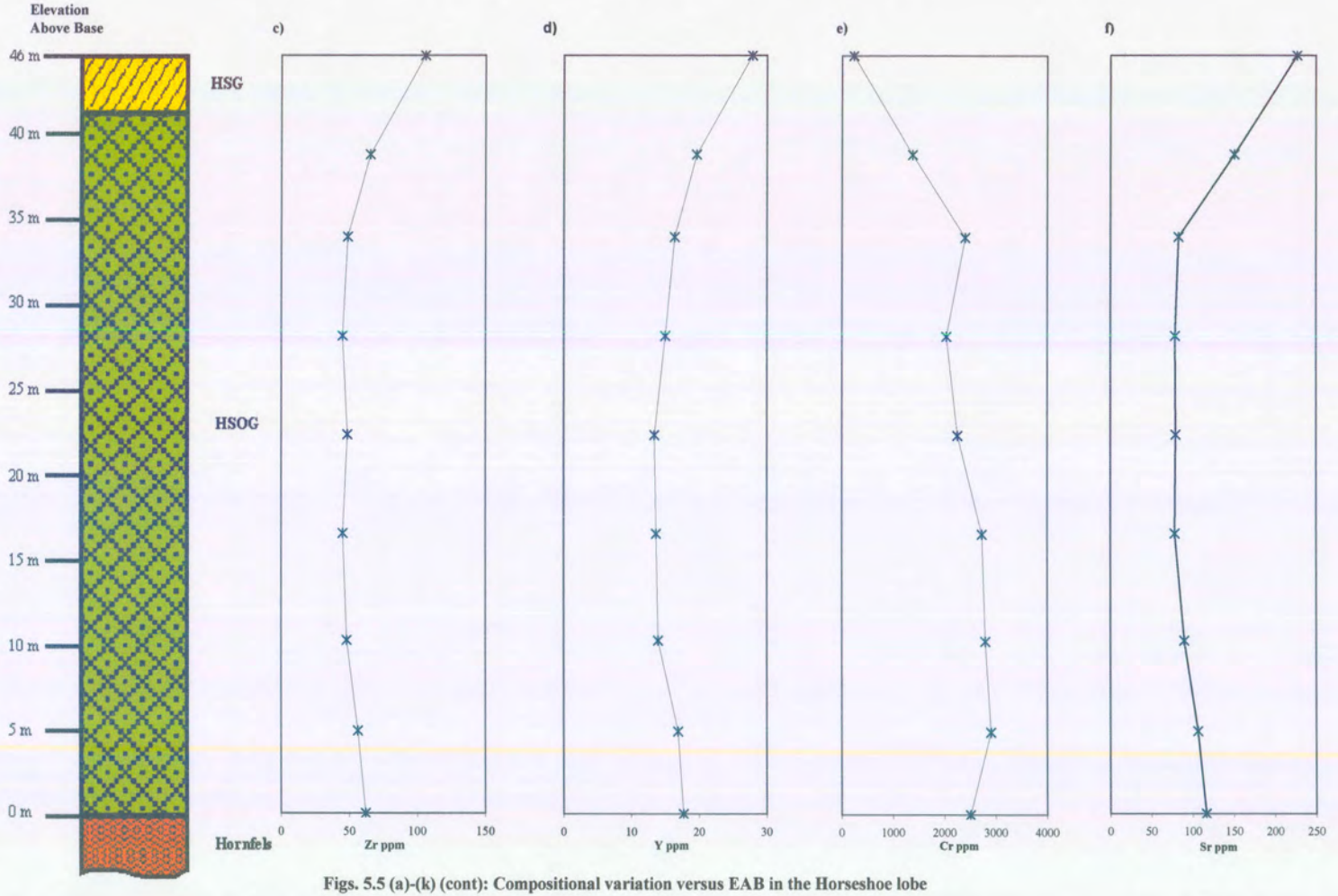

Figs. 5.5 (a)-(k) (cont): Compositional variation versus EAB in the Horseshoe lobe

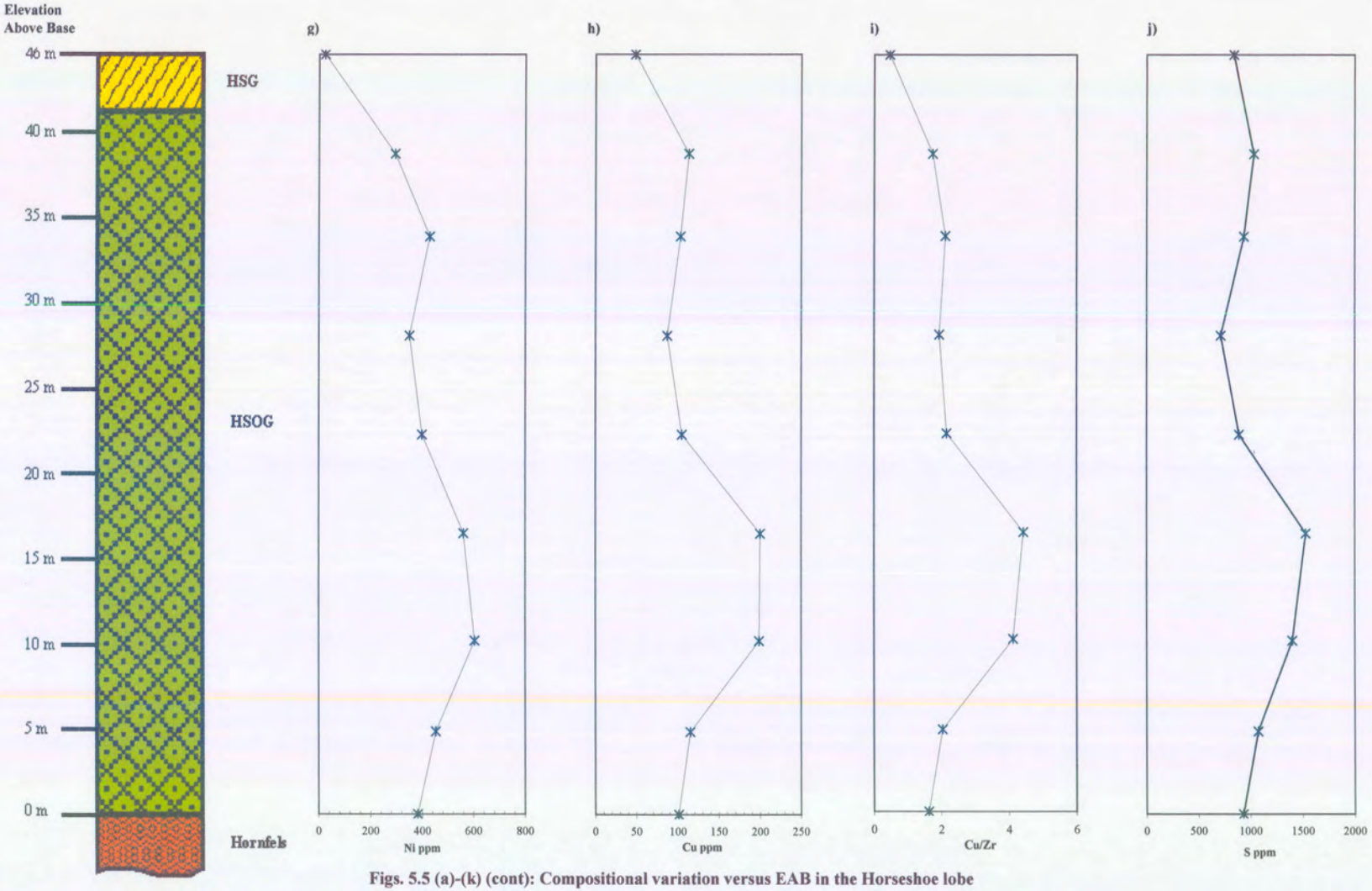

Figs. 5.5 (a)-(k) (cont): Compositional variation versus EAB in the Horseshoe lobe

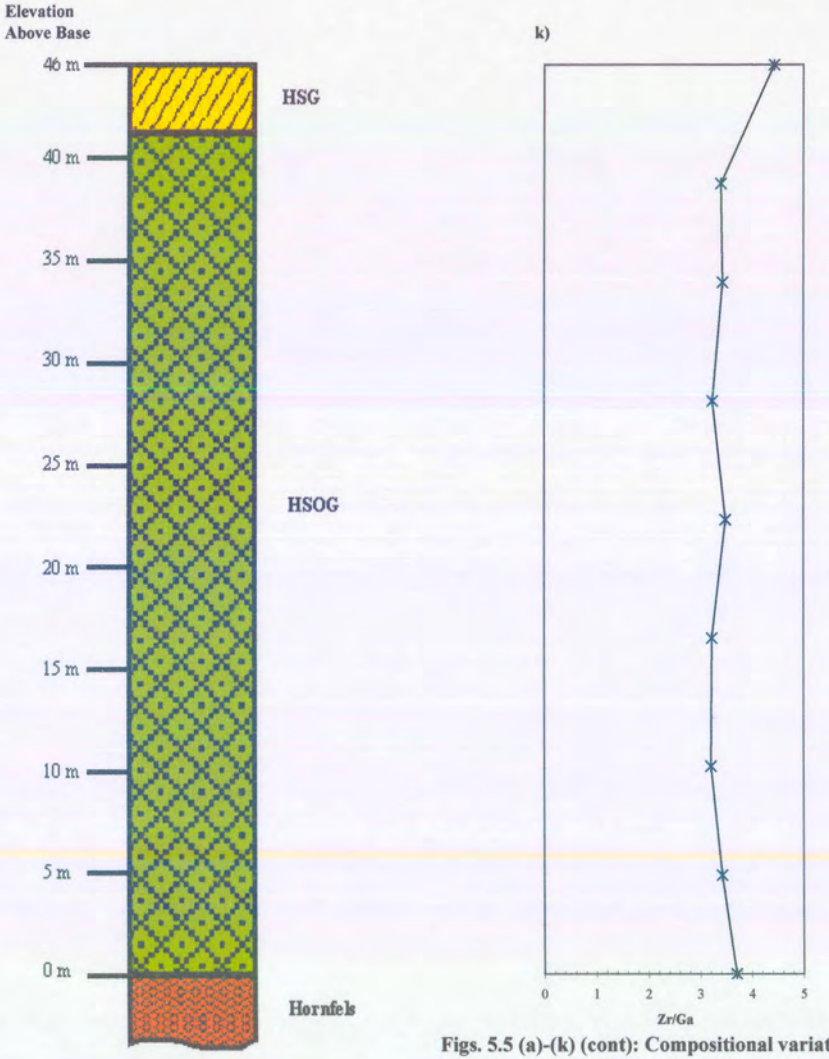

Figs. 5.5 (a)-(k) (cont): Compositional variation versus EAB in the Horseshoe lobe

the PU, COG, CG and the UOG units of the Ingeli lobe are not developed at Horseshoe.

Zr and Y (figs. 5.5 c-d) show similar trends as in the Ingeli lobe, with elevated values at the base and the top of the intrusion, and lower values in the central part of the intrusion. Estimated trapped melt proportions are around 50 % in the HSOG assuming Karoo dolerite as parental magma.

The concentrations of Cr and Sr closely match those of olivine and plagioclase, respectively.

Ni, Cu and S (figs. 5.5 g, h and j) show a distinct peak at 10-15 m above the base of the intersection. Based on the Cu/Zr ratio, it is evident that most of the HSOG is enriched in Cu relative to Zr, with values between 1.5 and 4.5. These values are similar to those observed in much of the BOG and PU of the Ingeli lobe, but the high values seen towards the top of the PU in the Ingeli lobe are not observed at Horseshoe.

Zr/ Ga ratios are between 3 and 4, similar to the BOG unit in the Ingeli lobe and possibly suggesting a common lineage between the two lobes.

6. Stream Sediment Geochemistry

6.1 Introduction

In the late autumn and early winter of 2000, Falconbridge Ventures of Africa conducted a regional stream sediment survey over a known area of mineralization in the MAC, in the Waterfall Gorge area and eleven other streams around the Insizwa lobe.

The objectives were as follows:

1. To determine which sample type and elements (or combination of elements) give the best contrast and longest dispersion. To this effect, three sieved fractions (-75, +75-180, and +180-250 microns) and a panned concentrate were taken at each sampling site.
2. To investigate the dispersion of sulphide and gossanous grains and check the potential for hydromorphic anomalies.
3. To assess the possibility of detecting ultramafic lithologies from stream sediment data.
4. To establish a minimum sampling density and devise a sampling strategy for a regional survey including recommendations for sample collection, analysis and interpretation.

The results of that study are summarized in Pedley (2000).

The objectives of using stream sediments in the present study are as follows.

1. To delineate areas of possible ultramafic lithologies (since these lithologies are the most likely hosts of magmatic sulphide deposits).

2. Using Pedley (2000) as a model, to try and pinpoint areas of sulphide mineralization that may have been missed during the initial mapping around the Ingeli lobe.

An orientation stream sediment survey was conducted from late September through October of 2000 during the wettest part of spring, with the idea of letting the fresh rains flush the organic materials in the stream beds farther off the lobe. Thirty-three stream sediment samples were collected by sieving around the Ingeli lobe and these were analysed by XRF at the University of Pretoria. All analyses are listed in Appendix (IV). Low totals (those below 98%) are most likely caused by high loss on ignition and fusing of the samples for extended periods of time to dissolve chromite particles (Loubscher, personal communication March, 2001). Fig. 6.1 shows a map of the sampling sites around the Ingeli lobe. Nine samples were further studied using ICP-OES to detect trace amounts of Pt and Pd and these results can also be found in Appendix (IV). Two size fractions were collected at each stream site; the -250 to + 75, and the -75 micron fraction. Only 1st order streams (the smallest streams), and 2nd order streams (those that are formed by the joining of two 1st order streams) where sampled in this survey. 3rd order streams (streams that are formed by the joining of two 2nd order streams) and decoupled streams (where the stream channels get wider downstream, and an alluvial flood plain is developed) were not sampled. In the latter case a geochemical signal of a sulphide occurrence may not be detected in the sediment because it never enters the stream channel (Fletcher 2000)).

Figure 6.1: Stream sediment sample localities

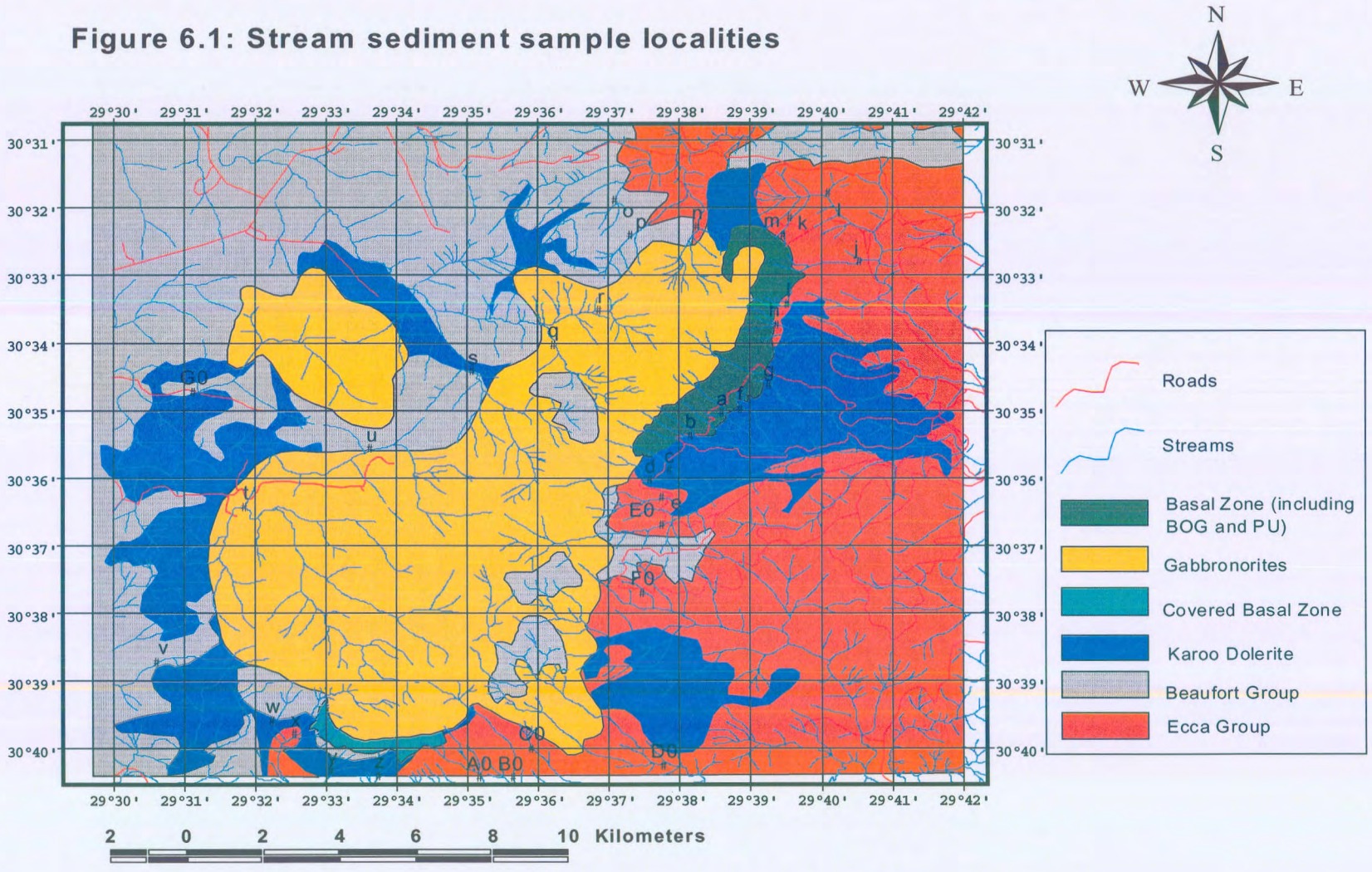

6.2 Sampling Procedure

A brief description of each stream is given in Appendix IV. Samples were taken from 1st and 2nd order streams, in the following environments: (i) fast moving shallow riffle areas, (ii) between boulders, (iii) beneath small waterfalls from the coarse washed sediment and (iv) other areas where hydrodynamic "traps" could be distinguished, i.e., behind large boulders or potholes in the bedrock (Plate 22). Most samples were collected within 1000 m of the contact with the floor rocks, as tenors drop off dramatically beyond that distance (Pedley 2000).

All sieving was carried out in the field (except two streams where sieving was done at Falconbridge Ventures of Africa). All material was wet sieved in the streams using 20 cm diameter, stainless steel "Scapa Test Sieves" (Plate 23). Bulk samples were first run through the 2000 micron fraction to remove pebbles, then through the 250, and 75 micron fraction sieves to give the 2 fractions collected. Material that had been sieved into the two size fractions was placed into thick, 2 litre polythene bags, and left to settle. When settling had occurred, most of the water could be drained off and the sample could then be dried by leaving it in the open air for 2-3 days. Dried samples were then placed in small polythene bags, ready for analysis.

Plate 22: Typical 2nd order stream that was sampled around the Ingeli lobe.

Plate 23: Sieving process using the 2000 micron sieve to get rid of the larger grain fraction.

Panned concentrates were not collected because Pedley (2000) and other workers (Stendal and Theobald, 1994) have reported problems with the "nugget" effect, which may lead to erratic Pt and Pd values.

6.3 Different Methods of Analysis

Major and minor elements were determined by XRF. Pt and Pd were determined by ICP-OES at Set Point Technologies. The detection limit for this technique for Pt and Pd is <10 ppb. Partial analysis techniques, using aqua regia and dilute hydrochloric acid, are commonly used to detach weakly bonded metal ions in order to improve the contrast between the metal in sulphide and the metal found in silicates. However, Chao and Sanzalone (1977) found that these methods may cause partial destruction of the silicate matrix if the samples are taken from highly weathered areas. Pedley (2000) found this to be true and the contrast between total analysis and partial analysis was not significant. Therefore, in this study total analysis is used to reduce cost and to attain higher precision. The -75 micron fraction produced the most reliable results. Often, silicates containing Ni are not broken down and are concentrated in the larger size fraction. These silicates produce high Ni background values that may prevent the detection of sulphides. In contrast, base metals tend to be quickly broken down and are concentrated in the -75 micron fraction. This is even more applicable in environments where the rates of weathering and erosion are high (Butt, 1995).

6.4 Fe and Mn Oxides

Metals in solution that have been derived from buried sulphides may precipitate in streams on amorphous oxides of Fe and Mn. These oxides can give misleading positive or negative anomalies. To account for these anomalies it is usually desirable to selectively extract those metals (Ni, Cu and Co) which are loosely attached using a technique like an enzyme leach. However, in an environment such as the Basal Zone of the MAC and where silicate weathering is intense, the interpretation of an enzyme leach is difficult (Peachy and Allen, 1977). Pedley (2000) found that around the Insizwa lobe partial extraction produce results that were similar to total extraction methods, and thus it was felt that a total extraction method is adequate for a large-scale orientation survey such as the one conducted here.

6.5 Binary Variation Diagrams

The thirty-three stream samples were broken into different groupings based on the lithology the stream drained before it made contact with the floor rocks. The three stream types include: BZS (Basal Zone streams), CBS (Covered Basal Zone streams), and GNS (gabbronorite streams). The concentration data for various elements in the stream sediment samples are plotted in the diagrams (Figs. 6.2 a-c).

Figure 6.2 a shows a positive correlation between Cu and Co. It appears that most streams draining Basal Zone rocks have Cu and Co values above background

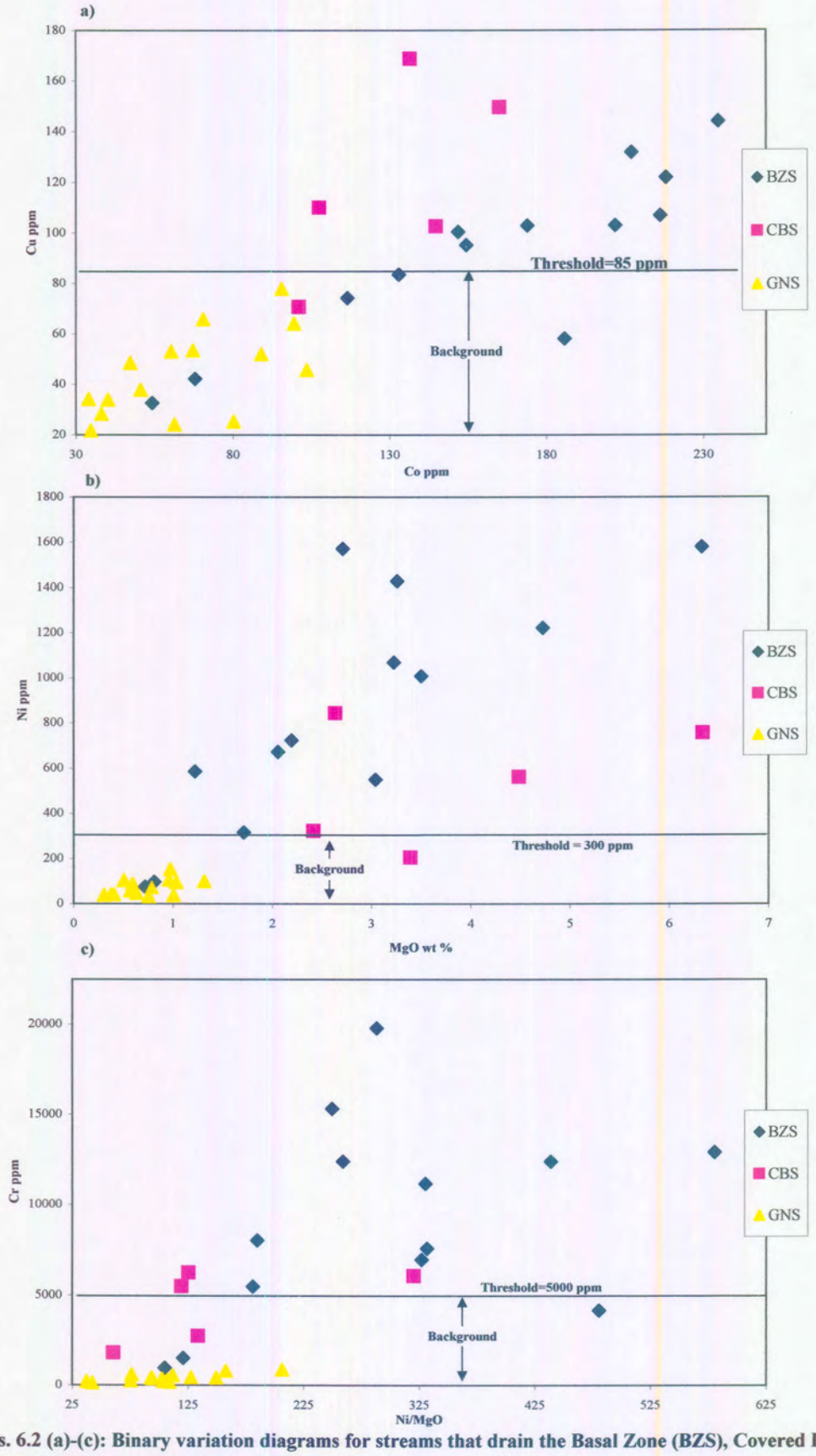

Figs. 6.2 (a)-(c): Binary variation diagrams for streams that drain the Basal Zone (BZS), Covered Basal Zone(CBS), and Gabbronorites (GNS)

values. The background value (the normal range of concentrations for an element in an area excluding mineralized samples) (Levinson, 1974)) seems to be composed of nearly all (GNS) samples. If the threshold (upper limit of normal background for a particular element) is placed at 85 ppm Cu, then the plot is most likely showing anomalous values coming from cumulus sulphides of the Basal Zone rocks.

Figures 6.2 (b)-(c); show a good correlation between Ni and MgO and between Cr and Ni/MgO indicating that Ni and Cr contents are useful to delineate areas that are composed of ultramafic lithologies. The two samples from the BZS that plot with the gabbronorites through all of the binary variation diagrams drain first the Basal Zone, then dolerite, and then possibly the floor rocks which appear to have diluted the Ni, Cu, Co, and Cr contents.

6.6 Pt and Pd

Figures 6.3 (a)-(c) show bar graphs of Pt and Pd plotted with Cu, Ni/MgO and Co in the nine selected streams. The six BZS streams all have higher Pt and Pd tenors than the 3 GSN streams. The elevated Pt and Pd values of stream j, with 205 ppb Pt, and 100 ppb Pd, are of particular interest and may indicate an enhanced potential for Ni-Cu-PGE mineralization of the Waterfall Gorge type.

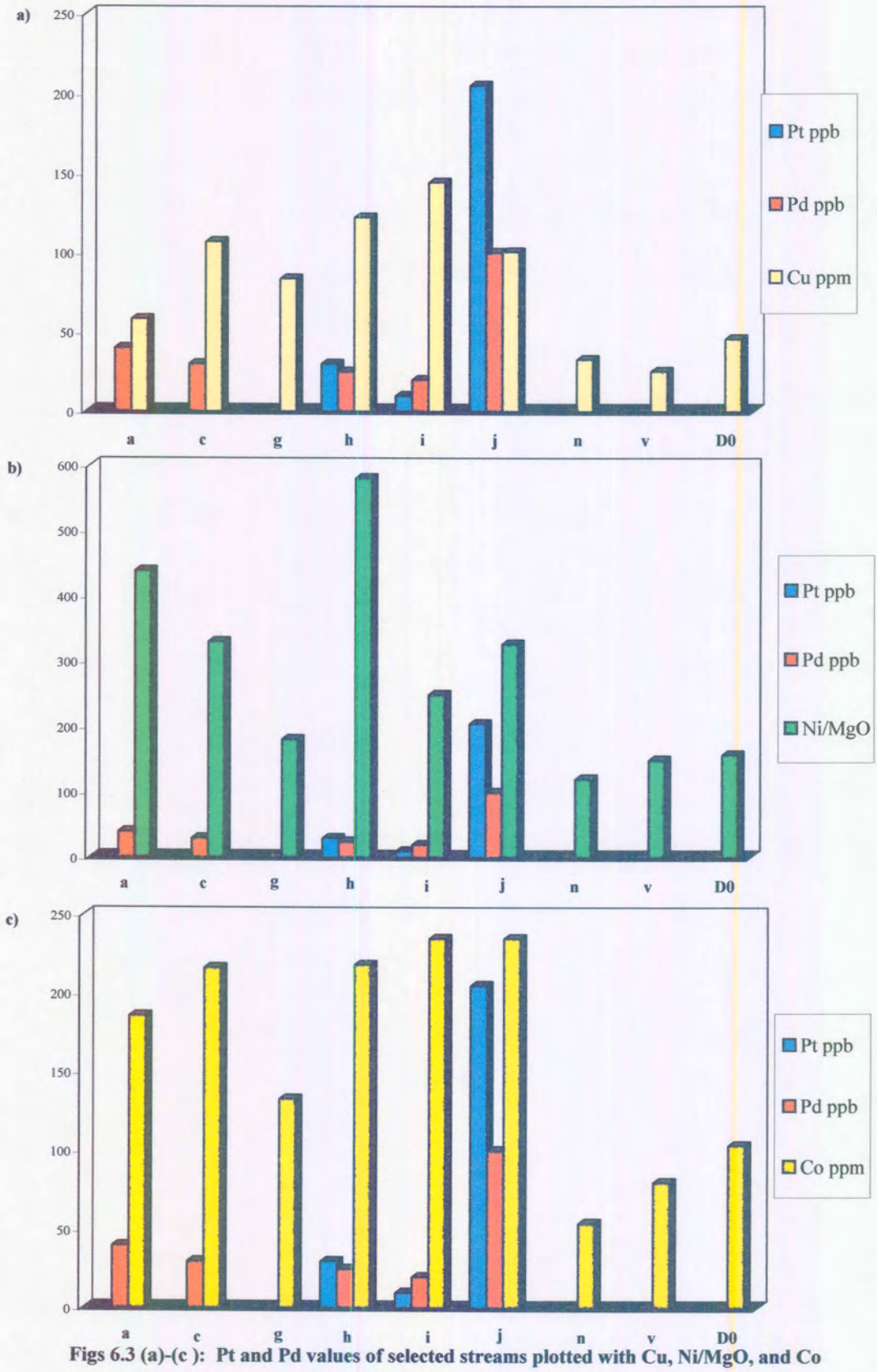

Figs 6.3 (a)-(c): Pt and Pd values of selected streams plotted with Cu, Ni/MgO, and Co

7. DISCUSSION

7.1 Introduction

Past workers on the Mount Ayliff Complex have used whole rock geochemistry, mineral chemistry, Sr isotopes and geophysics to formulate numerous models on the shape, size and regional extent of the Complex and on the nature of the parent magmas. In the following compilation I first present a summary of the different models proposed and how they may be applied to the Ingeli and Horseshoe lobes. I will then evaluate the potential of the Ingeli and Horseshoe lobes for magmatic Ni-Cu-PGE sulphide ores.

7.2 Lithological Comparison between the Different Lobes of the MAC

The rocks of the MAC can be sub-divided into three zones: The Basal Zone is comprised of olivine rich rocks. The Central Zone consists mainly of gabbronorites which comprise most of the preserved mountain masses. The Roof Zone is comprised of granites, quartz diorites, and monzonites (Scholtz, 1936) and is eroded in many parts of the complex.

The rocks of the Basal Zone consist of four sub-units: A chilled basal contact zone, a basal olivine gabbronorite, a lherzolite (PU), and a troctolite unit. The chilled contact zone and the troctolite are exposed at Insizwa, Tabankulu and Ingeli (Maske, 1966) but were not found in the Tiger Hoek Peak traverse or in the Horseshoe lobe. This is possibly partly due to poorer exposure (e.g. the absence of adits). The Horseshoe lobe is made up almost entirely of olivine melagabbro,

with little lherzolitic or gabbroic rocks. It is therefore lithologically distinct from the other lobes. In the Ingeli lobe, the basal olivine gabbronorite is much thicker than at Tabankulu or Insizwa, (150 m versus 10-25 m, (Lightfoot and Naldrett, 1983)), The overlying lherzolite unit makes up the bulk of the Basal Zone rocks and is developed at Insizwa, Ingeli (where it is called the PU unit), Tonti, and Tabankulu. The thickness of the lherzolite appears to be broadly similar in the four lobes (e.g. Lightfoot (1984), Maier (2002)), but considerable internal variation in thickness in the Insizwa lobe has been documented by Marsh and Allen (2002).

The gabbronorites of the Central Zone can reach 150 m at Tabankulu (Lightfoot and Naldrett, 1983) and over 600 m at Insizwa (Maier et al. 2002). At Ingeli, the Central Zone rocks at Tiger Hoek Peak are found to be over 300 m thick but it appears likely that the top contact of the Central Zone has been eroded in places not capped by the Roof Zone. In the Horseshoe lobe, gabbroic rocks make up less than 5 m of the intrusion.

The Roof Zone was found by Scholtz (1936) and Maske (1966) to be located only on the top of the Insizwa and Ingeli lobes. The best development of this rock type is found at Ingeli Peak, where it is found to be approximately 60 m thick (Maske, 1966).

Basal sulphides have been found in the Insizwa lobe, primarily at Waterfall Gorge, at Tabankulu, Tonti (unpublished company reports) and in the Horseshoe lobe. No basal sulphides were found in the Ingeli lobe, but the stream sediment survey suggests that the Basal Zone at Ingeli is enriched in Cu relative to the Central Zone, suggesting the presence of sporadic basal mineralization in this lobe as well.

In summary, the present study confirms that there are considerable lithological similarities between the Insizwa, Ingeli, Tonti and Tabankulu lobes, but that the Horseshoe lobe forms a distinct type of intrusion characterized by much reduced thickness and a more primitive bulk composition.

7.3 The Nature of the Parental Magma

In figures 7.1a-d and 7.2 a-c the data from the Basal Zone of the Insizwa lobe are plotted with those from Ingeli, Tonti and Horseshoe. Most samples plot on a common olivine control line, suggesting that the Basal Zone cumulates crystallized from a common parental magma of Karoo dolerite composition. The estimate of parental magma comes from Marsh and Eales (1984) and is the most sensible choice because it is derived from a large amount of spatially widely distributed samples and because it appears to be coherent with most of the observed compositional variation. Some of the more evolved samples from Insizwa appear to plot on a slightly different olivine control line than the other data from the other lobes, possibly due to the presence of cumulus plagioclase and

clinopyroxene. The present data provides no evidence for the presence of a high-MgO basaltic magma in the Mount Ayliff Complex as suggested by Cawthorn (1980), Tischler (1981), Cawthorn et al. (1985), and Cawthorn et al. (1992).

7.4 Interconnectivity of the Lobes of the MAC

Scholtz (1936) suggested that the lobes of the MAC were originally interconnected prior to erosion. The present study supports this model, in that both the Ingeli and the Insizwa lobes show a distinct peak in Cu contents towards the top of the Basal Zone (Fig. 7.3). The similarity in the patterns could be explained by similar (magmatic or hydrothermal) processes in the interconnected intrusion. In contrast, the occurrence of such a very similar Cu distribution pattern in two unrelated intrusions would seem to be too much of a coincidence.

7.5 Flow Direction of Magmas in the MAC

Olivine compositional data (Fig. 7.4) shows that olivine from Horseshoe and Tabankulu are depleted in Ni relative to Fo contents, while those from Insizwa and Ingeli are relatively undepleted. If the lobes crystallized from a common magma then one could suggest that the magmas streamed from north to south, becoming progressively more depleted in Ni due to localized sulphide segregation in the chamber. This is in agreement with the interpretations of Ferre et al. (2002).

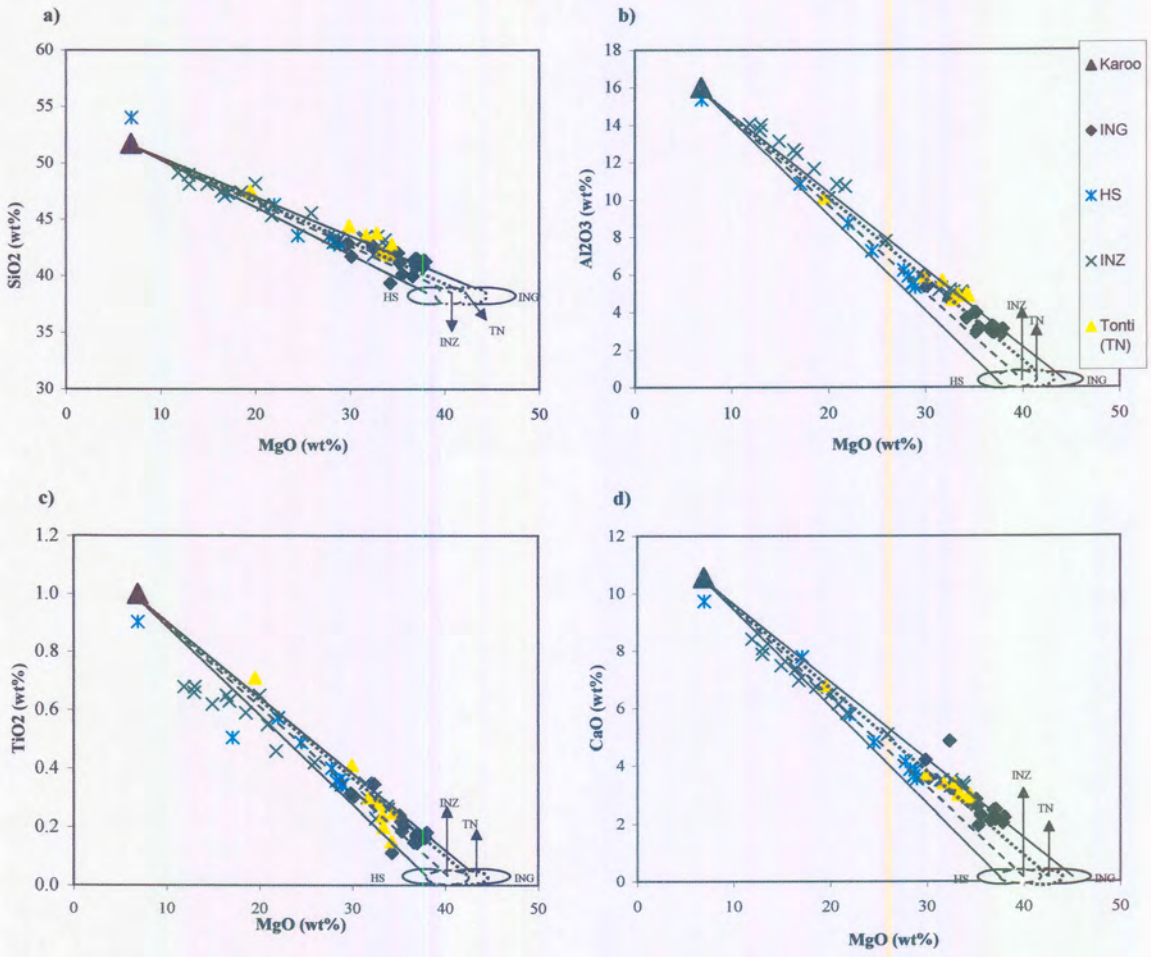

Fig. 7.1 (a)-(d) Major-element geochemistry of the Basal Zone of the Insizwa (INZ) and Tonti (TN) lobes plotted with data from the Ingeli and Horseshoe lobes. Open circles indicate approximate compositional range of olivines from the different Mount Ayliff lobes. TN data is from Cawthorn et al. (1992). INZ data is from Lightfoot and Naldrett (1984) and Cawthorn et al. (1992)

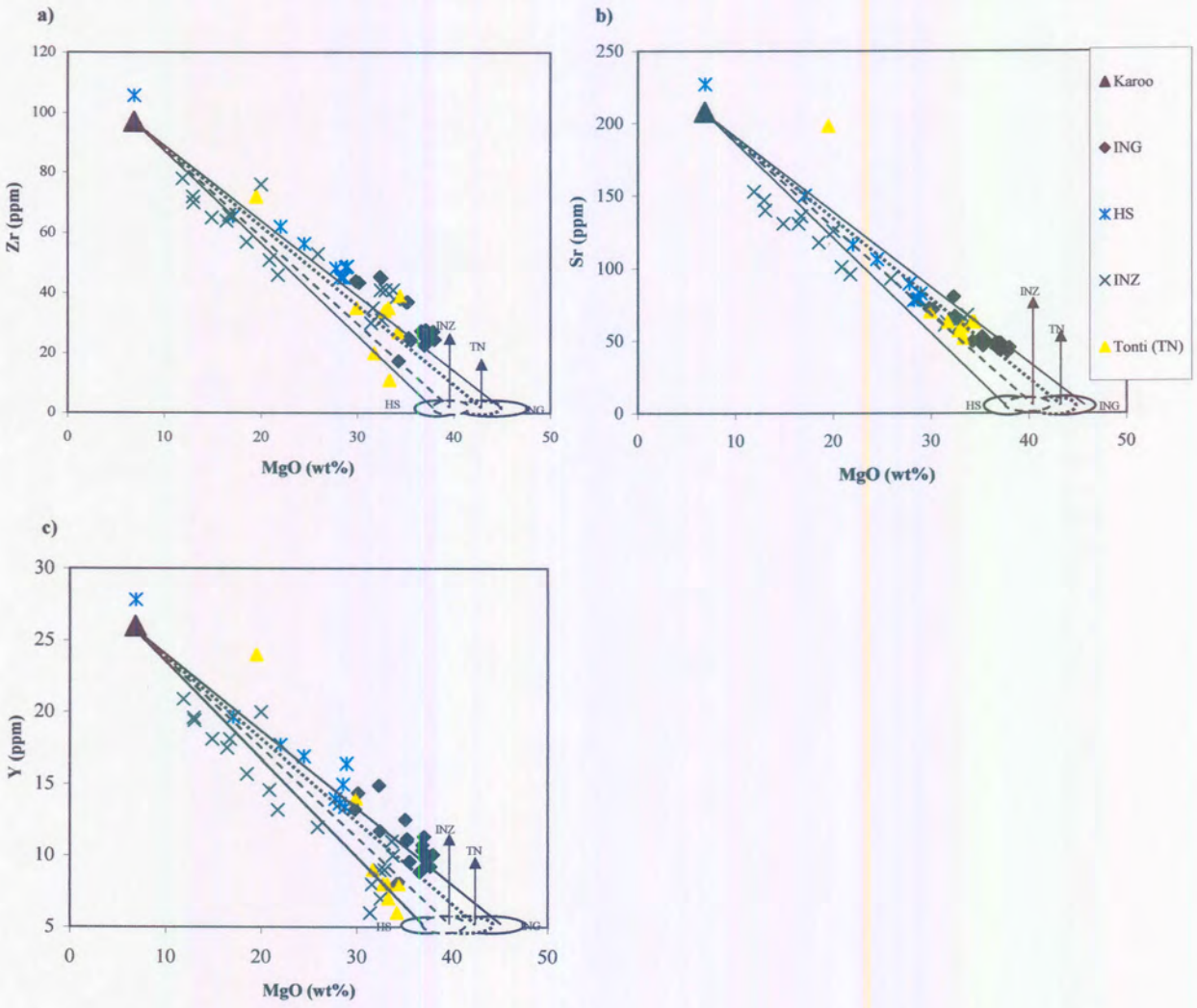

Fig 7.2 (a)-(c) Minor element geochemistry of the Basal Zone of the Insizwa (INZ) and Tonti (TN) plotted with data from the Ingeli and Horseshoe lobes. Open circles indicate approximate compositional range of olivines from the different Mount Ayliff lobes. TN data is from Cawthorn et al. (1984). INZ data is from Lightfoot and Naldrett (1984) and Cawthorn et al. (1992).

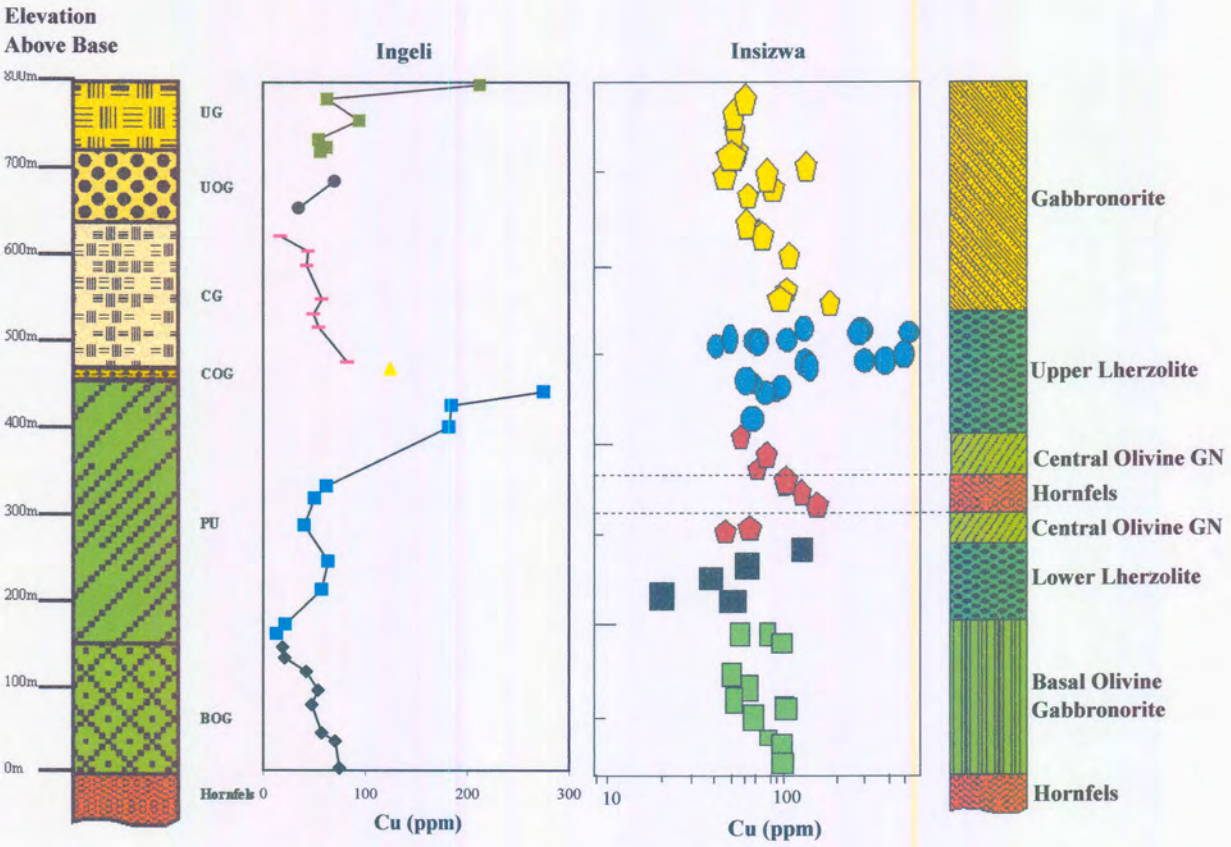

Fig. 7.3 Cu variation in borehole INS96-02 of the Insizwa lobe, compared to data from Ingeli. Diagrams show Cu enrichment at the top of the Basal Zone in both lobes. Insizwa diagram addapted from Marsh and Allen (2002).

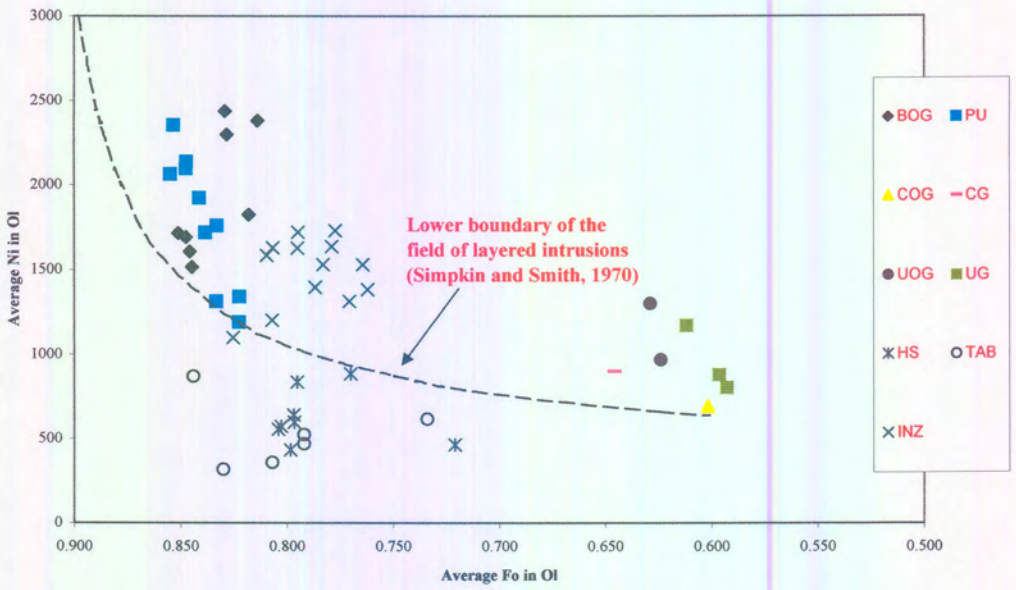

Fig. 7.4 Plot of Ni concentration versus forsterite content for olivine from Waterfall Gorge (INZ) and Tabankulu (TAB) Basal Zone units plotted with data from the Ingeli, and Horseshoe lobes. INZ and TAB data from Lightfoot and Naldrett (1983, 1984).

7.6 Open or Closed System Crystallization?

Scholtz (1936) argued that the Mount Ayliff Complex crystallized as a closed magmatic system. In contrast, Marsh and Allen (2002) suggested that the variable Sr-isotope ratios imply that the Insizwa lobe was a large open magmatic system that saw repeated injections of fresh magma that deposited the cumulate crystals while the melt moved on elsewhere. The data presented in the present study show that there is an absence of highly evolved rocks (SiO_2 > than 60 %) in the Horseshoe and Ingeli lobes. Further, the Horseshoe lobe is made up mostly of ultramafic rocks, capped by a thin layer of gabbro. This is best explained by a model whereby the lobe was formed by repeated influxes of primitive magma that precipitated the cumulates, while the residual melt was flushed out, i.e. an open magmatic system. Finally ratios of incompatible trace elements show considerable variation in different units of the Ingeli lobe (Fig 5.4) possibly indicating the intrusion of compositionally contrasting magmas.

7.7 The Origin of the Crustal Component

Scholtz (1936), Cawthorn (1980) and Tischler (1981) suggested that the parental magmas that formed the Basal Zone of the Complex were contaminated with a crustal component. They used as evidence the relatively high SiO_2, Na_2O and K_2O contents found in the chilled marginal zone. The presence of a crustal component is confirmed by high Sr-isotopic ratios (Maier et al. 2002). Incompatible trace element ratios in the Ingeli lobe suggest that within the ultramafic rocks there are

some subtle compositional variations, with the basal rocks having the largest crustal component (Figs. 5.4 q-v). Kerrich and Wyman (1996) argue that crustal contamination of primitive magmas is apparent on primitive mantle normalized diagrams from the conjunction of Nb (Ta), P, and Ti depletions. The Basal Zone rocks of the Ingeli lobe do show depletions in Nb, and Ti, indicating a crustal component (Figs. 5.3 a-b). However, it is less clear whether the crustal component originates from crustal assimilation within the Ingeli chamber, assimilation before emplacement, or whether the parental magmas represent partial melts of enriched continental lithosphere. Maier et al. (2002) proposed in situ contamination, while Lightfoot and Naldrett (1984) favored contamination prior to emplacement, and Marsh and Eales (1984) favored a lithospheric mantle source.

7.8 The Potential for Sulphide Ores; in the Ingeli and Horseshoe lobes, MAC

Naldrett (1999) indicated that there are a number of geological features that are common to many of the world's largest Ni-Cu sulphide deposits. These are: (i) a parental magma of basic-ultrabasic composition that crystallized large amounts of olivine, (ii) The abundance of sulphur in the adjacent country rocks, (iii) evidence of depletion of chacophile elements in the host silicate magmas, (iv) interaction of the silicate magma with the country rocks, e.g. the presence of country rock xenoliths in the magma, (v) the occurrence of mineralization within or close to a magma conduit.

In the MAC, several of these criteria are met, i.e., the intrusions are interpreted as sub-volcanic staging chambers to the Karoo flood basalts, they contain thick olivine cumulate units, metal depletion is evident in some, but not all, of the lobes, and interaction with the country rocks is documented by the presence of xenoliths, notably at the Waterfall Gorge Ni-sulphide occurrence (Lightfoot and Naldrett 1984).

However, one critical component seems absent, i.e. the abundance of sulphides in the country rocks. As a result, localized partial melting of the sediments produced small-scale sulphide segregation (Maier et al. 2002), possibly due to the lowering of the S-solubility in response to the addition of SiO_2 to the magma (Irvine, 1975), but large-scale sulphide segregation failed to occur.

However, stream sediment data collected around the Ingeli lobe suggest that streams h, i and j are enriched in metals and could be examined in more detail for a localized event like that of Waterfall Gorge type in the Insizwa lobe.

There are several small showings of sulphides at the base of the Horseshoe lobe. In addition, the whole-rock and olivine compositions are strongly depleted in Ni. This indicates that the floor rocks of the Horseshoe lobe may offer a better potential for sulphide ores than the Ingeli lobe. However, the lack of Co depletion in the ultramafic rocks suggests that any sulphide segregation event that did occur

8. Conclusions

This work has presented the results of a petrographical, lithological, lithogeochemical, and stream sediment investigation of the Ingeli and Horseshoe lobes of the Mount Ayliff Complex (MAC) in the Eastern Cape, South Africa. Comparisons were made to the other lobes of the MAC, particularly with regard to the potential of the intrusions to host magmatic Ni-Cu-PGE sulphide ores of economic importance.

Based on their lithologies, the Ingeli, Insizwa, Tabankulu and Tonti lobes appear to be genetically related to each other. The Horseshoe lobe is of much reduced thickness and its bulk composition is more mafic than that of the other lobes.

On the basis of whole-rock geochemistry, it appears that the magmas that formed the MAC were of Karoo dolerite lineage. The intrusions were formed from multiple injections of this magma but accumulated variable amounts of olivine.

Some localized contamination with country rocks caused isolated sulphide segregation. As a result, the magmatic sulphide potential at the MAC is probably small. However, stream sediment data from Ingeli indicates the possible presence of sulphide ores in the Basal Zone of that lobe.

References:

Bruynzeel, D., 1957, A petrographic study of the Waterfall Gorge profile at Insizwa: University of Stellenbosch Annals, v. 39, p. 341-360.

Butt, C.R.M.,1995, Geochemical exploration for base-metals in deeply weathered terrain. Co-operative research Centre for Landscape Evolution and Mineral Exploration, CSIRO Exploration and Mining, Perth, Australia.

Cawthorn, R.G., 1980, High-MgO Karoo tholeiite and the formation of the Ni-Cu sulphide mineralization in the Insizwa intrusion, Transkei: South African Journal of Science, v. 76, p. 467-470.

Cawthorn, R.G., and Groves, D.I., 1985, Magnesian ilmenite: clue to high-Mg parental magma of the Insizwa complex, Transkei: Canadian Mineralogist, v. 23, p. 609-618.

Cawthorn, R.G., de Wet, M., Maske, S., Groves, D.I., and Cassidy, K.F., 1986, Nickel sulphide potential of the Mount Ayliff intrusion (Insizwa Complex), Transkei: South African Journal of Science, v. 82, p. 572-576.

Cawthorn, R.G., Sander, B.K., and Jones, I.M., 1992, Evidence for the trapped liquid shift effect in the Mount Ayliff intrusion, South Africa: Contributions to Mineralogy and Petrology, v. 111, p. 194-202.

Cawthorn, R.G., and Kruger, F.J., 2002, Sulphide genesis in the Insizwa Intrusion, South Africa: Geochemical Constraints: Abstract for International Platinum Symposium, unpublished.

Chao, T.T., and Sanzalone, R.F., 1977, The chemical dissolution of sulphide minerals: The Journal of Research of the U.S. Geological Survey, v. 5, No. 4, July- Aug. p. 409-412.

DeDecker, R.H., 1981, Geology of the Kokstad area. 1:250 000 Geological Sheet 3028 Kokstad and explanation: Geological survey of South Africa, Pretoria.

Dodd, D., 2000, Insizwa joint venture project final report on exploration activities from 1995 to 2000: Falconbridge Ventures of Africa (proprietary Limited), Bulletin S 571.

Dowsett, J.S., and Reid, N.T., 1967, An exploration programme for Nickel and Copper in differentiated intrusives of East Griqualand and Pondoland: Transactions of the Geological Survey of South Africa, v. LXX, p 67-79.

Du Toit, A.L., 1910, Report on the Cu-Ni deposits of the Insizwa intrusion, Mount Ayliff, East Griqualand. 15th Annual Report, Cape of Good Hope Geological Communications, Department of Mines, Cape Town, pp.111.

Eales, H.V., Marsh, J.S., 1979, High-Mg tholeiitic rocks and their significance in the Karroo Central Province: South African Journal of Science, v. 75, p. 400-404.

Ferre, E.C., Bordarier, C., Marsh, J.S., 2002, Magma flow inferred from AMS fabrics in a layered mafic sill, Insizwa , South Africa: Technophysics, *in press.*

Fletcher, W.K., 2000, Lecture notes. Advances in design and interpretation of stream sediment surveys: 5th International Symposium on Environmental Geochemistry, unpublished.

Harmer, R.E., 2000, Unpublished report: Economic Geology Department, Council for Geoscience, Pretoria, South Africa.

Irvine, T.N., 1975, Crystallization sequences of the Muskox intrusion and other layered intrusions. II. Origin of Chromite layers and similar deposits of other magmatic ores. Geochimica et Cosmochimica Acta 39, p. 991-1020.

Karpetra, W.P., and Johnston, M.R., 1979. The geology of the Umtata area: sheet 3128, scale 1:250 000. Geologic Survey of South Africa, Pretoria.

Kerrich R., and Wyman D.A., 1996, The trace element systematics of igneous rocks in mineral exploration: an overview, In Wyman, D.A., ed., Trace Element Geochemistry of Volcanic Rocks: Applications for Massive Sulphide Exploration: Geological Association of Canada, Short Coarse Notes, v. 12, p. 1-50.

Le Maitre, R.W., Bateman P., Dudek, A., Keller, J., Lameyre, J., Le Bas, M.J., Sabine, P.A., Schmid, R., Sorensen, H., Streckeisen, A., Wooley, A.R. and Zanettin, B. (1989) A classification of Igneous rocks and Glossary Terms: Recommendations of the International Union of Geological Sciences Subcommission on the Systematics of Igneous Rocks. Blackwell Scientific, Oxford.

Levinson, A.A., 1974, Introduction to Exploration Geochemistry, Second Edition. Applied Publishing Ltd., Illinois.

Li, C., and Naldrett, A.J., 1998, Geology and petrology of the Voisey's Bay intrusion: reaction of olivine with sulphide and silicate liquids: Lithos, v. 47, p. 1-31.

Lightfoot, P.C., and Naldrett, A.J., 1983, The geology of the Tabankulu section of the Insizwa Complex, Transkei, Southern Africa, with reference to the nickel sulphide potential: Transactions of the Geological Society of South Africa, v. 86, p. 69-187.

Lightfoot, P.C., and Naldrett, A.J., 1984, Chemical variation in the Insizwa Complex, Transkei, and the nature of the parent magma: Canadian Mineralogist, v. 22, p. 111-123.

Lightfoot, P.C., Naldrett, A.J. and Hawksworth, C.J., 1984, The Geology and geochemistry of the Waterfall Gorge Section of the Insizwa Complex with particular reference to the origin of the nickel sulphide deposits: Economic Geology, v. 79, p. 1857-1879.

Lightfoot, P.C., Naldrett, A.J., and Hawksworth, C.J., 1987, Re-evaluation of the chemical variation in the Insizwa Complex, Transkei: Canadian Mineralogist, v. 25, p. 79-90.

Maier, W.D., 1991, Geochemical and petrological trends in the UG2-Merensky unit interval of the upper critical zone in the western Bushveld Complex, unpublished PhD-thesis, Rhodes University.

Maier, W.D., Barnes, S.J., and de Waal, S.A., 1998, Exploration for magmatic Ni-Cu-PGE sulphide deposits: a review of recent advances in the use of geochemical tools, and their application to some South African ores: South African Journal of Geology., v.101, p.237-253.

Maier, W.D., and Li, C., 2000, Magmatic Ni-Cu-PGE sulphide ore deposits: genesis and exploration. In: Maier, W.D., Li. C., de Waal, S.A., and Harmer, R.E., Short course on magmatic Cu-Ni-PGE sulphide deposits, Department of Earth Sciences, University of Pretoria, p.1-61.

Maier, W.D., Marsh, J.S., Barnes, and S.J., Barnes, 2002, The distribution of the platinum-group elements and gold in the Insizwa lobe, Mount Ayliff Complex, South Africa: implications for Ni-Cu-PGE sulphide exploration in the Karoo Igneous Province: Economic Geology, *in press.*

Marsh, J.S., and Eales, H.V., 1984, The chemistry and petrogenesis of igneous rocks of the Karoo central area, Southern Africa. In: Erklank, A.J., ed., Petrogenesis of the volcanic rocks of the Karoo Province, Geological Society of South Africa, Special Publication, v. 13, p. 27-67.

APPENDIX I

Traverse Log of Tiger Hoek Peak, Ingeli Mountain

Height in metres

722.50 - 796.87	Coarse grained plagioclase cumulate (UG)
637.50 - 722.50	Plagioclase cumulate with cumulus olivine (UOG)
471.00 - 637.50	Plagioclase cumulate (CG)
453.50 - 471.00	Plagioclase cumulate with cumulus olivine (COG)
167.18 - 435.50	Massive olivine cumulate (PU)
000.00 - 167.18	Olivine cumulate containing cumulus plagioclase (BOG)

Traverse Log of the Horseshoe Lobe

42.00 - 46.00	Fined grained plagioclase cumulate (HSG)
00.00 - 42.00	Olivine cumulate containing cumulus plagioclase (HSOG)

Modal Analyses

Rock Unit	BOG	BOG	BOG	BOG	BOG	BOG	BOG	BOG	PU	PU	PU	PU
Sample	**IT-3**	**IT-4**	**IT-5**	**IT-6**	**IT-7**	**IT-8**	**IT-10**	**IT-11**	**IT-12**	**IT-13**	**IT-14**	**IT-15**
Olivine	62.5	58.5	65.1	60.5	69.7	67.7	75.7	74.7	77.5	76.2	81.7	78.7
Intercumulus Plag	17.5	21.5	17.4	18	14.5	15.2	13	15.5	9.7	11.7	9.2	6.2
Cumulus Plag	0	1.7	0	0.2	0	0	0	0	0	0	0	0
Orthopyroxene	13.5	10.2	11	13.7	5	8.2	6	3.2	8.5	5.5	3.7	5.7
Clinopyroxene	3	4.5	4.1	5.2	6.2	5.2	3	4	2.2	4.2	2.5	5.5
Mica	1.5	1	0.5	0.7	1.7	1	0	0.2	0.5	0	1	0.2
Orthoclase	0	0	0	0	0	0	0	0	0	0	0	0
Oxides	2	2.5	1.7	1.5	2.7	2.5	2.2	2.2	1.2	2.2	1.7	1.7
Sulfides	0	0	0	0	0	0	0	0	0	0	0	1.7
Quartz	0	0	0	0	0	0	0	0	0	0	0	0
Amphibole	0	0	0	0	0	0	0	0	0	0	0	0
Accessories	0.7	0.2	0.2	0	0.2	0.2	0.7	0.2	0	0.2	0	0

Modal Analyses

Rock Unit	PU	PU	PU	PU	PU	PU	COG	CG	CG	CG	CG	CG
Sample	**IT-16**	**IT-17**	**IT-18**	**IT-19**	**IT-20**	**IT-21**	**IT-22**	**IT-23**	**IT-24**	**IT-25**	**IT-26**	**IT-27**
Olivine	80.2	70.7	78.7	79	84.2	76.2	6	0	0	0	3	1
Intercumulus Plag	8	9.5	4.2	9.7	7	4.7	5.2	1	0.2	0	2	2.7
Cumulus Plag	0	0	0	0	0	0	55.1	77.2	63	61.2	62	57.7
Orthopyroxene	4	12.2	0.7	1.5	2	11.5	14.7	15.2	17.5	12	16	15.7
Clinopyroxene	4.7	4.7	12	6.7	4.7	3.2	18	5.2	19	26.2	17	21.7
Mica	0.2	0	0.2	0	0.2	0.5	0.2	0	0	0	0	0
Orthoclase	0	0	0	0	0	0	0	0	0	0	0	0.2
Oxides	2.5	2.7	3.2	2	1	3.2	0	0.5	0.2	0	0	0.5
Sulfides	0.2	0	0.7	1	0.7	0.5	0	0.7	0.2	0.5	0	0.2
Quartz	0	0	0	0	0	0	0	0	0	0	0	0
Amphibole	0	0	0	0	0	0	0	0	0	0	0	0
Accessories	0.2	0.2	0.2	0	0	0	0	0	0	0	0	0

Modal Analyses

Rock Unit	CG	CG	UOG	UOG	UG	UG	UG	UG	UG	UG	HSG	HSOG
Sample	**IT-28**	**IT-29**	**IT-30**	**IT-31**	**IT-32**	**IT-33**	**IT-34**	**IT-35**	**IT-36**	**IT-37**	**Hs8**	**Hs9**
Olivine	0	4	6	5.5	3.7	2.5	0.5	0.2	0	0.7	0	20.5
Intercumulus Plag	0	0	0	0	0	0	0	0	0	0	0	40
Cumulus Plag	58.7	62.9	66.9	61.7	57.2	63	63.7	60.2	59.2	63.9	57.7	1.2
Orthopyroxene	20.2	14.5	6.7	11.7	5.2	7.2	4.2	10.2	16.5	1.7	1.5	15.2
Clinopyroxene	20.5	17.2	18.2	18	30.2	26.2	29.5	24.7	20.5	29.5	37	21.2
Mica	0	0	0	0	0	0	0	0	0.5	0.2	0	0
Orthoclase	0	1	0.2	2.2	1	0	0.2	1.7	1.7	1	1.5	0
Oxides	0.5	0.2	0.7	0	0	0	0	0.2	0	0	0.5	0.2
Sulfides	0	0	0.5	0.7	1.2	0.2	1.2	0.5	1.5	2.2	1.7	0.7
Quartz	0	0	0	0	0	0	0.2	0.2	0	0.5	1	0
Amphibole	0	0	0.5	0	1.2	0.7	0.2	1.7	0	0	0.2	0
Accessories	0	0	0	0	0.2	0	0	0	0	0	0	0

Modal Analyses

Rock Unit	HSOG	HSOG	HSOG	HSOG	HSOG	HSOG	HSOG
Sample	**Hs10**	**Hs11**	**Hs12**	**Hs13**	**Hs14**	**Hs15**	**Hs18**
Olivine	65.6	64.5	58.5	59.5	55.2	45.2	40.5
Intercumulus Plag	21	18	22	15	21	29	34
Cumulus Plag	2	1.2	2.5	1.9	2.7	3.3	3.9
Orthopyroxene	10	14.9	15.1	15.1	14.5	10.7	18.4
Clinopyroxene	0.5	0	1.6	6.3	4	8.5	0.2
Mica	0	0	0	1.2	0.7	1.7	2.3
Orthoclase	0	0	0	0	0	0	0
Oxides	0.5	0	0	0.2	1.2	0.7	0.5
Sulfides	0	0.2	0	0	0.2	0.7	0
Quartz	0	0	0	0	0	0	0
Amphibole	0	0	0	0	0	0	0
Accessories	0	0	0	0	0	0	0

CIPW Norms for the Ingeli lobe

Rock	BOG	BOG	BOG	BOG	BOG	BOG	BOG	BOG	PU	PU	PU	PU	PU
Sample	**IT-3**	**IT-4**	**IT-5**	**IT-6**	**IT-7**	**IT-8**	**IT-10**	**IT-11**	**IT-12**	**IT-13**	**IT-14**	**IT-15**	**IT-16**
Q	0	0	0	0	0	0	0	0	0	0	0	0	0
or	0	1.4	1.48	1.5	1.37	0	0.66	0.6	0.54	0.66	0.96	0.6	0.59
ab	0	2.08	0.97	0.26	0.26	0	0.26	0.26	0.26	0.26	0.26	0.26	0.25
an	11.35	14.84	14.03	12.13	10.18	7.66	8.54	8.44	7.67	7.77	7.26	7.73	8.11
lc	1.76	0	0	0	0	1.19	0	0	0	0	0	0	0
ne	2.68	0	0	0	0	0.14	0	0	0	0	0	0	0
C	0	0	0	0	0	0	0	0	0	0	0	0	0
ac	0	0	0	0	0	0	0	0	0	0	0	0	0
ns	0	0	0	0	0	0	0	0	0	0	0	0	0
Di wo	5.51	2.63	1.73	1.59	1.59	3.45	1.53	1.62	1.23	1.3	1.16	1.1	1.18
Di en	4.06	1.96	1.28	1.18	1.2	2.61	1.16	1.23	0.93	0.98	0.88	0.83	0.9
Di fs	0.91	0.41	0.28	0.26	0.22	0.48	0.21	0.22	0.17	0.19	0.15	0.15	0.16
Hy en	0	18.95	20.3	19.33	15.97	0	13.9	12.87	14.87	13.86	13.65	11.77	12
Hy fs	0	4	4.36	4.23	2.96	0	2.51	2.31	2.8	2.67	2.36	2.16	2.12
Ol fo	55.32	38.91	39.91	43.36	49.87	64.1	54.84	55.77	54.53	55.21	56.92	58.16	57.77
Ol fa	13.73	9.06	9.47	10.47	10.21	14.79	10.94	11.05	11.34	11.74	10.85	11.76	11.26
mt	4.91	5.06	5.49	5.06	5.62	5.11	5.04	5.24	5.28	4.97	5.18	5.1	5.25
he	0	0	0	0	0	0	0	0	0	0	0	0	0
Il	0.68	0.6	0.59	0.52	0.46	0.41	0.35	0.33	0.31	0.33	0.31	0.33	0.34
ap	0.11	0.11	0.11	0.11	0.09	0.07	0.07	0.07	0.07	0.07	0.07	0.07	0.07
Total	101.03	100	100	100	100	100.01	100	100	100	100	100	100	100

CIPW Norms for the Ingell lobe

Rock	PU	PU	PU	PU	PU	COG	CG	CG	CG	CG	CG	CG	CG
Sample	**IT-17**	**IT-18**	**IT-19**	**IT-20**	**IT-21**	**IT-22**	**IT-23**	**IT-24**	**IT-25**	**IT-26**	**IT-27**	**IT-28**	**IT-29**
Q	0	0	0	0	0	0	2.18	3.41	3.13	1.62	0	1.76	0
or	0.36	0.66	0.54	0.25	0.68	1.29	1.44	1.14	1.55	1.34	1.71	1.69	1.43
ab	0.26	0.26	0.26	0.27	0.26	7.66	12.44	11.83	13.61	13.88	9.95	15.12	17.11
an	8.42	8.22	7.91	10.28	8.57	41.17	52.67	44.07	41.14	38.64	35.38	35.37	37.91
lc	0	0	0	0	0	0	0	0	0	0	0	0	0
ne	0	0	0	0	0	0	0	0	0	0	2.04	0	0
C	0	0	0	0	0	0	0	0	0	0	0	0	0
ac	0	0	0	0	0	0	0	0	0	0	0	0	0
ns	0	0	0	0	0	0	0	0	0	0	0	0	0
Di wo	1.16	0.98	0.72	1.64	1.26	0.72	2.28	10.15	10.32	12.22	16.68	11.8	8.95
Di en	0.88	0.74	0.53	1.22	0.93	0.51	1.62	7.14	7.05	8.43	11.3	7.83	5.9
Dl fs	0.17	0.14	0.12	0.25	0.21	0.14	0.46	2.13	2.44	2.78	4.07	3.09	2.4
Hy en	12.97	10.85	17.33	11.93	11.14	9.3	19.07	13.37	13.21	13.03	0	14.19	14.76
Hy fs	2.46	2.13	3.85	2.44	2.56	2.56	5.42	3.99	4.58	4.3	0	5.59	5.99
Ol fo	55.84	57.34	50.54	53.43	56.06	26.29	0	0	0	0	11.16	0	1.4
Ol fa	11.68	12.44	12.39	12.07	14.23	7.99	0	0	0	0	4.44	0	0.63
mt	5.47	5.87	5.36	5.96	3.61	1.87	1.94	2.22	2.26	3.04	2.61	2.88	2.89
he	0	0	0	0	0	0	0	0	0	0	0	0	0
il	0.29	0.29	0.37	0.22	0.39	0.42	0.41	0.5	0.61	0.59	0.61	0.62	0.57
ap	0.04	0.07	0.09	0.05	0.09	0.09	0.07	0.07	0.09	0.13	0.07	0.07	0.07
Total	100	100	100	100	100	100	100	100	100	100	100	100	100

CIPW Norms for the Ingeli lobe

Rock	UOG	UOG	UG	UG	UG	UG	UG	UG
Sample	**IT-30**	**IT-31**	**IT-32**	**IT-33**	**IT-34**	**IT-35**	**IT-36**	**IT-37**
Q	0	0	0	0.86	1.47	0	2.87	1.97
or	1.66	1.64	0	1.21	1.74	1.97	2.6	2.41
ab	16.43	7.27	0	15.54	17.63	8.78	18.43	21.77
an	38.64	36.26	29.42	33.19	32.01	29.35	31.41	34.65
lc	0	0	2.08	0	0	0	0	0
ne	0	5.45	11.42	0	0	6.39	0	0
C	0	0	0	0	0	0	0	0
ac	0	0	0	0	0	0	0	0
ns	0	0	0	0	0	0	0	0
Di wo	9.98	15.14	21.33	12.44	9.9	17.24	10.2	9.35
Di en	6.48	9.97	13.88	7.87	6.09	10.52	5.91	5.2
Di fs	2.8	4.06	5.95	3.76	3.23	5.73	3.8	3.78
Hy en	12.47	0	0	14.06	14.8	0	12.05	9.34
Hy fs	5.39	0	0	6.72	7.86	0	7.75	6.79
Ol fo	1.41	10.79	8.93	0	0	9.54	0	0
Ol fa	0.67	4.84	4.22	0	0	5.74	0	0
mt	3.31	3.51	3.44	3.45	4.01	3.6	3.38	3.38
he	0	0	0	0	0	0	0	0
il	0.67	0.94	1.3	0.84	1.12	1.02	1.36	1.18
ap	0.09	0.13	0.2	0.06	0.15	0.11	0.22	0.18
Total	100	100	102.18	100	100	100	100	100

Appendix II

The major rock forming minerals, (olivine, plagioclase, orthopyroxene, and clinopyroxene), were analysed using a fully automated wavelength dispersive JEOL CXA-733 Superprobe at Rhodes University, Grahamstown, South Africa. The operating conditions of the microprobe were: 30 nA beam current and 15 kV accelerating voltage.

The following is a table of average detection limits for the 4 phases analysed:

wt%	SiO2	Al2O3	TiO2	Cr2O3	FeO	MnO	MgO	NiO	CaO	Na2O	K2O
OL	0.048	0.015	0.016	0.055	0.054	0.051	0.012	0.050	0.013	0.020	0.017
OPX	0.048	0.016	0.017	0.057	0.057	0.051	0.013	0.050	0.014	0.021	0.018
CPX	0.049	0.015	0.018	0.059	0.057	0.057	0.014	0.050	0.015	0.022	0.019
PL	0.047	0.013			0.053	0.053			0.014	0.019	0.013
Total Ave	0.048	0.015	0.017	0.193	0.055	0.053	0.013	0.050	0.014	0.021	0.017

Average Olivine analyses

unit	BOG	BOG	BOG	BOG	BOG	BOG	BOG	BOG	PU	PU	PU	PU	PU
wt%	IT-3	IT-4	IT-5	IT-6	IT-7	IT-8	IT-10	IT-11	IT-12	IT-13	IT-14	IT-15	IT-16
SiO2	38.71	40.13	39.17	39.68	39.13	40.07	39.55	39.70	40.72	39.96	40.79	40.46	39.87
FeO	17.44	15.98	16.39	16.55	14.97	14.52	14.17	14.30	14.97	15.10	13.86	14.28	14.18
MnO	0.25	0.22	0.21	0.25	0.22	0.21	0.20	0.27	0.21	0.21	0.21	0.24	0.20
MgO	41.25	43.25	44.64	41.70	45.72	44.63	45.47	44.59	44.49	43.95	45.78	44.48	46.28
NiO	0.29	0.29	0.31	0.22	0.19	0.20	0.22	0.22	0.24	0.22	0.26	0.27	0.30
CaO	0.10	0.05	0.04	0.07	0.04	0.06	0.06	0.07	0.08	0.05	0.06	0.06	0.06
TOTAL	98.04	99.91	100.76	98.48	100.28	99.69	99.67	99.14	100.72	99.48	100.96	99.78	100.88
n	4	4	4	5	4	4	4	4	4	4	4	4	4

Average Cations (based on 4 Oxygens)

	IT-3	IT-4	IT-5	IT-6	IT-7	IT-8	IT-10	IT-11	IT-12	IT-13	IT-14	IT-15	IT-16
Si	1.00	1.01	0.98	1.02	0.98	1.01	0.99	1.00	1.01	1.01	1.01	1.01	0.99
Fe	0.37	0.34	0.34	0.36	0.31	0.30	0.30	0.30	0.31	0.32	0.29	0.30	0.29
Mn	0.01	0.00	0.00	0.01	0.00	0.00	0.00	0.01	0.00	0.00	0.00	0.01	0.00
Mg	1.61	1.63	1.67	1.60	1.71	1.67	1.70	1.68	1.65	1.65	1.69	1.66	1.71
Ni	0.01	0.01	0.01	0.00	0.00	0.00	0.00	0.00	0.00	0.00	0.01	0.01	0.01
Ca	0.00	0.00	0.00	0.00	0.00	0.00	0.00	0.00	0.00	0.00	0.00	0.00	0.00

1 Standard Deviation (wt%)

	It-3	It-4	It-5	It-6	It-7	It-8	It-10	It-11	It-12	It-13	It-14	It-15	It-16
SiO2	0.54	0.36	0.17	0.28	0.99	0.43	0.38	0.24	0.90	0.20	0.40	0.19	0.25
FeO	0.19	0.34	0.34	0.16	0.13	0.18	0.03	0.22	0.15	0.24	0.31	0.15	0.13
MnO	0.01	0.04	0.02	0.04	0.01	0.07	0.04	0.03	0.02	0.05	0.04	0.03	0.05
MgO	1.35	1.18	0.30	0.34	1.52	0.28	0.69	0.29	1.34	0.53	0.44	1.19	0.48
NiO	0.02	0.04	0.03	0.02	0.04	0.02	0.03	0.02	0.03	0.05	0.01	0.02	0.03
CaO	0.02	0.01	0.02	0.01	0.02	0.02	0.02	0.01	0.01	0.02	0.02	0.03	0.02

Average Olivine analyses

unit	PU	PU	PU	PU	PU	COG	CG	UOG	UOG	UG	UG	UG	HSOG
wt%	IT-17	IT-18	IT-19	IT-20	IT-21	It-22	IT-29	IT-30	IT-31	IT-32	IT-33	IT-35	HS-10
SiO2	39.07	39.35	39.30	39.51	39.22	36.73	36.96	36.00	36.15	35.69	35.87	35.25	39.28
FeO	14.52	15.56	16.56	15.66	16.47	30.37	31.00	31.96	31.99	35.60	34.61	34.91	18.05
MnO	0.21	0.24	0.21	0.19	0.24	0.42	0.39	0.40	0.41	0.42	0.42	0.41	0.27
MgO	45.17	43.51	43.08	43.86	42.73	31.41	31.67	29.91	30.13	27.25	28.70	28.53	42.24
NiO	0.27	0.22	0.20	0.17	0.17	0.08	0.11	0.16	0.14	0.15	0.11	0.10	0.07
CaO	0.06	0.10	0.09	0.09	0.06	0.05	0.07	0.07	0.08	0.05	0.10	0.08	0.14
TOTAL	99.31	98.97	99.44	99.48	98.89	99.06	100.20	98.50	98.90	99.16	99.82	99.28	100.05
n	4	4	3	4	4	3	3	4	3	2	3	2	4

Average Cations (based on 4 Oxygens)

	IT-17	IT-18	IT-19	IT-20	IT-21	It-22	IT-29	IT-30	IT-31	IT-32	IT-33	IT-35	HS-10
Si	0.99	1.00	1.00	1.00	1.00	1.01	1.00	1.00	1.00	1.00	1.00	0.99	1.00
Fe	0.31	0.33	0.35	0.33	0.35	0.70	0.70	0.74	0.77	0.77	0.80	0.82	0.39
Mn	0.00	0.01	0.00	0.00	0.01	0.01	0.01	0.01	0.01	0.01	0.01	0.01	0.01
Mg	1.70	1.65	1.63	1.66	1.63	1.28	1.28	1.25	1.21	1.21	1.19	1.19	1.60
Ni	0.01	0.00	0.00	0.00	0.00	0.00	0.00	0.00	0.00	0.00	0.00	0.00	0.00
Ca	0.00	0.00	0.00	0.00	0.00	0.00	0.00	0.00	0.00	0.00	0.00	0.00	0.00

1 Standard Deviation (wt%)

	It-17	It-18	It-19	It-20	It-21	It-22	It-29	It-30	It-31	It-32	It-33	It-35	HS-10
SiO2	0.48	0.26	0.24	0.49	0.49	0.10	0.18	0.19	0.33	0.03	0.15	0.14	0.35
FeO	0.20	0.05	0.37	0.47	0.16	0.02	0.33	0.63	1.24	0.02	0.48	0.70	0.31
MnO	0.03	0.04	0.06	0.05	0.03	0.03	0.05	0.04	0.01	0.05	0.04	0.04	0.04
MgO	0.64	0.48	0.33	0.41	0.09	0.44	0.27	0.36	0.61	0.84	0.87	0.17	0.40
NiO	0.04	0.03	0.01	0.02	0.03	0.05	0.04	0.05	0.03	0.04	0.03	0.03	0.02
CaO	0.02	0.01	0.02	0.02	0.01	0.01	0.01	0.02	0.01	0.00	0.03	0.01	0.03

Average Olivine analyses

unit	HSOG	HSOG	HSOG	HSOG	HSOG	HSOG
wt%	HS-11	HS-12	HS-13	HS-14	HS-15	HS-18
SiO2	39.22	39.02	39.00	38.92	39.09	38.79
FeO	18.82	18.61	18.25	18.95	19.14	21.18
MnO	0.29	0.29	0.24	0.27	0.28	0.29
MgO	41.82	40.84	41.67	41.68	41.50	39.80
NiO	0.04	0.08	0.08	0.10	0.10	0.11
CaO	0.17	0.14	0.15	0.16	0.17	0.12
TOTAL	100.36	98.97	99.38	100.07	100.28	100.30
n	3	4	4	4	4	4

Average Cations (based on 4 Oxygens)

	HS-11	HS-12	HS-13	HS-14	HS-15	HS-18
Si	1.00	1.01	1.00	1.00	1.00	1.00
Fe	0.40	0.40	0.39	0.41	0.41	0.46
Mn	0.01	0.01	0.01	0.01	0.01	0.01
Mg	1.59	1.57	1.59	1.59	1.58	1.53
Ni	0.00	0.00	0.00	0.00	0.00	0.00
Ca	0.00	0.00	0.00	0.00	0.00	0.00

1 Standard Deviation (wt%)

	HS-11	HS-12	HS-13	HS-14	HS-15	HS-18
SiO2	0.20	0.11	0.30	0.44	0.19	0.30
FeO	0.53	0.19	0.36	0.69	0.86	0.83
MnO	0.02	0.04	0.05	0.04	0.04	0.04
MgO	0.43	0.29	0.25	0.40	0.45	0.55
NiO	0.01	0.03	0.02	0.01	0.05	0.02
CaO	0.04	0.03	0.03	0.06	0.02	0.04

Average Orthopyroxene analyses

Unit	BOG	BOG	BOG	BOG	BOG	BOG	BOG	BOG	PU	PU	PU	PU	PU
wt%	IT-3	IT-4	It-5	IT-6	IT-7	IT-8	IT-10	IT-11	IT-12	IT-13	IT-14	IT-15	IT-16
SiO2	55.40	56.82	55.29	55.98	55.86	55.76	54.85	55.40	56.40	55.56	55.75	56.40	55.59
Al2O3	1.45	1.17	1.18	1.57	1.20	1.40	1.65	1.32	1.37	1.33	1.23	1.46	1.45
TiO2	0.39	0.42	0.34	0.29	0.44	0.33	0.39	0.27	0.23	0.29	0.38	0.20	0.24
Cr2O3	0.50	0.40	0.36	0.61	0.39	0.53	0.68	0.47	0.52	0.49	0.43	0.51	0.52
FeO	10.29	10.13	10.16	10.01	9.35	8.98	7.39	8.83	9.51	9.30	8.71	8.93	8.87
MnO	0.21	0.26	0.22	0.21	0.20	0.21	0.17	0.21	0.25	0.22	0.18	0.23	0.25
MgO	29.99	29.85	31.38	28.65	31.38	30.05	27.08	31.66	30.35	30.20	31.19	30.59	31.10
NiO	0.06	0.09	0.07	0.05	0.06	0.10	0.05	0.04	0.07	0.03	0.09	0.05	0.11
CaO	2.00	1.91	1.73	2.28	1.97	2.10	8.38	2.20	2.09	2.19	1.81	2.23	2.21
Na2O	0.04	0.03	0.05	0.03	0.05	0.03	0.20	0.04	0.06	0.03	0.04	0.03	0.02
TOTAL	100.33	101.07	100.79	99.67	100.89	99.49	100.83	100.44	100.86	99.63	99.81	100.63	100.36
n	3	4	4	4	3	3	3	3	2	3	3	3	3

Average Cations (based on 6 Oxygens)

	IT-3	IT-4	It-5	IT-6	IT-7	IT-8	IT-10	IT-11	IT-12	IT-13	IT-14	IT-15	IT-16
Si	1.95	1.98	1.94	1.98	1.95	1.97	1.94	1.94	1.97	1.96	1.96	1.97	1.95
Al	0.06	0.05	0.05	0.07	0.05	0.06	0.07	0.05	0.06	0.06	0.05	0.06	0.06
Ti	0.01	0.01	0.01	0.01	0.01	0.01	0.01	0.01	0.01	0.01	0.01	0.01	0.01
Cr	0.67	0.92	0.89	0.88	0.87	1.12	0.77	0.95	1.10	0.60	1.05	1.01	1.04
Fe	0.30	0.30	0.30	0.30	0.27	0.27	0.22	0.26	0.28	0.27	0.26	0.26	0.26
Mn	0.01	0.01	0.01	0.01	0.01	0.01	0.00	0.01	0.01	0.01	0.01	0.01	0.01
Mg	1.57	1.55	1.64	1.51	1.63	1.58	1.42	1.65	1.58	1.59	1.63	1.59	1.62
Ni	0.00	0.00	0.00	0.00	0.00	0.00	0.00	0.00	0.00	0.00	0.00	0.00	0.00
Ca	0.08	0.07	0.07	0.09	0.07	0.08	0.32	0.08	0.08	0.08	0.07	0.08	0.08
Na	0.00	0.00	0.00	0.00	0.00	0.00	0.01	0.00	0.00	0.00	0.00	0.00	0.00

1 Standard Deviation (wt%)

	It-3	It-4	It-5	It-6	It-7	It-8	It-10	It-11	It-12	It-13	It-14	It-15	It-16
SiO2	1.27	1.07	0.76	0.79	0.30	0.35	1.17	0.23	0.88	1.18	0.98	0.18	0.48
Al2O3	0.24	0.48	0.42	0.19	0.44	0.31	0.53	0.03	0.09	0.34	0.06	0.21	0.17
TiO2	0.24	0.13	0.18	0.07	0.23	0.11	0.07	0.04	0.00	0.14	0.14	0.02	0.05
Cr2O3	0.15	0.14	0.17	0.06	0.17	0.05	0.33	0.04	0.05	0.17	0.04	0.06	0.07
FeO	0.36	0.46	0.22	0.22	0.43	0.16	2.70	0.08	0.10	0.24	0.04	0.13	0.02
MnO	0.02	0.05	0.03	0.03	0.06	0.04	0.01	0.03	0.02	0.03	0.06	0.04	0.01
MgO	1.32	0.45	0.48	0.57	0.92	1.93	8.14	0.08	0.18	0.56	0.62	0.31	0.27
NiO	0.05	0.03	0.02	0.03	0.04	0.04	0.01	0.03	0.01	0.04	0.02	0.02	0.03
CaO	0.24	0.54	0.60	0.11	0.70	0.27	10.96	0.08	0.01	0.39	0.23	0.02	0.11
Na2O	0.00	0.02	0.01	0.03	0.02	0.01	0.27	0.04	0.01	0.01	0.01	0.01	0.03

Average Orthopyroxene analyses

unit	PU	PU	PU	PU	COG	CG	CG	CG	CG	CG	CG	CG	UOG
wt%	IT-17	It-18	IT-19	IT-21	IT-22	IT-23	IT-24	IT-25	IT-26	IT-27	IT-28	IT-29	It-30
SiO2	55.15	56.26	55.38	55.20	53.07	54.62	55.57	55.36	54.99	54.36	53.58	54.33	52.99
Al2O3	1.36	1.10	1.36	1.07	0.77	1.47	0.98	0.92	0.98	0.83	0.71	0.85	0.69
TiO2	0.24	0.48	0.23	0.76	0.38	0.12	0.15	0.18	0.18	0.19	0.41	0.47	0.37
Cr2O3	0.52	0.48	0.60	0.31	0.07	0.51	0.26	0.14	0.18	0.09	0.06	0.01	0.12
FeO	9.13	9.53	10.30	10.57	18.44	13.11	14.09	14.62	13.77	16.44	18.58	18.05	19.53
MnO	0.24	0.23	0.27	0.27	0.43	0.30	0.28	0.32	0.27	0.35	0.44	0.38	0.36
MgO	30.68	30.01	29.15	29.64	23.83	27.36	26.93	26.13	26.58	25.12	23.23	24.07	23.49
NiO	0.05	0.07	0.07	0.03	0.04	0.04	0.00	0.02	0.00	0.02	0.02	0.01	0.05
CaO	2.15	1.68	2.25	1.61	1.37	2.05	2.41	2.32	2.48	2.31	1.95	1.87	0.98
Na2O	0.04	0.04	0.11	0.08	0.02	0.01	0.02	0.04	0.04	0.01	0.03	0.04	0.01
TOTAL	99.56	99.88	99.70	99.54	98.41	99.59	100.68	100.05	99.46	99.73	99.02	100.08	98.60
n	4	1	1	1	2	3	2	4	3	4	4	2	1

Average Cations (based on 6 Oxygens)

	IT-17	It-18	IT-19	IT-21	IT-22	IT-23	IT-24	IT-25	IT-26	IT-27	IT-28	IT-29	It-30
Si	1.95	1.98	1.97	1.96	1.98	1.96	1.98	1.99	1.98	1.98	1.99	1.99	1.98
Al	0.06	0.05	0.06	0.05	0.03	0.06	0.04	0.04	0.04	0.04	0.03	0.04	0.03
Ti	0.01	0.01	0.01	0.02	0.01	0.00	0.00	0.00	0.00	0.01	0.01	0.01	0.01
Cr	1.06	0.01	0.02	0.01	0.00	0.02	0.01	0.00	0.01	0.00	0.00	0.00	0.00
Fe	0.27	0.28	0.31	0.31	0.58	0.39	0.42	0.44	0.42	0.50	0.58	0.55	0.61
Mn	0.01	0.01	0.01	0.01	0.01	0.01	0.01	0.01	0.01	0.01	0.01	0.01	0.01
Mg	1.62	1.57	1.54	1.57	1.32	1.48	1.43	1.40	1.43	1.37	1.28	1.31	1.31
Ni	0.00	0.00	0.00	0.00	0.00	0.00	0.00	0.00	0.00	0.00	0.00	0.00	0.00
Ca	0.08	0.06	0.09	0.06	0.05	0.08	0.09	0.09	0.10	0.09	0.08	0.07	0.04
Na	0.00	0.00	0.01	0.01	0.00	0.00	0.00	0.00	0.00	0.00	0.00	0.00	0.00

1 Standard Deviation (wt%)

	It-17	It-18	It-19	It-21	It-22	It-23	It-24	It-25	It-26	It-27	It-28	It-29	It-30
SiO2	0.51	0.00	0.00	0.00	0.21	0.35	0.07	0.39	0.22	0.54	0.43	0.66	0.00
Al2O3	0.19	0.00	0.00	0.00	0.03	0.09	0.07	0.07	0.08	0.03	0.09	0.16	0.00
TiO2	0.09	0.00	0.00	0.00	0.02	0.01	0.02	0.03	0.02	0.01	0.05	0.12	0.00
Cr2O3	0.08	0.00	0.00	0.00	0.01	0.07	0.03	0.08	0.01	0.03	0.02	0.02	0.00
FeO	0.22	0.00	0.00	0.00	0.13	1.36	0.52	0.73	1.02	0.88	0.41	0.09	0.00
MnO	0.04	0.00	0.00	0.00	0.07	0.06	0.03	0.04	0.04	0.04	0.04	0.07	0.00
MgO	0.28	0.00	0.00	0.00	0.21	0.66	1.03	0.69	1.09	0.35	0.27	0.13	0.00
NiO	0.02	0.00	0.00	0.00	0.01	0.02	0.00	0.03	0.00	0.03	0.02	0.00	0.00
CaO	0.09	0.00	0.00	0.00	0.01	0.13	0.09	0.07	0.28	0.05	0.12	0.26	0.00
Na2O	0.02	0.00	0.00	0.00	0.01	0.01	0.00	0.01	0.01	0.01	0.02	0.04	0.00

Average Orthopyroxene analyses

unit	HSOG	HSOG
wt%	HS-15	HS-18
SiO2	55.13	54.34
Al2O3	1.24	1.47
TiO2	0.41	0.75
Cr2O3	0.24	0.22
FeO	11.88	13.57
MnO	0.26	0.30
MgO	28.90	27.61
NiO	0.03	0.00
CaO	1.95	2.04
Na2O	0.03	0.06
TOTAL	100.08	100.35
n	4	1

Average Cations (based on 6 Oxygens)

	HS-15	HS-18
Si	1.96	1.95
Al	0.05	0.06
Ti	0.01	0.02
Cr	0.01	0.01
Fe	0.35	0.41
Mn	0.01	0.01
Mg	1.53	1.47
Ni	0.00	0.00
Ca	0.07	0.08
Na	0.00	0.00

1 Standard Deviation (wt%)

	HS-15	HS-18
SiO2	0.34	0.00
Al2O3	0.53	0.00
TiO2	0.20	0.00
Cr2O3	0.14	0.00
FeO	1.21	0.00
MnO	0.08	0.00
MgO	0.28	0.00
NiO	0.03	0.00
CaO	0.53	0.00
Na2O	0.02	0.00

Average Clinopyroxene analyses

unit	UOG	UOG	UG	UG	UG	UG	UG	UG	HSG	HSOG	HSOG	HSOG	HSOG
wt%	IT-30	IT-31	IT-32	IT-33	IT-34	IT-35	IT-36	IT-37	HS-8	HS-10	HS-11	HS-12	HS-13
SiO2	51.61	51.53	51.87	51.75	53.62	50.57	51.57	51.18	52.42	52.99	53.13	53.47	53.02
Al2O3	1.85	2.07	1.86	1.81	1.53	1.65	1.19	1.60	1.43	2.02	2.07	2.18	2.16
TiO2	0.40	0.42	0.50	0.49	0.66	0.66	0.54	0.61	0.49	0.47	0.51	0.28	0.31
FeO	0.44	0.72	0.32	0.32	0.28	0.23	0.10	0.20	0.11	0.89	0.94	0.58	0.65
Cr2O3	8.67	8.92	10.02	10.47	10.72	11.08	12.70	13.25	11.89	5.88	6.21	6.03	5.93
MnO	0.24	0.20	0.22	0.25	0.23	0.28	0.31	0.29	0.28	0.16	0.18	0.22	0.22
MgO	15.44	15.38	15.58	14.63	14.42	14.13	14.04	14.29	15.83	18.66	18.58	18.86	18.64
NiO	0.04	0.01	0.01	0.02	0.02	0.05	0.02	0.01	0.01	0.02	0.03	0.02	0.01
CaO	19.50	19.01	18.59	19.09	18.89	19.61	18.72	18.02	17.13	18.38	17.99	17.26	17.88
Na2O	0.28	0.28	0.24	0.28	0.28	0.27	0.29	0.23	0.18	0.25	0.27	0.22	0.23
TOTAL	98.48	98.55	99.20	99.10	100.64	98.53	99.46	99.68	99.79	99.73	99.90	99.12	99.03
n	4	4	4	4	3	3	4	4	4	4	2	3	2

Average Cations (based on 6 Oxygens)

	IT-30	IT-31	IT-32	IT-33	IT-34	IT-35	IT-36	IT-37	HS-8	HS-10	HS-11	HS-12	HS-13
Si	1.94	1.94	1.94	1.95	1.98	1.93	1.95	1.94	1.96	1.94	1.94	1.96	1.95
Al	0.08	0.09	0.08	0.08	0.07	0.07	0.05	0.07	0.06	0.09	0.09	0.09	0.09
Ti	0.01	0.01	0.01	0.01	0.02	0.02	0.02	0.02	0.01	0.01	0.01	0.01	0.01
Cr	0.01	0.02	0.01	0.01	0.01	0.01	0.00	0.01	0.00	0.03	0.03	0.02	0.02
Fe	0.27	0.28	0.31	0.33	0.33	0.35	0.40	0.42	0.37	0.18	0.19	0.18	0.18
Mn	0.01	0.01	0.01	0.01	0.01	0.01	0.01	0.01	0.01	0.00	0.01	0.01	0.01
Mg	0.87	0.86	0.87	0.82	0.80	0.80	0.79	0.81	0.88	1.02	1.01	1.03	1.02
Ni	0.00	0.00	0.00	0.00	0.00	0.00	0.00	0.00	0.00	0.00	0.00	0.00	0.00
Ca	0.79	0.77	0.75	0.77	0.75	0.80	0.76	0.73	0.69	0.72	0.70	0.68	0.70
Na	0.02	0.02	0.02	0.02	0.02	0.02	0.02	0.02	0.01	0.02	0.02	0.02	0.02

1 Standard Deviation (wt %)

	It-30	It-31	It-32	It-33	It-34	It-35	It-36	It-37	HS-8	HS-10	HS-11	HS-12	HS-13
SiO2	0.21	0.79	0.38	0.34	2.26	0.32	0.33	0.01	1.23	0.50	0.75	0.30	0.44
Al2O3	0.09	0.13	0.17	0.38	0.04	0.01	0.34	0.01	0.19	0.16	0.34	0.22	0.15
TiO2	0.07	0.21	0.15	0.14	0.19	0.04	0.15	0.00	0.18	0.35	0.36	0.03	0.01
Cr2O3	0.05	0.19	0.15	0.06	0.09	0.10	0.06	0.00	0.06	0.07	0.04	0.05	0.02
FeO	1.21	1.10	1.35	0.57	0.34	1.12	1.36	0.07	3.37	0.05	0.14	0.46	0.48
MnO	0.03	0.04	0.07	0.02	0.10	0.05	0.05	0.00	0.10	0.04	0.02	0.03	0.05
MgO	0.51	0.65	0.41	0.14	0.09	0.41	0.49	0.03	2.21	0.73	1.01	0.44	0.59
NiO	0.03	0.01	0.02	0.03	0.01	0.02	0.02	0.00	0.03	0.02	0.01	0.04	0.01
CaO	1.15	1.10	0.79	0.48	0.66	1.30	2.09	0.10	0.63	0.60	0.31	0.98	2.07
Na2O	0.04	0.04	0.03	0.05	0.03	0.03	0.02	0.00	0.03	0.05	0.08	0.03	0.05

Average Clinopyroxene analyses

unit	HSOG	HSOG
wt%	HS-14	HS-15
SiO2	52.37	51.93
Al2O3	2.35	2.47
TiO2	0.54	0.71
FeO	0.59	0.62
Cr2O3	6.07	6.58
MnO	0.22	0.21
MgO	18.06	17.94
NiO	0.02	0.01
CaO	18.47	18.25
Na2O	0.26	0.19
TOTAL	98.95	98.91
n	4	1

Average Cations (based on 6 Oxygens)

	HS-14	HS-15
Si	1.93	1.92
Al	0.10	0.11
Ti	0.02	0.02
Cr	0.02	0.02
Fe	0.19	0.20
Mn	0.01	0.01
Mg	0.99	0.99
Ni	0.00	0.00
Ca	0.73	0.72
Na	0.02	0.01

1 Standard Deviation (wt %)

	HS-14	HS-15
SiO2	0.19	0.00
Al2O3	0.27	0.00
TiO2	0.24	0.00
Cr2O3	0.07	0.00
FeO	0.29	0.00
MnO	0.04	0.00
MgO	0.53	0.00
NiO	0.01	0.00
CaO	0.74	0.00
Na2O	0.04	0.00

Average Plagioclase analyses

unit	BOG	BOG	BOG	BOG	BOG	BOG	BOG	BOG	PU	PU	PU	PU	PU
wt%	IT-3	IT-4	IT-5	IT-6	IT-7	IT-8	IT-10	IT-11	IT-12	IT-13	IT-14	IT-15	IT-16
SiO2	50.92	52.80	50.17	51.84	50.22	51.55	50.51	50.82	51.64	51.15	51.68	51.80	51.79
Al2O3	31.04	30.51	31.82	31.06	30.91	30.89	30.86	31.96	32.19	32.25	31.09	30.79	30.77
FeO	0.20	0.20	0.19	0.17	0.22	0.16	0.19	0.20	0.24	0.20	0.22	0.20	0.19
MnO	0.03	0.03	0.01	0.01	0.00	0.02	0.01	0.00	0.03	0.00	0.01	0.00	0.01
CaO	13.24	12.19	13.71	12.54	13.13	13.14	13.80	13.48	14.01	13.97	13.09	13.06	12.94
Na2O	3.80	4.46	3.55	4.27	3.97	3.99	3.76	3.66	3.45	3.52	3.84	3.88	3.96
K2O	0.25	0.34	0.26	0.33	0.31	0.32	0.30	0.32	0.21	0.29	0.33	0.33	0.35
TOTAL	99.49	100.53	99.72	100.22	98.76	100.06	99.43	100.45	101.77	101.38	100.26	100.06	100.00
n	4	4	4	4	2	3	2	4	2	4	4	4	4

Cations (based on 8 Oxygens)

	IT-3	IT-4	IT-5	IT-6	IT-7	IT-8	IT-10	IT-11	IT-12	IT-13	IT-14	IT-15	IT-16
Si	2.33	2.38	2.29	2.35	2.31	2.34	2.31	2.30	2.31	2.30	2.34	2.35	2.35
Al	1.67	1.62	1.71	1.66	1.68	1.65	1.67	1.71	1.70	1.71	1.66	1.65	1.65
Fe	0.01	0.01	0.01	0.01	0.01	0.01	0.01	0.01	0.01	0.01	0.01	0.01	0.01
Mn	0.00	0.00	0.00	0.00	0.00	0.00	0.00	0.00	0.00	0.00	0.00	0.00	0.00
Ca	0.65	0.59	0.67	0.61	0.65	0.64	0.68	0.65	0.67	0.67	0.63	0.64	0.63
Na	0.34	0.39	0.31	0.37	0.35	0.35	0.33	0.32	0.30	0.31	0.34	0.34	0.35
K	0.01	0.02	0.02	0.02	0.02	0.02	0.02	0.02	0.01	0.02	0.02	0.02	0.02

1 Standard Deviation (wt %)

	It-3	It-4	It-5	It-6	It-7	It-8	It-10	It-11	It-12	It-13	It-14	It-15	It-16
SiO2	0.91	2.85	1.01	2.43	0.00	0.83	1.71	0.84	0.00	0.30	0.85	1.44	1.69
Al2O3	0.62	2.08	0.63	1.01	0.00	0.22	1.62	0.32	0.00	0.48	0.61	0.99	1.39
FeO	0.03	0.05	0.02	0.02	0.00	0.04	0.02	0.03	0.00	0.03	0.05	0.05	0.03
MnO	0.02	0.03	0.01	0.02	0.00	0.00	0.02	0.01	0.00	0.00	0.01	0.00	0.01
CaO	0.59	2.47	0.56	1.30	0.00	0.24	1.25	0.27	0.00	0.29	0.75	0.98	1.40
Na2O	0.32	1.37	0.32	0.78	0.00	0.21	0.57	0.22	0.00	0.16	0.53	0.58	0.68
K2O	0.05	0.12	0.06	0.09	0.00	0.04	0.04	0.09	0.00	0.03	0.06	0.08	0.13

Average Plagioclase analyses

unit	PU	PU	PU	PU	PU	COG	CG	CG	CG	CG	CG	CG	CG
wt%	IT-17	IT-18	IT-19	IT-20	IT-21	IT-22	IT-23	IT-24	IT-25	IT-26	IT-27	IT-28	IT-29
SiO2	51.13	50.94	51.54	50.25	55.32	50.86	48.44	48.99	49.47	50.14	49.92	51.26	51.83
Al2O3	31.10	31.37	30.59	32.12	28.24	31.55	33.71	33.03	32.67	32.30	32.02	30.95	31.23
FeO	0.21	0.22	0.21	0.24	0.17	0.33	0.14	0.31	0.35	0.35	0.39	0.29	0.39
MnO	0.01	0.02	0.03	0.02	0.01	0.02	0.01	0.02	0.01	0.00	0.01	0.01	0.01
CaO	13.48	13.45	12.75	14.19	10.09	13.81	15.89	15.59	15.12	14.61	14.56	13.52	13.26
Na2O	3.57	3.65	3.95	3.45	5.58	3.54	2.43	2.56	2.82	2.88	3.04	3.51	3.83
K2O	0.32	0.32	0.30	0.24	0.40	0.23	0.16	0.18	0.21	0.26	0.26	0.30	0.29
TOTAL	99.81	99.96	99.36	100.51	99.81	100.35	100.78	100.68	100.66	100.55	100.21	99.84	100.85
n	4	3	4	4	4	4	4	4	4	2	4	4	4

Cations (based on 8 Oxygens)

	IT-17	IT-18	IT-19	IT-20	IT-21	IT-22	IT-23	IT-24	IT-25	IT-26	IT-27	IT-28	IT-29
Si	2.33	2.31	2.35	2.28	2.49	2.31	2.20	2.08	2.06	2.27	2.27	2.33	2.34
Al	1.67	1.68	1.65	1.72	1.50	1.69	1.80	1.66	1.61	1.73	1.72	1.66	1.66
Fe	0.01	0.01	0.01	0.01	0.01	0.01	0.01	0.01	0.01	0.01	0.01	0.01	0.02
Mn	0.00	0.00	0.00	0.00	0.00	0.00	0.00	0.00	0.00	0.00	0.00	0.00	0.00
Ca	0.66	0.66	0.62	0.69	0.49	0.67	0.77	0.71	0.68	0.71	0.71	0.66	0.64
Na	0.31	0.33	0.35	0.30	0.49	0.31	0.21	0.21	0.23	0.25	0.27	0.31	0.33
K	0.02	0.02	0.02	0.01	0.02	0.01	0.01	0.01	0.01	0.01	0.02	0.02	0.02

1 Standard Deviation (wt %)

	It-17	It-18	It-19	It-20	It-21	It-22	It-23	It-24	It-25	It-26	It-27	It-28	It-29
SiO2	0.39	0.54	1.32	0.42	2.13	1.83	0.95	0.97	23.87	1.18	1.38	0.62	1.26
Al2O3	0.77	0.32	0.95	0.23	1.42	0.98	0.38	0.49	15.72	1.38	1.04	0.83	1.12
FeO	0.03	0.04	0.02	0.03	0.05	0.01	0.03	0.06	0.18	0.05	0.01	0.01	0.09
MnO	0.01	0.02	0.04	0.02	0.02	0.02	0.03	0.02	0.01	0.00	0.01	0.02	0.03
CaO	0.25	0.13	1.30	0.27	1.64	1.46	0.31	0.63	7.33	1.03	1.05	0.57	0.70
Na2O	0.19	0.06	0.60	0.18	0.84	0.69	0.14	0.26	1.29	0.48	0.58	0.26	0.35
K2O	0.05	0.02	0.10	0.02	0.15	0.04	0.04	0.04	0.10	0.06	0.11	0.04	0.08

Average Plagioclase analyses

unit	UOG	UOG	UG	UG	UG	UG	UG	UG	HSG	HSOG	HSOG	HSOG	HSOG
wt%	IT-30	IT-31	IT-32	IT-33	IT-34	IT-35	IT-36	IT-37	HS-8	HS-10	HS-11	HS-12	HS-13
SiO2	50.52	50.31	51.61	51.61	52.85	49.97	52.04	52.01	51.55	51.03	50.99	51.78	51.12
Al2O3	30.92	31.94	31.48	31.48	30.38	31.05	29.80	29.92	30.15	30.45	31.04	29.96	30.83
FeO	0.35	0.41	0.42	0.42	0.33	0.39	0.38	0.46	0.65	0.33	0.24	0.29	0.26
MnO	0.03	0.01	0.02	0.02	0.02	0.00	0.02	0.01	0.00	0.01	0.00	0.01	0.01
CaO	13.39	13.78	13.32	13.32	11.35	13.80	12.50	12.81	13.08	13.15	13.59	12.59	13.33
Na2O	3.60	3.51	3.78	3.78	4.10	3.67	4.25	4.17	4.13	3.69	3.61	3.79	3.51
K2O	0.30	0.28	0.32	0.32	0.38	0.25	0.30	0.31	0.23	0.25	0.23	0.26	0.24
TOTAL	99.10	100.24	100.94	100.94	99.42	99.12	99.30	99.69	99.79	98.89	99.69	98.67	99.30
n	3	3	4	4	4	4	4	4	4	4	3	4	4

Cations (based on 8 Oxygens)

	IT-30	IT-31	IT-32	IT-33	IT-34	IT-35	IT-36	IT-37	HS-8	HS-10	HS-11	HS-12	HS-13
Si	2.32	2.29	2.33	2.33	2.40	2.30	2.38	2.37	2.35	2.33	2.32	2.38	2.34
Al	1.67	1.71	1.67	1.67	1.63	1.68	1.61	1.61	1.62	1.66	1.68	1.62	1.66
Fe	0.01	0.02	0.02	0.02	0.01	0.02	0.01	0.02	0.02	0.01	0.01	0.01	0.01
Mn	0.00	0.00	0.00	0.00	0.00	0.00	0.00	0.00	0.00	0.00	0.00	0.00	0.00
Ca	0.66	0.67	0.64	0.64	0.55	0.68	0.61	0.63	0.64	0.66	0.67	0.62	0.65
Na	0.32	0.31	0.33	0.33	0.36	0.33	0.38	0.37	0.36	0.31	0.31	0.34	0.31
K	0.02	0.02	0.02	0.02	0.02	0.01	0.02	0.02	0.01	0.01	0.01	0.01	0.01

1 Standard Deviation (wt %)

	It-30	It-31	It-32	It-33	It-34	It-35	It-36	It-37	HS-8	HS-10	HS-11	HS-12	HS-13
SiO2	0.58	0.97	1.23	0.70	1.38	1.51	0.70	0.96	0.62	1.76	0.57	1.88	0.20
Al2O3	0.41	1.06	0.90	0.36	0.89	1.07	0.62	0.97	0.73	1.72	0.64	1.49	0.16
FeO	0.04	0.07	0.07	0.02	0.05	0.05	0.04	0.07	0.34	0.14	0.14	0.06	0.09
MnO	0.01	0.01	0.02	0.01	0.02	0.01	0.04	0.02	0.01	0.01	0.00	0.01	0.02
CaO	0.25	0.54	1.12	0.47	1.51	1.31	0.78	1.00	0.68	1.86	0.49	1.45	0.26
Na2O	0.12	0.27	0.54	0.24	0.32	0.71	0.42	0.64	0.35	0.78	0.25	0.71	0.09
K2O	0.03	0.05	0.06	0.06	0.04	0.06	0.05	0.05	0.03	0.09	0.04	0.09	0.02

Average Plagioclase analyses

unit	HSOG	HSOG	HSOG
wt%	HS-14	HS-15	HS-18
SiO2	51.73	53.93	51.64
Al2O3	30.31	29.31	30.23
FeO	0.28	0.31	0.43
MnO	0.00	0.01	0.05
CaO	12.85	11.49	12.77
Na2O	3.79	4.64	3.81
K2O	0.28	0.35	0.27
TOTAL	99.25	100.04	99.18
n	4	4	4

Cations (based on 8 Oxygens)

	HS-14	HS-15	HS-18
Si	2.36	2.46	2.36
Al	1.63	1.53	1.63
Fe	0.01	0.01	0.02
Mn	0.00	0.00	0.00
Ca	0.63	0.52	0.62
Na	0.34	0.44	0.34
K	0.02	0.02	0.02

1 Standard Deviation (wt %)

	HS-14	HS-15	HS-18
SiO2	0.44	3.43	0.52
Al2O3	0.54	2.36	0.39
FeO	0.05	0.03	0.06
MnO	0.00	0.02	0.03
CaO	0.48	2.81	0.38
Na2O	0.18	1.56	0.27
K2O	0.05	0.11	0.05

Appendix III

Whole Rock Geochemical Analysis

X-Ray Fluorescence

Apparatus: ARL 9400XP+ Wavelength dispersive XRF Spectometer

Sample Preparation: Samples were dried and roasted at 1000°C to determine % loss on ignition. ***Major element analysis*** was executed on fused beads, following the standard method used in the XRF and XRD laboratory of the University of Pretoria, as adapted from H. Bennett and G. Oliver's proposed methods in "XRF Analysis of Ceramics, Minerals and Applied Materials" John Wiley and Son 1992: p 67-93.

5 grams of the sample were weighed, and then roasted overnight in 110° oven, and then weighed again. This pre-roasting was conducted to evaporate excess water from the sample. 1 gram pre-roasted sample + 6 grams Lithium Tetra Borate flux were mixed in a 5 % Au/Pt crucible and fused at 1000°C in a muffle furnace with occasional swirling. The glass disks are poured into a pre-heated Pt/Au mould, and the bottom surface of the disk is analysed. ***Trace elements*** were analysed on pressed powder pellets, using an adaption of the method used described by J.S. Watson in "Fast, Simple Method of Powder Pellet Preparation for X-Ray Fluorescence Analysis", X-Ray Spectrometry, Vol.25 1996, p173-174, and using saturated Mowoil 40-88 solution as a binder.

Calibration: The XRF Spectrometer was calibrated with certified reference materials. The NBSGSC fundamental parameter program was used for matrix correction of major elements as well as Cl, Co, Cr, V, Sc, and S. The Rh Compton peak ratio method was used for other trace elements.

Standard Deviation and Limit of Detection for XRF:

	std.dev.(%)	LOD
SiO_2	0.4	0.02
TiO_2	0.03	0.0032
Al_2O_3	0.3	0.01
Fe_2O_3	0.3	0.0097
MnO	0.0065	0.0013
MgO	0.1	0.0118
CaO	0.07	0.01
Na_2O	0.11	0.0265
K_2O	0.06	0.005
P_2O_5	0.08	0.01
Cr_2O_3	0.0053	0.0006
NiO	0.01	0.0013
V_2O_5	0.0018	0.0008
ZrO_2	0.005	0.0009
CuO	0.0037	0.0003

Values for elements indicated with * should be considered semi-quantitative

	std dev.(ppm)	LOD
As*	10	3
Cu	3	2
Ga	2	2
Mo	1	1
Nb	3	2
Ni	6	3
Pb	3	3
Rb	4	2
Sr	4	3
Th	2	3
U	2	3
W*	10	6
Y	4	3
Zn	4	4
Zr	6	10
Ba	14	5
Ce	14	6
Cl*	100	11
Co	6	3
Cr	40	15
F*	500	400
La	24	5
S*	300	40
Sc	5	1
V	10	1

ICP-MS Analysis, from University of Cape Town, SA

Apparatus: Perkin Elmer / Sciex Elan 6000 inductively coupled plasma mass spectrometer equipped with an acid-resistant cross flow nebuliser, a *Ryton*™ Scott-type spraychamber and a Perkin Elmer AS 90 autosampler.

Sample Preparation: In the case of solid samples analysed by laser ablation ICP-MS and liquid samples analyzed by solution ICP-MS, sample preparation may be minimal. Rock samples to be analysed by solution ICP-MS have to be dissolved by *acid digestion*. Various digestion methods involving a range of different ultra clean acids (e.g. HF, HNO_3, HCl, $HClO_4$, aqua regia) may be used to dissolve various types of materials. Digestion in a microwave oven may speed up the procedure and help to ensure that all of the sample material is dissolved. Fusion procedures using one of a number of fluxing agents may be required to dissolve refractory minerals such as Zircon in some instances. For quantitative analysis, it is crucial that all of the sample material is entirely dissolved. One of the simple acid digestion procedures involves the digestion of 50-100 mg of fine, homogenous sample powder in a mixture of HNO_3 and HF in heated, closed Teflon beakers, followed by evaporation to complete dryness and two further stages of digestion in HNO_3 and evaporation. The final stage of sample preparation involves dissolution in ~2 % HNO_3 internal standard stock solution containing 10 ppb of all the internal standards required for analysis. Most rock samples have to be diluted by a factor of at least 1000-2000 times in order to lower the total dissolved solid content of the final solution to a level at which a clogging of interface cone orifices is not a problem.

Calibration: For quantitative ICP-MS analysis, calibration is most commonly achieved by *external standardization*. The signal intensities of all the analyte isotopes are measured in a blank as well as in one or more artificial or natural standards with different, known analyte concentrations that cover the concentration range of interest. The (hopefully) linear relationship between the blank-corrected standards on a diagram of signal intensity vs. concentration is used to establish a calibration curve that may be used to calculate the concentration of the analytes in samples of unknown composition. Isotopes commonly used as internal standards in solution ICP-MS include ^{9}Be, ^{45}Sc, ^{89}Y, ^{103}Rh, ^{115}In, and ^{209}Bi.

Analytical Range and Detection Limits: The analytical range of solution ICP-MS extends from the ppt (parts per trillion) to the ppm (parts per million) regions. Solution ICP-MS combines perfectly with a good major an minor element technique such as X-ray fluorescence spectrometry (XRF). For most elements that can be determined by solution ICP-MS, best-scenario theoretical detection limits are in the ppt range (some in the ppb range).

Accuracy and Precision: In most cases, accuracies and precisions of ~ 1-3 % may be expected for solution ICP-MS for all elements. Accuracies and precisions of ~ 1-10 % are typical for most elements analysed by laser ablation ICP-MS.

XRF WR Data																			
Height m	3	34.37	43.75	76.56	93.75	115.62	131.25	143.75	159.37	170.31	210.93	243.75	285.93	317.18	331.25	400	425	440.62	467.18
Rock	BOG	BOG	BOG	BOG	BOG	BOG	BOG	BOG	PU	PU	PU	PU	PU	PU	PU	PU	PU	PU	COG
%	IT-3	IT-4	IT-5	IT-6	IT-7	IT-8	IT-10	IT-11	IT-12	IT-13	IT-14	IT-15	IT-16	IT-17	IT-18	IT-19	IT-20	IT-21	IT-22
SiO2	38.34	42.87	41.74	42.51	42.04	41.19	41.52	41.33	41.53	41.24	41.40	40.82	41.31	40.94	40.01	41.28	39.38	40.18	43.17
TiO2	0.35	0.31	0.30	0.27	0.24	0.22	0.18	0.17	0.16	0.17	0.16	0.17	0.18	0.15	0.15	0.19	0.11	0.20	0.21
Al2O3	5.39	5.95	5.38	4.70	4.00	3.98	3.26	3.22	2.93	2.97	2.85	2.95	3.12	3.16	3.12	2.99	3.70	3.20	16.16
Fe2O3	15.20	13.48	13.95	14.89	14.05	14.08	14.02	14.07	14.65	14.75	13.82	14.45	14.19	14.76	15.24	16.23	14.82	16.12	9.85
MnO	0.21	0.19	0.19	0.20	0.19	0.19	0.19	0.19	0.20	0.20	0.18	0.19	0.19	0.19	0.20	0.21	0.20	0.21	0.12
MgO	32.32	29.82	30.15	32.44	35.06	35.21	36.87	37.08	37.05	36.85	37.81	37.68	37.98	36.93	36.60	35.29	34.22	35.53	18.19
CaO	4.87	4.21	3.57	3.22	2.84	2.6	2.46	2.49	2.15	2.19	2.03	2.09	2.23	2.25	2.12	1.95	2.76	2.30	8.34
Na2O	0.57	0.24	0.11	<0.03	<0.03	0.01	<0.03	<0.03	<0.03	<0.03	<0.03	<0.03	<0.03	<0.03	<0.03	<0.03	<0.03	<0.03	0.87
K2O	0.37	0.23	0.24	0.25	0.23	0.23	0.11	0.10	0.09	0.11	0.16	0.10	0.10	0.06	0.11	0.09	0.04	0.11	0.21
P2O5	0.05	0.05	0.05	0.05	0.04	0.05	0.03	0.03	0.03	0.03	0.03	0.03	0.03	0.02	0.03	0.04	0.02	0.04	0.04
Cr2O3	0.42	0.62	0.77	0.51	0.58	0.57	0.80	0.56	0.54	0.57	0.56	0.69	0.85	0.98	0.74	0.54	0.62	0.57	0.28
NiO	0.18	0.19	0.20	0.16	0.18	0.17	0.16	0.17	0.16	0.17	0.20	0.19	0.22	0.21	0.20	0.17	0.16	0.17	0.02
V2O5	0.02	0.02	0.03	0.02	0.02	0.02	0.02	0.02	0.02	0.02	0.02	0.02	0.02	0.02	0.02	0.02	0.02	0.02	<0.01
ZrO2	<0.01	<0.01	0.05	<0.01	<0.01	<0.01	<0.01	<0.01	<0.01	<0.01	<0.01	<0.01	<0.01	<0.01	<0.01	<0.01	<0.01	<0.01	<0.01
LOI	0.18	0.56	2.53	-0.55	0.61	0.16	0.02	0.19	0.69	0.41	0.49	-0.11	-0.23	-0.35	0.67	-0.47	2.97	0.01	1.69
TOTAL	98.48	98.74	99.25	98.69	100.09	98.68	99.46	99.64	100.22	99.70	99.73	99.30	100.19	99.34	99.20	98.53	99.01	98.67	99.15
ppm	IT3	IT4	IT5	IT6	IT7	IT8	IT10	IT11	IT12	IT13	IT14	IT15	IT16	IT17	IT18	IT19	IT20	IT21	IT22
As	9	10	9	8	9	8	8	9	9	8	7	7	9	10	8	9	10	9	9
Cu	74	70	57	47	54	42	21	19	13	22	57	63	40	50	62	182	185	275	125
Ga	14	15	16	15	13	13	12	13	12	13	12	12	13	13	12	12	12	12	18
Mo	2	4	3	2	3	2	3	2	2	2	3	2	2	2	4	3	3	<1	2
Nb	4	4	4	3	3	4	2	3	2	2	3	3	4	2	4	2	2	3	3
Ni	1265	1517	1533	1270	1376	1311	1275	1346	1271	1339	1571	1530	1743	1656	1526	1373	1210	1390	149
Pb	<3	7	5	<3	6	5	4	5	4	4	<3	<3	<3	6	<3	<3	<3	6	6
Rb	11	12	10	10	10	11	9	7	5	7	10	6	7	5	7	5	5	7	9
Sr	81	72	72	67	52	53	49	49	45	45	43	45	46	46	49	47	50	50	206
Th	<3	6	<3	<3	<3	4	5	4	<3	<3	<3	<3	<3	4	<3	4	4	<3	<3
Y	15	13	14	12	13	11	11	10	11	10	10	9	10	9	9	11	8	10	11
Zn	90	84	88	97	85	83	83	84	85	84	77	82	84	83	87	105	86	95	51
Zr	45	44	43	45	37	37	26	28	28	26	27	25	25	23	27	25	17	24	32
Cl	1114	1173	1578	1064	1503	906	868	1679	1269	945	870	722	1055	730	1368	553	1377	928	845
Co	127	122	129	134	135	137	140	140	144	155	145	143	144	144	156	150	150	155	84
Cr	2872	4151	4924	3416	3732	3731	3988	3492	3332	3607	3427	4289	5273	5872	4358	3410	3494	3455	1785
S	404	458	429	242	395	355	297	308	322	274	420	393	322	388	358	1538	1604	2209	638
Sc	15	14	13	13	11	13	12	12	11	11	13	12	13	11	11	14	10	12	<1
V	113	114	119	102	89	82	84	78	76	76	73	75	78	78	87	90	72	92	70

XRF WR Data																		
Height m	475	515.62	531.25	548.43	587.5	604.68	621.87	654.68	685.93	720.31	725	734.37	756.25	781.25	796.87	46	40	35	29
Rock	CG	CG	CG	CG	CG	CG	CG	UOG	UOG	UG	UG	UG	UG	UG	UG	HSG	HSOG	HSOG	HSOG
%	IT-23	IT-24	IT-25	IT-26	IT-27	IT-28	IT-29	IT-30	IT-31	IT-32	IT-33	IT-34	IT-35	IT-36	IT-37	HS8	HS10	HS11	HS12
SiO2	49.90	50.91	51.59	49.79	47.65	50.65	50.31	49.99	46.15	42.71	52.15	50.58	45.85	50.88	50.88	54.05	42.79	43.05	43.19
TiO2	0.21	0.26	0.32	0.30	0.32	0.32	0.30	0.35	0.50	0.67	0.45	0.58	0.53	0.70	0.61	0.90	0.34	0.36	0.34
Al2O3	21.68	18.42	17.91	16.68	16.04	15.88	17.38	17.64	17.14	15.06	15.77	15.30	14.99	15.23	17.08	15.37	5.34	5.55	5.56
Fe2O3	5.10	5.41	6.17	6.37	8.35	7.44	7.94	8.13	9.36	10.01	9.50	9.97	11.21	10.10	9.37	10.93	15.23	15.39	15.29
MnO	0.09	0.11	0.12	0.13	0.16	0.16	0.14	0.13	0.15	0.17	0.16	0.18	0.21	0.18	0.16	0.17	0.20	0.20	0.20
MgO	8.15	8.09	8.05	8.36	10.95	8.62	9.00	8.37	10.25	10.43	8.97	8.25	9.57	7.02	5.71	6.92	28.94	28.59	28.78
CaO	11.57	13.62	13.23	13.40	15.29	12.58	11.91	12.62	14.82	15.99	13.01	11.17	14.16	11.11	11.38	9.73	3.55	3.65	3.86
Na2O	1.45	1.38	1.60	1.60	1.63	1.75	2.01	1.94	2.07	2.44	1.88	2.06	2.41	2.13	2.53	2.16	0.22	0.25	0.30
K2O	0.24	0.19	0.26	0.22	0.29	0.28	0.24	0.28	0.28	0.44	0.21	0.29	0.33	0.43	0.40	0.80	0.29	0.35	0.31
P2O5	0.03	0.03	0.04	0.06	0.03	0.03	0.03	0.04	0.06	0.09	0.03	0.07	0.05	0.10	0.08	0.15	0.07	0.07	0.08
Cr2O3	0.15	0.12	0.08	0.09	0.05	0.06	0.06	0.11	0.10	0.09	0.07	0.05	0.06	0.04	0.04	0.04	0.37	0.34	0.35
NiO	<0.01	<0.01	<0.01	<0.01	<0.01	<0.01	0.02	0.02	0.02	<0.01	0.02	<0.01	<0.01	<0.01	<0.01	<0.01	0.05	0.05	0.05
V2O5	0.02	0.04	0.04	0.04	0.05	0.05	0.03	0.03	0.04	0.04	0.04	0.04	0.04	0.04	0.04	0.04	0.03	0.03	0.03
ZrO2	<0.01	<0.01	<0.01	<0.01	<0.01	<0.01	<0.01	0.01	<0.01	<0.01	0.01	<0.01	<0.01	<0.01	<0.01	<0.01	<0.01	0.00	0.00
LOI	0.25	0.26	0.23	0.23	0.16	0.09	-0.11	-0.03	-0.02	0.06	-0.15	-0.17	-0.17	0.89	-0.06	-0.02	1.48	1.30	0.88
TOTAL	98.87	98.86	99.65	97.28	100.97	97.92	99.28	99.62	100.94	98.23	102.11	98.38	99.26	98.87	98.22	101.25	98.90	99.17	99.23
ppm	IT23	IT24	IT25	IT26	IT27	IT28	IT29	IT30	IT31	IT32	IT33	IT34	IT35	IT36	IT37	HS8	HS10	HS11	HS12
As	8	9	8	8	7	9	8	8	7	8	9	9	8	8	9	9	9	9	8
Cu	83	54	49	58	43	44	17	35	70	56	62	54	94	62	212	48	103	87	105
Ga	22	23	21	22	22	19	21	22	21	21	20	22	22	24	24	24	14	14	14
Mo	2	2	3	2	3	3	3	<1	2	3	2	3	3	2	2	3	2	<1	3
Nb	4	2	4	2	3	3	3	3	4	5	3	5	5	5	5	7	4	3	4
Ni	72	48	39	34	30	43	126	139	143	117	125	113	121	72	29	24	429	351	400
Pb	5	<3	10	<3	<3	4	<3	<3	<3	4	4	4	<3	<3	5	7	6	7	4
Rb	10	8	14	10	10	11	11	9	7	13	4	10	8	14	12	26	12	10	11
Sr	244	227	235	226	234	239	263	244	242	238	218	232	240	240	267	227	83	79	79
Th	<3	4	5	<3	<3	<3	4	<3	<3	5	<3	<3	<3	4	<3	4	<3	<3	<3
Y	9	13	14	13	14	15	14	14	17	21	16	18	17	23	21	28	16	15	13
Zn	31	34	40	40	47	47	44	51	50	57	60	63	64	73	63	88	101	93	94
Zr	24	28	33	28	29	28	27	34	37	52	27	44	38	59	47	106	49	45	49
Cl	260	322	324	180	391	223	357	457	510	553	385	648	487	693	347	312	993	672	495
Co	24	28	30	34	40	41	48	45	45	43	52	56	54	51	45	52	132	126	130
Cr	1120	835	417	491	283	340	289	528	495	431	383	275	304	220	211	231	2401	2032	2249
S	241	188	137	118	152	21	212	136	217	163	219	71	74	34	70	840	937	714	891
Sc	5	17	18	19	25	30	17	15	18	20	29	27	23	29	24	26	14	16	14
V	109	185	183	201	211	230	160	148	158	191	210	205	193	223	210	213	121	108	116

XRF WR Data					
Height m	23	17	11	5	0
Rock	HSOG	HSOG	HSOG	HSOG	HSOG
%	HS13	HS14	HS15	HS16	HS18
SiO2	42.98	43.52	43.56	48.69	46.31
TiO2	0.36	0.40	0.49	0.56	0.57
Al2O3	5.93	6.26	7.27	13.97	8.74
Fe2O3	15.13	14.69	13.70	10.47	13.25
MnO	0.20	0.19	0.19	0.53	0.18
MgO	28.24	27.78	24.48	3.45	22.01
CaO	3.88	4.16	4.83	12.93	5.78
Na2O	0.31	0.40	0.66	1.17	0.88
K2O	0.30	0.30	0.43	1.90	0.46
P2O5	0.09	0.08	0.10	1.27	0.11
Cr2O3	0.45	0.46	0.46	<0.01	0.42
NiO	0.08	0.08	0.06	0.10	0.05
V2O5	0.03	0.03	0.03	0.03	0.03
ZrO2	<0.01	<0.01	<0.01	<0.01	<0.01
LOI	0.62	1.14	1.36	4.10	0.44
TOTAL	98.58	99.50	97.63	99.17	99.26
ppm	HS13	HS14	HS15	HS16	HS18
As	9	8	10	20	8
Cu	200	199	115	174	101
Ga	14	15	16	21	17
Mo	2	3	<1	3	2
Nb	3	3	5	9	5
Ni	561	604	454	713	383
Pb	6	4	9	39	6
Rb	12	10	16	87	16
Sr	78	90	106	234	116
Th	<3	<3	4	17	4
Y	14	14	17	40	18
Zn	89	90	87	120	85
Zr	45	48	56	85	62
Cl	473	623	398	216	583
Co	125	121	107	71	98
Cr	2730	2793	2905	55	2504
S	1530	1398	1076	4847	932
Sc	14	13	18	13	16
V	113	120	137	130	144

ICP-MS analyses

Height	0	43.75	76.56	115.62	210.93	285.93	331.25	400	440.62	467.18	475	548.43	621.87
Sample	**It-3**	**It-5**	**It-6**	**It-8**	**It-14**	**It-16**	**It-18**	**It-19**	**It-21**	**It-22**	**It-23**	**It-26**	**It-29**
Sc	16.6	14.8	13.7	12.3	10.7	10.6	10.4	12.1	10.9	6.49	12.2	30.5	26
Se	n.d	n.d	n.d	n.d	n.d	n.d	n.d	n.d	n.d	n.d	n.d	n.d	n.d
Rb	7.95	6.9	6.73	5.92	6.13	2.59	2.95	2.17	3.08	6.32	5.84	5.51	6.01
Sr	68.2	60.4	57	40.8	32.1	36.5	36.5	33	39.1	193	234	218	244
Y	8.45	7	6.77	5.39	3.56	3.76	3.37	3.72	4.59	4.93	4.83	7.75	7.54
Zr	43.1	30.2	30.1	24.5	12.5	15.6	11.3	11.5	15	23.4	10.4	20.9	22.6
Nb	2.79	2.15	2.17	1.41	0.95	1.06	0.86	0.81	1.1	1.71	1.3	1.43	1.49
Mo	0.48	0.43	0.43	0.34	0.21	0.25	0.22	0.25	0.3	0.27	0.21	0.22	0.2
Sb	0.042	0.033	0.021	0.015	0.015	n.d.	n.d.	n.d.	0.027	0.018	0.043	0.027	0.021
Cs	0.21	0.18	0.11	0.13	0.32	0.068	0.061	0.055	0.057	0.011	0.035	0.015	0.025
Ba	68.8	61.7	52.4	39.8	31.5	25.2	33.8	24.3	36.3	57.7	57.8	61.4	69.4
La	4.86	4	4.04	3.48	2.18	2.12	1.93	1.75	2.03	3.1	2.83	2.89	3.05
Ce	9.96	8.44	8.77	7.52	4.78	4.49	4.21	3.8	4.46	6.65	5.89	6.35	6.81
Pr	9.96	8.44	8.77	7.52	4.78	4.49	4.21	3.8	4.46	6.65	5.89	6.35	6.81
Nd	5.35	4.51	4.52	3.96	2.5	2.31	2.23	2.07	2.58	3.51	3.12	3.85	3.97
Sm	1.27	1.06	1.02	0.87	0.55	0.52	0.51	0.51	0.63	0.81	0.75	1.01	1.03
Eu	0.38	0.32	0.3	0.22	0.17	0.17	0.15	0.16	0.21	0.39	0.49	0.49	0.58
Gd	1.49	1.27	1.21	0.98	0.66	0.63	0.61	0.6	0.75	0.89	0.81	1.26	1.22
Tb	0.24	0.2	0.2	0.16	0.1	0.1	0.1	0.1	0.13	0.14	0.13	0.22	0.2
Dy	1.63	1.37	1.26	1.01	0.67	0.68	0.65	0.67	0.84	0.9	0.87	1.41	1.39
Ho	0.32	0.28	0.27	0.22	0.14	0.14	0.13	0.15	0.18	0.19	0.18	0.3	0.29
Er	0.95	0.8	0.74	0.6	0.4	0.43	0.36	0.44	0.5	0.51	0.54	0.86	0.82
Tm	0.13	0.12	0.11	0.09	0.06	0.064	0.055	0.064	0.075	0.08	0.081	0.13	0.12
Yb	0.91	0.75	0.75	0.58	0.41	0.43	0.38	0.47	0.5	0.5	0.51	0.81	0.79
Lu	0.14	0.11	0.11	0.091	0.064	0.068	0.063	0.068	0.08	0.079	0.083	0.12	0.12
Hf	1.08	0.74	0.77	0.62	0.33	0.39	0.29	0.29	0.4	0.55	0.3	0.58	0.58
Ta	0.32	0.25	0.22	0.21	0.15	0.15	0.15	0.14	0.28	0.31	0.25	0.24	0.25
Pb	2.05	1.75	1.39	1.31	0.71	0.54	0.79	0.86	1.84	1.57	1.44	1.19	2.46
Th	0.93	0.79	0.78	0.66	0.56	0.38	0.33	0.31	0.31	0.58	0.42	0.43	0.65
U	0.23	0.2	0.21	0.17	0.17	0.11	0.088	0.087	0.081	0.15	0.1	0.11	0.2

ICP-MS analyses

Height	720.31	781.25	796.87
Sample	**It-32**	**It-36**	**It-37**
Sc	30.3	33.7	30.1
Se	n.d	1.7	n.d
Rb	6.99	9.61	8.38
Sr	225	225	253
Y	14	16.8	14.5
Zr	42.4	47.1	39.5
Nb	4.63	4.57	3.49
Mo	0.26	0.26	0.16
Sb	n.d.	0.016	0.022
Cs	0.018	0.14	0.15
Ba	107	141	121
La	5.2	6.33	4.95
Ce	11.4	13.8	10.9
Pr	11.4	13.8	10.9
Nd	7.09	8.42	6.84
Sm	1.84	2.17	1.82
Eu	0.73	0.88	0.84
Gd	2.28	2.69	2.29
Tb	0.38	0.44	0.39
Dy	2.5	2.98	2.59
Ho	0.54	0.64	0.55
Er	1.53	1.78	1.57
Tm	0.22	0.26	0.23
Yb	1.42	1.72	1.48
Lu	0.21	0.26	0.22
Hf	1.08	1.26	1.02
Ta	0.43	0.43	0.34
Pb	2.08	1.81	1.74
Th	0.65	0.88	0.63
U	0.16	0.23	0.15

Appendix IV

Stream sediment geochemistry

Major and Trace elements:

The procedure for analysis of major and trace elements is the same as for whole rock geochemistry.

Pt and Pd

Pt and Pd were analysed in the following manner:

The instrument used is a Varian Vista Pro ICP with axial configuration and a CCD detector. Detection limits are for fire assay finished by ICP. The samples are prepared by splitting in a riffle splitter to create a sample of about 500 g. This is then milled so that 90 % of the material passes through a 106 micrometer screen. The sample is then fire assayed in charges of 50 g using various collectors in appropriate fluxes. A blank, duplicate, and reference standard are included in each batch of 35 samples. The resultant prill is dissolved by in house methods at Set Point Technologies. Pt and Pd are analysed for using ICP appropriate standards.

Stream Log

The following is a log of the various streams sampled, including a brief description and ph values.

a- This stream is well below the floor contact with country rocks. There is a large variety of different lithologies in the float including rocks from the Central Zone. Stream contains some clay material; ph is 6. GPS- S 30° 35. 032', E 029° 38.619'

b- This sample was taken below the Basal Zone contact of the intrusion, however, stream does not appear to cut through outcrop of any rock type in the immediate area. Boulders line the stream and clays and organics fill the voids between boulders. Sample was taken from behind a boulder trap; ph is 6. GPS- S 30° 35.372', E 029°38'.171

c- The sample was taken below the Jack Se dam and the known hornfels contact. The dam will most likely affect metal tenors. The bed load mostly consists of hornfels with the odd piece of lower gabbronorite mixed in. Sample was taken from a boulder trap; ph is 6. GPS- S 30° 35.885', E 029°37.874

d- The mud tends to be thick along the banks of this stream. Small clasts of lower gabbronorite are mixed in the mud matrix. Sample was taken from a trap directly down stream from where a small spring enters the main stream; ph is 7. GPS- S 30° 36.028, E 029°37.602

e- This is a large stream below the intrusive contact with the hornfels. The sample was taken below the road, and less than a km below the floor contact. The outcropping rocks appear to be hornfels; ph is 6. GPS- S 30° 36.284, E 029°37.777

f- The sample was taken from a small stream by a road cut that exposes hornfels. The bed load is fine grained, and contains coarse angular fragments of hornfels throughout; ph is 6.5. GPS- S 30° 34.970, E 029° 38.879

g- Sample was taken from a large stream below the floor contact of the lobe. The sample was collected below a logged out section of the Weza forest plantation where a house/office has been built. Most of the bed load consists of fist sized

cobbles. Many boulders are found and they offer a number of quality sediment traps; ph is 6. GPS- S 30°34.619, E 029° 39.291

h- Sample was taken below the hornfels contact and down stream from a large waterfall. Sediment is fine, but appears free of organic material and clay. The sample was taken behind small boulders where traps could be found; ph is 6. GPS- S 30°33.731, E 029°39.391

i- The sample was taken dry and later sieved up-stream in the stream bed where water was found. No ph measurement. GPS- S 30°33.426, E 029°39.551

j- The sample was taken from an area well below the hornfels contact with the intrusion. The area is quite overgrown, and contains little water. The water is slow moving and contains fine silt material. The sample was taken in a faster flowing stretch of water were sediment was clean and free of organic material; ph is 6. GPS- S 30°32.801, E 029°40.551

k- The sample was taken from a stream that has an abundance of hydrodynamic traps, and coarse grained material. Most of the larger clasts in the stream bed are hornfels that are thumb sized; ph is 6. GPS- S 30°32.143, E 029°39.571

l- Sample was taken below the convergence of two perennial streams. This stream has very little in the way of suitable sediment, or traps. This stream is in the natural Ingeli forest and not the Weza plantation; ph is 6. GPS- S 30°31.774, E 029°40.119

m- Sample was taken below a dolerite hill. This stream runs through boulders, brush, and overburden before being exposed. The bed load consists of clasts ultramafic

rocks. The sample was taken in the riffles of the fast flowing water; ph is 6. GPS- S 30°32.400, E 029°39.490

n- Sample was taken on a dolerite exposure, and down-stream from the convergence of two streams. The water clarity is milky here and sample was taken from a depression in the dolerite were the sediment had been trapped; ph is 6.GPS- S 30°32.275, E 029°38.268

o- Sample was taken from a small stream above the town of Ingeli. Sample was taken below dolerite contact with hornfels. This stream contains high amounts of organics and very little quality sediment. The stream maybe too far below the floor rock contact of the Ingeli lobe; ph is 6. GPS- S 30°31.895, E 029°37.102

p- Sample was taken above town of Ingeli. The sample was later sieved at the Falconbridge offices. No ph measurement. GPS- S 30°32.407, E 029°37.319

q- This sample was taken below the contact with the hornfels, but above the major stream confluence near the Clover Combined School where local settlement is quite abundant. Most of the boulders are hornfels and dolerites; ph 6. GPS- S 30°34.028, E 029°36.241

r- Sample was taken from a stream that appears to drain the gabbroic areas of the lobe. The Basal Zone rocks are not exposed here. The sample was taken from behind a boulder where the water was clean, and the sediment lacked organic material and clays; ph is 6. GPS- S 30°33.515, E 029°36.892

s- Sample was taken from a large stream that is flanked on one side by a ridge of dolerite. The clasts in the stream bed tend to be dolerites, gabbroic rocks and hornfels; ph is 6. GPS- S 30°34.422, E 029°35.094

t- This sample was taken from a slow moving stream that did not have an abundance of suitable sediment. The stream cuts both gabbros and dolerites farther upstream; ph is 6. GPS- S 30°36.426, E 029°31.878

u- Sample was taken below an area where the hornfels bedrock is exposed in several places. Sediment was found to lie within cracks found in the hornfels; ph is 6. GPS- S 30°35.562, E 029°33.655

v- Sample was taken above the town of Lower Brooks' Neck. Sediment seems to be mostly made up of hornfels, although dolerite clasts can also be found. Most of the sediment is pebble to cobble sized. Red staining is also found on the banks of the stream; ph is 6. GPS- S 30° 713, E 029°30.635

w- Sample was taken from a non-perennial stream that barely drains the lowest section of the lobe. The stream is full of dolerite and hornfels boulders; ph is 6. GPS-S 30°39.591, E 029°32.264

x- The sample was taken from perennial stream that has cut a large gorge in the in situ bedrock hornfels; ph is 6. GPS- S 30°39.778, E 029°32.588

y- The sample was taken from a stream that cuts across a dolerite outcrop, and may not come into contact with the Ingeli lobe; ph is 6. GPS- S 30°40.318, E 029°33.019

z- Stream above little a settlement. The country rock is dolerite, but hornfels clasts are also found in the stream bed; ph is 6. GPS- S 30°40.395, E 029°33.763

A0- The sample was taken at the convergence of many non-perennial streams that cut the dolerite and hornfels. Many dolerite boulders are found in the float; ph is 6. GPS- S 30°40.428, E 029°35.183

B0- The sample was taken from a non-perennial stream below the dense natural tree line. This sample could be ½ km too far from the contact with the floor rocks. Strong weather made sieving at this cite impossible, so sieving was carried out at the Falconbridge offices; ph is 6. GPS- S 30°40.425, E 029°35.660

C0- The sample was taken in a stream that drained the natural forest. The cliff on the right side of the stream is made of dolerite. The stream bed is dominated by large gabbro boulders. Sample was taken from a boulder trap; ph is 6. GPS- S 30°39.990, E 029°35.918

D0- This stream mainly cuts through dolerite and natural forest; ph is 6. GPS- S 30°40.247, E 029°37.792

E0- This stream flows off the Ingeli lobe, and through a concrete pipe. Sample was taken below this pipe because there is not enough water found above it; ph is 6. GPS- S 30°36.689, E 029°37.762

F0- The sample was taken in mixed natural forest/plantation area. Hornfels boulders dominate stream bed and the sample was taken below one of these boulders; ph is 6. GPS- S 30°37.700, E 029°37.500

G0- The sample was taken in a stream that drains a small gabbroic lobe to the northwest of the Ingeli lobe; ph is 6.GPS- S 30°34.730, E 029°31.162

XRF analyses for stream sediments in the Ingeli lobe

Streams	a	b	c	d	e	f	g	h	i	j	k	l	m	n	o
SiO2	35.70	30.79	29.99	33.86	38.65	37.55	35.52	33.51	33.93	38.34	38.69	55.11	44.74	60.65	69.23
TiO2	1.09	1.02	1.82	1.36	1.28	1.13	1.29	1.07	0.92	1.62	1.24	1.89	2.53	2.33	2.17
Al2O3	15.37	15.97	16.56	12.97	20.86	12.18	14.91	13.91	11.40	17.22	17.21	15.01	13.58	11.64	8.40
Fe2O3	23.58	25.72	29.41	21.88	14.76	23.12	18.56	26.38	25.35	21.28	20.81	12.24	18.21	11.66	9.46
MnO	0.25	0.26	0.72	0.23	0.19	0.34	0.21	0.26	0.29	0.18	0.50	0.19	0.30	0.18	0.24
MgO	3.26	3.22	2.19	3.50	0.96	4.73	3.04	2.71	6.33	2.06	1.22	0.72	1.71	0.81	0.38
CaO	0.72	1.01	0.71	1.16	0.74	0.63	1.40	0.59	1.21	0.55	0.55	0.56	1.82	1.03	0.71
Na2O	0.84	0.24	0.26	0.31	0.29	0.23	0.35	0.21	0.30	0.24	0.22	0.20	0.54	0.44	0.54
K2O	0.48	0.46	0.43	0.47	1.01	0.47	0.76	0.33	0.37	0.49	0.79	1.60	0.55	0.91	1.42
P2O5	0.12	0.13	0.09	0.13	0.18	0.14	0.19	0.12	0.15	0.12	0.12	0.16	0.09	0.10	0.06
Cr2O3	1.57	1.43	1.90	3.15	0.11	3.67	1.04	2.50	2.82	1.31	0.85	0.19	1.49	0.28	0.05
NiO	0.23	0.19	0.15	0.17	0.03	0.20	0.11	0.26	0.26	0.12	0.12	0.03	0.07	0.04	0.03
V2O5	0.06	0.07	0.09	0.09	0.04	0.09	0.06	0.07	0.08	0.07	0.05	0.04	0.09	0.05	0.03
ZrO2	<0.01	0.02	0.18	0.11	0.10	0.06	0.10	0.09	0.08	0.13	0.11	0.19	0.18	0.28	0.41
LOI	16.05	18.12	13.98	18.16	18.15	14.04	19.85	16.31	16.36	15.58	15.84	11.09	11.34	9.38	5.98
TOTAL	99.32	98.66	98.48	97.56	97.36	98.58	97.40	98.33	99.83	99.31	98.32	99.22	97.23	99.79	99.12
Traces															
ppm	a	b	c	d	e	f	g	h	i	j	k	l	m	n	o
As	3.00	5.72	5.62	5.36	9.76	3.47	6.61	8.32	7.21	7.30	8.03	10.54	5.95	5.38	5.72
Cu	58.14	131.96	106.87	102.84	64.11	102.99	83.48	122.01	144.12	100.43	95.22	42.26	74.24	32.68	34.17
Ga	14.99	23.09	23.24	17.38	25.78	21.91	19.70	13.78	18.73	16.84	17.00	22.95	18.33	2.00	17.14
Mo	1.77	2.28	2.52	3.40	2.72	1.00	3.67	2.95	2.50	2.25	3.14	2.49	<1	2.04	<1
Nb	36.05	10.33	14.88	12.64	19.40	13.60	14.59	15.40	11.01	16.75	17.20	19.30	21.30	20.70	17.37
Ni	1429.36	1069.86	724.14	1009.64	107.03	1223.36	550.57	1572.56	1579.79	672.97	586.51	75.49	316.63	97.82	41.00
Pb	10.60	10.04	14.65	11.87	43.81	16.55	22.70	21.11	13.45	14.41	29.48	28.68	14.66	18.80	21.44
Rb	22.10	31.51	24.34	27.28	70.87	35.30	45.10	25.53	23.73	32.88	57.52	99.01	25.55	48.39	59.26
Sr	22.95	45.45	31.20	41.33	39.24	27.93	58.34	31.41	46.67	32.58	44.53	52.15	64.91	50.46	51.17
Th	5.58	9.21	7.46	4.98	20.12	10.25	13.66	15.73	9.16	5.28	16.42	15.44	9.93	8.33	11.63
U	3.00	<3	<3	<3	4.84	3.00	<3	4.94	<3	<3	<3	<3	<3	4.04	3.53
Y	15.47	28.99	24.87	28.21	55.00	29.88	28.43	28.59	20.84	30.56	35.70	35.42	27.85	28.98	28.72
Zn	149.76	134.41	147.41	183.35	113.84	187.79	122.14	135.10	158.20	106.60	108.68	111.66	103.54	67.38	39.70
Zr	162.91	214.68	426.35	308.33	249.89	236.51	242.87	227.35	196.84	303.33	255.56	469.78	445.15	597.24	675.51
Cl	236.31	199.06	115.08	259.80	281.28	361.63	313.10	135.10	135.15	114.11	83.91	263.67	97.02	73.44	170.09
Co	185.79	207.13	216.30	173.94	99.49	201.99	132.89	218.10	234.83	151.87	154.45	67.97	116.50	54.27	34.09
Cr	12402.47	7587.86	11169.44	19794.11	544.69	18567.02	5481.11	12926.85	15328.80	6975.00	4156.38	959.26	8046.65	1514.05	182.50
S	63.71	603.68	488.10	564.67	481.38	105.59	722.99	477.71	629.08	352.44	354.12	348.17	288.31	235.13	169.09
Sc	28.28	63.15	69.70	45.62	54.63	29.86	46.74	51.13	40.56	56.96	51.23	33.85	48.47	34.87	22.58
V	421.11	339.33	471.91	464.95	258.40	364.71	299.93	330.53	339.44	322.80	261.00	200.53	407.89	223.82	136.60
Pt in ppb	<10		<10				<10	30	10	205				<10	
Pd in ppb	40		30				<10	25	20	100				<10	

XRF analyses for stream sediments in the Ingeli lobe

Streams	p	q	r	s	t	u	v	w	x	y	z	AO	BO	CO	DO	EO
SiO2	65.79	53.92	50.76	62.11	52.72	67.93	61.54	57.61	41.27	37.13	36.36	44.71	36.94	41.14	40.18	45.03
TiO2	2.57	1.93	2.49	1.87	1.95	2.29	1.87	1.17	1.00	1.07	0.98	0.96	1.69	2.71	1.70	1.54
Al2O3	9.04	14.68	14.12	10.51	13.30	6.81	13.39	14.04	12.56	16.84	12.06	15.83	16.14	14.85	18.22	22.82
Fe2O3	10.45	12.79	13.14	10.46	13.81	8.70	10.83	9.14	19.31	20.30	18.86	14.23	21.87	16.10	14.59	13.33
MnO	0.18	0.22	0.21	0.31	0.37	0.94	0.17	0.15	0.29	0.29	0.29	0.17	0.25	0.20	0.15	0.15
MgO	0.57	1.03	0.79	0.63	1.31	0.31	0.59	1.00	6.34	2.64	4.49	2.42	3.39	0.51	0.97	0.61
CaO	0.98	1.77	0.96	1.17	2.25	0.86	0.53	1.04	2.55	1.74	3.08	1.45	2.40	0.72	1.14	0.21
Na2O	0.56	0.79	0.39	0.60	0.72	0.88	0.54	0.47	0.77	0.52	0.61	0.35	0.57	0.27	0.33	0.16
K2O	1.12	0.97	0.84	1.22	0.62	1.16	1.59	1.65	0.87	0.52	0.53	1.07	1.25	0.72	0.86	1.14
P2O5	0.05	0.13	0.13	0.08	0.11	0.08	0.07	0.15	0.17	0.18	0.21	0.16	0.16	0.22	0.19	0.14
Cr2O3	0.09	0.07	0.08	0.06	0.13	0.10	0.07	0.05	1.24	1.18	1.21	0.51	0.31	0.12	0.09	0.06
NiO	0.03	0.03	0.03	0.03	0.03	0.02	0.03	0.03	0.16	0.15	0.12	0.07	0.05	0.02	0.03	0.02
V2O5	0.04	0.05	0.05	0.04	0.05	0.03	0.04	0.03	0.06	0.06	0.06	0.04	0.07	0.05	0.05	0.04
ZrO2	0.34	0.19	0.20	0.22	0.15	0.25	0.20	0.19	0.11	0.11	0.09	0.11	0.13	0.18	0.13	0.16
LOI	5.81	10.64	13.11	7.84	10.69	6.78	7.19	10.49	11.54	15.59	19.45	16.77	11.99	20.59	19.78	12.84
TOTAL	97.62	99.21	97.26	97.16	98.21	97.14	98.64	97.21	98.23	98.31	98.39	98.84	97.24	98.41	98.40	98.26
Traces																
ppm	p	q	r	s	t	u	v	w	x	y	z	AO	BO	CO	DO	EO
As	5.46	6.26	6.81	8.44	7.31	7.28	6.93	7.56	6.65	3.00	5.34	3.34	3.36	3.00	3.00	12.78
Cu	33.96	65.84	53.53	37.91	51.99	24.17	25.35	28.30	168.69	149.61	102.51	70.67	110.05	77.84	45.75	53.13
Ga	13.18	21.89	17.21	14.11	18.01	11.71	17.89	16.75	4.57	20.54	15.81	19.77	25.62	23.30	20.69	31.68
Mo	<1	1.97	1.81	<1	<1	<1	2.06	1.62	<1	1.00	3.76	1.00	1.00	1.00	3.24	1.78
Nb	18.07	18.49	19.97	18.69	13.62	19.59	93.64	14.69	7.78	9.97	8.82	11.30	14.87	18.88	61.41	26.07
Ni	58.74	96.18	74.06	47.75	100.37	39.04	88.80	37.66	757.18	844.38	563.16	323.24	205.82	104.54	153.28	65.36
Pb	17.34	17.30	8.32	21.23	13.95	7.01	23.85	19.70	5.65	9.82	7.04	14.98	11.24	16.00	17.09	32.26
Rb	51.30	41.62	41.35	56.43	28.14	43.25	75.05	95.33	38.31	29.37	24.24	60.49	59.15	41.50	35.30	73.92
Sr	56.02	88.37	55.27	77.17	80.31	68.00	66.97	83.78	100.16	66.42	72.23	62.13	96.56	41.82	62.66	16.52
Th	6.04	7.82	6.34	11.30	5.67	8.76	11.94	11.78	<3	6.65	4.16	8.62	6.43	11.09	6.72	25.33
U	<3	<3	<3	5.25	<3	3.75	3.00	4.98	<3	3.00	<3	3.00	3.00	3.00	3.00	6.16
Y	26.64	30.38	33.57	29.27	22.67	24.26	16.69	27.91	22.92	31.98	19.53	25.68	29.87	33.07	21.26	44.05
Zn	50.84	68.52	74.93	55.17	69.52	43.48	100.96	70.96	102.55	133.74	105.03	98.22	127.88	134.44	139.98	113.26
Zr	682.44	429.58	428.20	492.41	349.52	640.54	362.45	359.38	180.02	255.28	174.88	226.06	258.09	456.28	250.02	337.30
Cl	18.75	278.94	90.62	53.30	38.48	93.96	62.54	233.29	236.12	292.97	356.02	250.62	318.50	243.90	172.84	137.31
Co	40.21	70.53	67.28	50.53	89.01	61.39	80.20	38.09	136.58	165.10	144.76	101.05	107.51	95.52	103.52	60.30
Cr	393.28	397.56	376.57	253.68	591.12	425.79	416.24	209.67	5479.72	6068.32	6237.45	2741.76	1793.91	883.16	803.32	289.77
S	114.85	306.35	312.60	147.95	249.57	211.32	53.57	223.64	310.88	107.94	597.20	116.14	84.43	129.20	63.16	71.78
Sc	25.69	44.92	42.46	26.53	44.08	19.67	30.13	24.53	30.95	41.26	32.39	33.13	50.01	43.86	44.03	34.27
V	196.99	257.00	232.70	175.59	253.22	157.79	564.84	127.80	220.79	294.12	252.81	228.29	364.18	315.95	638.31	202.38
Pt in ppb				<10			<10								<10	
Pd in ppb				<10			<10								<10	

XRF analyses for stream sediments in the Ingeli lobe

Streams	FO	GO
SiO2	49.52	66.53
TiO2	1.54	1.59
Al2O3	17.87	10.53
Fe2O3	11.32	8.05
MnO	0.11	0.36
MgO	0.40	0.75
CaO	0.19	1.19
Na2O	0.26	0.85
K2O	0.88	2.42
P2O5	0.14	0.07
Cr2O3	0.04	0.03
NiO	0.02	0.03
V2O5	0.03	0.03
ZrO2	0.20	0.00
LOI	15.78	5.69
TOTAL	98.32	98.11
Traces		
ppm	FO	GO
As	12.48	7.73
Cu	48.50	21.69
Ga	27.49	13.99
Mo	1.64	1.00
Nb	24.33	18.41
Ni	42.05	31.95
Pb	31.97	17.44
Rb	56.60	93.82
Sr	23.47	81.83
Th	26.28	12.13
U	6.69	3.00
Y	50.37	25.27
Zn	72.12	51.91
Zr	409.62	385.31
Cl	231.07	298.72
Co	47.28	34.76
Cr	218.14	139.00
S	87.94	64.72
Sc	28.85	15.34
V	163.05	126.77
Pt in ppb		
Pd in ppb		